DEVELOPMENT AND COMPARISON OF COMPTON SUPPRESSION TECHNIQUES FOR LOW-LEVEL RADIONUCLIDE ANALYSIS

By

Frank R. Markwell

A DISSERTATION PRESENTED TO THE GRADUATE COUNCIL OF
THE UNIVERSITY OF FLORIDA
IN PARTIAL FULFILLMENT OF THE REQUIREMENTS FOR
THE DEGREE OF DOCTOR OF PHILOSOPHY IN
NUCLEAR ENGINEERING SCIENCES

UNIVERSITY OF FLORIDA

1972

ACKNOWLEDGEMENTS

The author wishes to express his appreciation to Dr. W.E. Bolch, Dr. M.J. Ohanian, Dr. C.E. Roessler, Dr. W.H. Ellis, and Dr. H.A. Bevis, members of his supervisory committee, for their advice and assistance in the preparation of this dissertation. He especially wishes to thank Dr. W.E. Bolch for the suggestion of the dissertation subject and for his encouragement and valuable advice. Special thanks are due Dr. C.E. Roessler for his aid, helpful suggestions and constructive criticism. Thanks are also expressed to Dr. W.H. Ellis for his helpful suggestions and encouragement.

Special appreciation is extended to the the staff members of the Nuclear Engineering Department and the Environmental Engineering Department in the University of Florida, without whom this work could not have been performed.

The author acknowledges the support by the Atomic Energy Commission for the award of a Special Fellowship in Nuclear Science and Engineering during his graduate studies and the support by Florida Power Corporation.

In addition, the author wishes to thank Nuclear Physics for the loan of the Ge(Li) spectrometer.

TABLE OF CONTENTS

		Page
ACKNOWLEDGEMENTS	.....	ii
LIST OF FIGURES	.....	vi
LIST OF TABLES	.....	ix
ABSTRACT	.....	x
Chapter		
I.	INTRODUCTION	1
II.	THEORY	4
	A. Ge(Li) Detector	4
	B. Anticoincidence Guarding	6
	C. Active-Sample Guarding	8
III.	EXPERIMENTAL SYSTEM	10
	A. Primary Detector	10
	B. Guard Detector	14
	C. Sample Detector	16
	D. Counting Room and Shielding	21
	E. Electronics	27
IV.	NaI(Tl) SYSTEM	33
	A. Configuration	33
	B. Electronics	33
V.	NaI(Tl) PERFORMANCE	39
	A. Detector Background	39
	B. Efficiency	39

TABLE OF CONTENTS -- continued

		Page
Chapter -- continued		
	C. Minimum Detectable Activity	42
	D. Peak-to-Compton Ratio	44
	E. Complex Spectrum	44
VI.	Ge(Li) SYSTEM PERFORMANCE	51
	A. System Background	51
	B. Efficiency	55
	C. Minimum Detectable Activity	55
	D. Peak-to-Compton Ratio	59
	E. Complex Spectrum	59
VII.	GUARDED SYSTEM PERFORMANCE	62
	A. System Background	62
	B. Guard-Detector Efficiency	64
	C. Photopeak Reduction	68
	D. Minimum Detectable Activity	69
	E. Peak-to-Compton Ratio	69
	F. Complex Spectrum	73
VIII.	ACTIVE SAMPLE SYSTEM	75
	A. Efficiency	75
	B. Minimum Detectable Activity	75
	C. Peak-to-Compton Ratio	76
	D. Separation of Decay Modes	76
IX.	COMPARISON OF SYSTEMS ON ENVIRONMENTAL SAMPLES	82

TABLE OF CONTENTS -- continued

Page

Chapter -- continued

A. Standard Samples 82

B. Air Sample 85

C. Water Samples 85

D. Solid Samples 88

X. EVALUATION OF DETECTION SYSTEMS 94

A. NaI(Tl) System 94

B. Unguarded Ge(Li) System 95

C. Guarded Ge(Li) System 95

D. Active-Sample System 96

XI. CONCLUSIONS 97

Appendices

A. ELECTRONIC CIRCUITS 100

B. GUARD-DETECTOR CHARACTERISTICS 105

C. SPECTRUM ENERGY CALIBRATION 110

D. EXAMPLE OF DIGITAL DATA 113

LIST OF REFERENCES 115

BIOGRAPHICAL SKETCH 117

LIST OF FIGURES

Figure		Page
1.	Effect of Compton suppression	7
2.	Guarded Ge(Li) system configuration	11
3.	Ge(Li) detector - side view	12
4.	Ge(Li) detector - frontal view	13
5.	Ge(Li) detector with extension collar	15
6.	Guard-detector photomultiplier tube	17
7.	Guard-detector with photomultiplier mounted	18
8.	Sample port mounted in guard detector	19
9.	Ge(Li) detector positioned in sample port	20
10.	Sample container with photomultiplier mounted	22
11.	Sample port for standard technique	23
12.	Sample port for active-sample technique	24
13.	Counting room and entrance	25
14.	Counting room	26
15.	Photomultiplier shielding	28
16.	Guarded Ge(Li) system electronics	29
17.	Ge(Li) system analyzer	30
18.	NaI(Tl) detector configuration	34
19.	NaI(Tl) crystal in lead shield	35
20.	NaI(Tl) system in counting room	36
21.	NaI(Tl) system electronics	38
22.	Background for NaI(Tl)	40

LIST OF FIGURES -- continued

Figure		Page
23.	NaI(Tl) photopeak efficiency	43
24.	Minimum theoretical detectable activity for NaI(Tl)	45
25.	Peak-and-Compton spectrum for NaI(Tl)	47
26.	Peak-to-Compton ratio for NaI(Tl)	48
27.	Complex NaI(Tl) spectrum	49
28.	Counting room background	52
29.	Ge(Li) background with Hg shielding	53
30.	Ge(Li) photopeak efficiency	56
31.	Minimum theoretical detectable activity for Ge(Li)	57
32.	Peak-to-Compton ratio for Ge(Li)	60
33.	Unguarded complex Ge(Li) spectrum	61
34.	Unguarded Ge(Li) background	63
35.	Guarded Ge(Li) background	65
36.	Guard-detector efficiency	67
37.	Minimum theoretical detectable activity for guarded Ge(Li)	70
38.	Peak-to-Compton ratio for guarded Ge(Li)	72
39.	Guarded complex Ge(Li) spectrum	74
40.	Active-sample minimum theoretical detectable activity for Ge(Li)	77
41.	Active-sample peak-to-Compton ratio	79
42.	Separation of decay modes	80

LIST OF FIGURES -- continued

Figure		Page
43.	Zn-65 source spectrum	83
44.	Complex standard-sample spectrum	84
45.	Air sample spectrum	86
46.	Water standard spectrum	87
47.	UFTR primary coolant water spectrum	89
48.	Soil sample spectrum	90
49.	Oyster sample spectrum	92
50.	Seaweed sample spectrum	93
51.	Sample-detector electronics circuit	101
52.	Guard-detector electronics circuit	102
53.	Ge(Li) threshold electronics	103
54.	System coincidence electronics	104
55.	Guard-detector light collection	106
56.	Guard-detector background	107
57.	Threshold calibration	108
58.	Ge(Li) calibration spectrum	111
59.	Ge(Li) calibration curve	112

LIST OF TABLES

Table		Page
1.	Background Count Rate for the NaI(Tl) System ..	41
2.	Theoretical Minimum Detectable Activities for the NaI(Tl) System	46
3.	Background Count Rate for the Ge(Li) System ...	54
4.	Theoretical Minimum Detectable Activities for the Ge(Li) System	58
5.	Background Count Rate for the Guarded Ge(Li) System	66
6.	Theoretical Minimum Detectable Activities for the Guarded Ge(Li) System	71
7.	Theoretical Minimum Detectable Activities for the Active-Sample Ge(Li) System	78
8.	Digital Data for Guarded Air Sample Spectrum ..	114

Abstract of Dissertation Presented to the Graduate Council in Partial Fulfillment of the Requirements for the Degree of Doctor of Philosophy in Engineering

DEVELOPMENT AND COMPARISON OF COMPTON SUPPRESSION TECHNIQUES FOR LOW-LEVEL RADIONUCLIDE ANALYSIS

By

Frank R. Markwell

December, 1972

Chairman: Dr. W. E. Bolch
Major Department: Nuclear Engineering Sciences

Optimum analysis of low-level radionuclides requires the removal of Compton interference from the gamma-ray spectrum. Significant Compton suppression can be achieved by employing high-efficiency guard detectors to detect the scattered gamma photons. However, high detection efficiency prohibits significant absorption between the primary detector and the guard detector, thus restricting the sample to one of small mass. When large-mass samples are used Compton suppression is greatly degraded.

To alleviate this problem a new concept has been developed and a system constructed, and evaluated which, in effect, makes the sample part of the guard detector. Restricted to optically clear samples, the system requires the addition of a liquid scintillator to the counting sample. This

"cocktail" is viewed by a separate photomultiplier tube and associated electronics which add its detected signal to the guard signal and both are used in anticoincidence with the primary detector. This scheme restores the performance of the system to that of the "small-sample" Compton reduction system. However, it also removes photopeaks due to simultaneous (preceding within 200 ns) β^+ or β^- decay in the sample which can also trigger the anticoincidence logic. Alternately, by requiring coincidence between the sample-scintillator detector and the primary detector, all electron capture and metastable states are excluded, leaving only a spectrum of photopeaks from short lived β^+ and β^- decay daughters but with partial Compton reduction. In short, this technique yields two spectra for each liquid sample, a "perfect" gamma spectrum of some excited states and a "not so perfect" gamma spectrum of the remaining excited states.

The complete detection system employs a 6% efficient (re 3x3 inch NaI(Tl)), 2.8 keV resolution Ge(Li) spectrometer as the primary detector arranged to extend 12 inches into the center of a 31 inch diameter by 26 inch long container of Pilot Chemical's high efficiency mineral oil scintillator. This scintillator, which acts as the guard detector, is viewed by a 15 inch Fairchild K2128 photomultiplier tube and both are shielded with 2.5 inches of mercury. The sample container arranged axially around the Ge(Li) crystal and viewed by a 2 inch diameter RCA 6655 photomultiplier tube, holds 1.5 litres (60% scintillator). The electronics include

preamplifier, threshold detectors, and logic circuits to give a timing uncertainty of less than 200 ns.

Comparison of this system with a 4x4 inch NaI(Tl) system and the unguarded Ge(Li) system shows it to have both superior peak-to-Compton ratios and superior minimum detectable activities for counting times as short as 40 minutes. In addition to maintaining the point source peak-to-Compton ratio for large water samples, the active-sample technique has the advantage of dividing the spectrum into two spectra according to the decay mode of the radionuclides.

CHAPTER I

INTRODUCTION

Gamma ray spectroscopy has been an important tool in the analysis of radionuclides for many years. The development of the NaI(Tl) detector opened the field and since then vast improvements in efficiency and reductions in interradionuclide interference have been made. Improvements in detector efficiency and resolution have reduced this interference but not eliminated it. The remaining interference is mostly due to the Compton continuum associated with photopeaks in the spectrum.

Since Compton scatter in the detector is only a partial energy release mechanism, a lower energy gamma photon may also exit the detector. This characteristic has been used in suppressing the Compton continuum.[1][2] The original systems for such suppressions employed NaI(Tl) as the primary detector surrounded by a large liquid scintillator which detected the Compton scattered photons leaving the primary detector and used them to eliminate such counts from the spectrum. Thus, this technique is denoted as anticoincidence guarding.

The development of the Ge(Li) detector has resulted in greatly improved resolution capabilities and reduced effects from the Compton continuum. The usefulness of such a detector

for low level radionuclide analysis has been shown previously by Cooper et al.[3] Soon thereafter investigators applied anticoincidence guarding to Ge(Li) detectors.[4][5][6][7] These systems, which suppressed the Compton continuum up to a factor of 6, employed plastic scintillators as the guard detector. Current investigators, using NaI(Tl) guards, report a Compton reduction for ^{137}Cs of up to 9 times,[8][9] and those using plastic scintillator guards report a reduction of 6 times.[10][11]

Significant Compton reduction can only be achieved by employing high-efficiency guard detectors. However, high detector efficiency prohibits significant absorption between the primary detector and the guard detector, thus restricting the sample to one of small mass. When large-mass samples are used, Compton suppression is greatly degraded.[7]

To alleviate this problem, a new concept is proposed which, in effect, makes the sample part of the guard detector. Restricted to clear water samples, the system would require the addition of a liquid scintillator to the counting sample. This "cocktail" would be viewed by a separate photomultiplier tube and associated electronics which would add its detected signal to the guard signal and both would be used in anti-coincidence with the primary detector. This scheme should restore the performance of the system to that of the "small-sample" Compton reduction system. However, it would also remove many photopeaks due to simultaneous (preceding within 200 ns) β^+ or β^- decay in the sample which could also trigger the anticoincidence logic. Alternately, by requiring coinci-

dence between the sample-scintillator detector and the primary detector, all electron capture and metastable states could be excluded, leaving only a spectrum of photopeaks from short-lived β^- and β^+ decay daughters but with partial Compton reduction. In short, this technique would yield two spectra from each liquid sample, a "perfect" gamma spectrum of some excited states and a "not so perfect" gamma spectrum of the remaining excited states.

Presented here are the design details of a liquid scintillator guarded Ge(Li) system with the active-sample option, as mentioned above, and the evaluation of this system for environmental radionuclide analysis with respect to their relative advantages over a 4x4 inch NaI(Tl) system.

CHAPTER II

THEORY

In this chapter the theory behind the active sample anticoincidence guarded Ge(Li) spectrometer is presented. Included are both the theory associated with the new active sample technique and the theory of anticoincidence guarding. The latter is presented since anticoincidence guarding is still a relatively new technique and not widely known.

A. Ge(Li) Detector

Interaction of a gamma photon with the primary detector can occur in one of several ways. These are photoelectric absorption, Compton scatter, and pair production. For germanium and typical gamma energies (<2MeV), only the first two are significant. Photoelectric absorption occurs when the gamma photon releases all of its energy in one interaction with a bound electron, and has the greatest probability for photon energies just above the ionization potential energy of that bound electron. Thus, this method of photon energy release is most significant for low energies and has approximately a $(h\nu)^{-3.5}$ probability dependance. Photoelectric absorption transfers all of its energy to the bound electron which in turn releases this energy by ionization and electronic

excitation of atoms in the immediate vicinity of the photon interaction.

The other interaction of significance is Compton scatter, which consists of a partial transferral of photon energy to the bound electron and the subsequent scatter of the photon (reduction in energy). This reaction has a $(h\nu)^{-1}$ probability dependance and thus is significant for energies higher than those significant for photoelectric absorption. Again the liberated electron from the photon interaction produces ionization and electronic excitation of atoms in its immediate vincinity.

Such interactions within the intrinsic region of a semiconductor produce electron-hole pairs having lifetimes long enough to allow their collection by an electric field. The result is a charge collection which is proportional to the gamma photon energy release within the semiconductor crystal. A count rate-energy release spectrum (charge collection) yields a peak corresponding to photoelectric absorption and a continuum of counts corresponding to the energy release in Compton scatter. Due to the physics of Compton scatter this continuum is approximated by a plateau from zero energy (no scatter) to a maximum energy signicantly less (typically 100-200 keV) than the photopeak energy (corresponding to the energy release in photon backscatter).

The ratio of probabilities of the two interactions depends upon the photon energy and the detector material. For germanium the photoelectric interaction and Compton scatter

are equally probable at 150 keV but at 1 MeV Compton scatter is 100 times more probable.[7]

B. Anticoincidence Guarding

The useful information from a Ge(Li) spectrum lies in the photopeak energy and amplitude since the gamma photon energy is characteristic of the radionuclide from which it originated and the amplitude is proportional to the quantity present. The Compton plateau is a continuum which, because of counting statistics, is erratic and thus obscures other photopeaks which may lie within this energy range. Anticoincidence guarding suppresses the counting of scatter events thereby removing this continuum and allowing recognition of small amplitude photopeaks within the energy range (see Figure 1).

To achieve this Compton suppression, those gamma photons which deposit only part of their energy in the primary detector must be recognized. By placing the primary detector within a high-efficiency detector, photons which are scattered in the primary detector can be detected again in the guard and thus recognized as being Compton scattered. These can then be prevented from being recorded in the spectrum. To obtain excellent Compton suppression, the guard detector must approach 100% detection (not energy collection) efficiency and photon absorption between the primary detector and the guard detector must be eliminated. Since good primary detection requires the radioactive sample to be placed in the center of the guard detector just adjacent to the primary detector, the sample itself can act as an

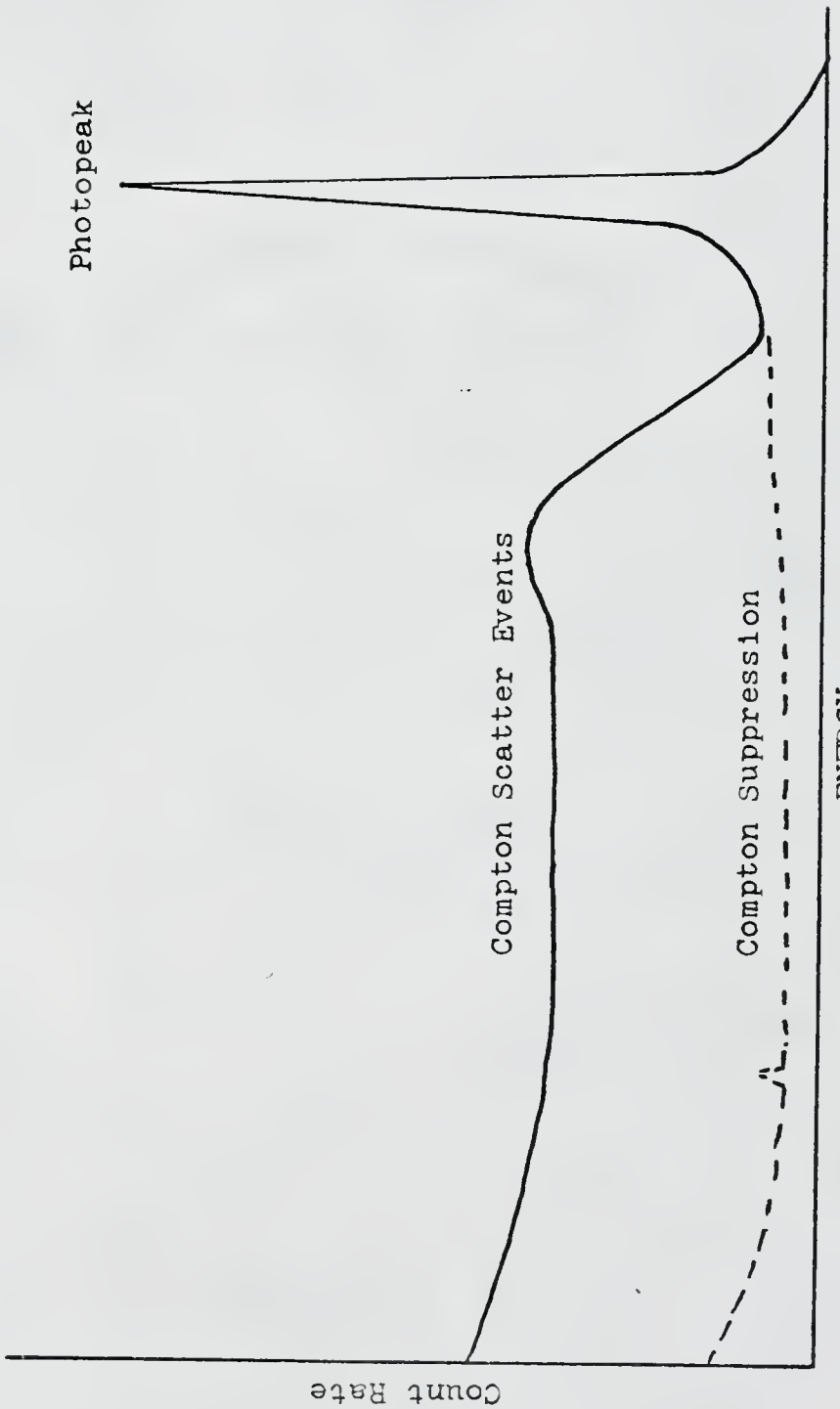

Fig. 1 Effect of Compton suppression.

unwanted absorber. Thus excellent Compton suppression in standard systems can be maintained only with small samples. In addition, large samples inherently yield a lower peak-to-Compton ratio due to Compton scatter in the sample before the photon reaches the primary detector.

An inherent disadvantage of anticoincidence guarding is the removal from the spectrum of those photopeaks associated with cascade gamma decay (2 or more simultaneous photons) and β^+ decay whose excited daughter decays simultaneously (yielding a simultaneous gamma decay photon and annihilation photons).

C. Active Sample Guarding

To eliminate degradation of Compton suppression and maintain excellent peak-to-Compton ratios, the sample must be used as a guard detector also. This allows recognition of sample-scattered photons which enter the primary detector and primary detector scattered photons which are absorbed back in the sample. The combined effects yield a peak-to-Compton ratio for large samples which approaches that for point source samples.

An inherent problem in this technique arises when a radionuclide in the sample decays by emission of a β^- particle to its excited daughter and then immediately emits a gamma photon. In this case gamma photons enter the primary detector at the same time that the β^- particles (poly-energetic) release their energy in the sample detector. Thus

the β particles can not be distinguished from the scattered gamma photons by the sample detector. Radionuclides having excited daughter lifetimes greater than the timing uncertainty of the detector system, and those radionuclides which decay by electron capture, are not affected by this phenomenon.

To restore these short-lived excited daughters from β^- decay and remove the long-lived and electron capture events, coincidence signals can be required between the sample detector and the primary detector, indicating β^- decay with an associated prompt gamma photon. This spectrum contains only photopeaks from these prompt gamma decay states but maintains only partial Compton suppression.

The active-sample technique, in addition to the normal guarded system spectrum, yields two additional simplified spectra - one spectrum of gamma photons from electron capture and metastable states maintaining total Compton suppression, and a second spectrum of prompt gamma photons from β^- decay maintaining partial Compton suppression.

CHAPTER III

EXPERIMENTAL SYSTEM

The complete active-sample experimental system consists of three detectors, the primary, the guard, and the sample detector. Figure 2 shows their relationship. This chapter gives both the component specifications and design parameters for each detector and establishes this relationship. In addition, the counting room is described and shielding considerations explained.

A. Primary Detector

In order to obtain the greatest resolution and thus the most discriminating and accurate spectrometer, a Ge(Li) detector was selected as the primary detector. The Ge(Li) detector yields by far the best photopeak resolution and the greatest peak-to-Compton ratio of any detector presently available.[12] However, the efficiency of the Ge(Li) detector is typically much less than other available detectors. Taking both properties into account, the Ge(Li) detector still yields a superior spectrum in most cases.[6]

The Ge(Li) detector, produced by Ortec, Inc. has a crystal volume of 34 cc which yields 6% efficiency (re 3x3 NaI(Tl)), 2.9 keV resolution, and 15 to 1 peak-to-Compton ratio for ^{60}Co. The detector as shown in Figures 3 and 4 includes a liquid

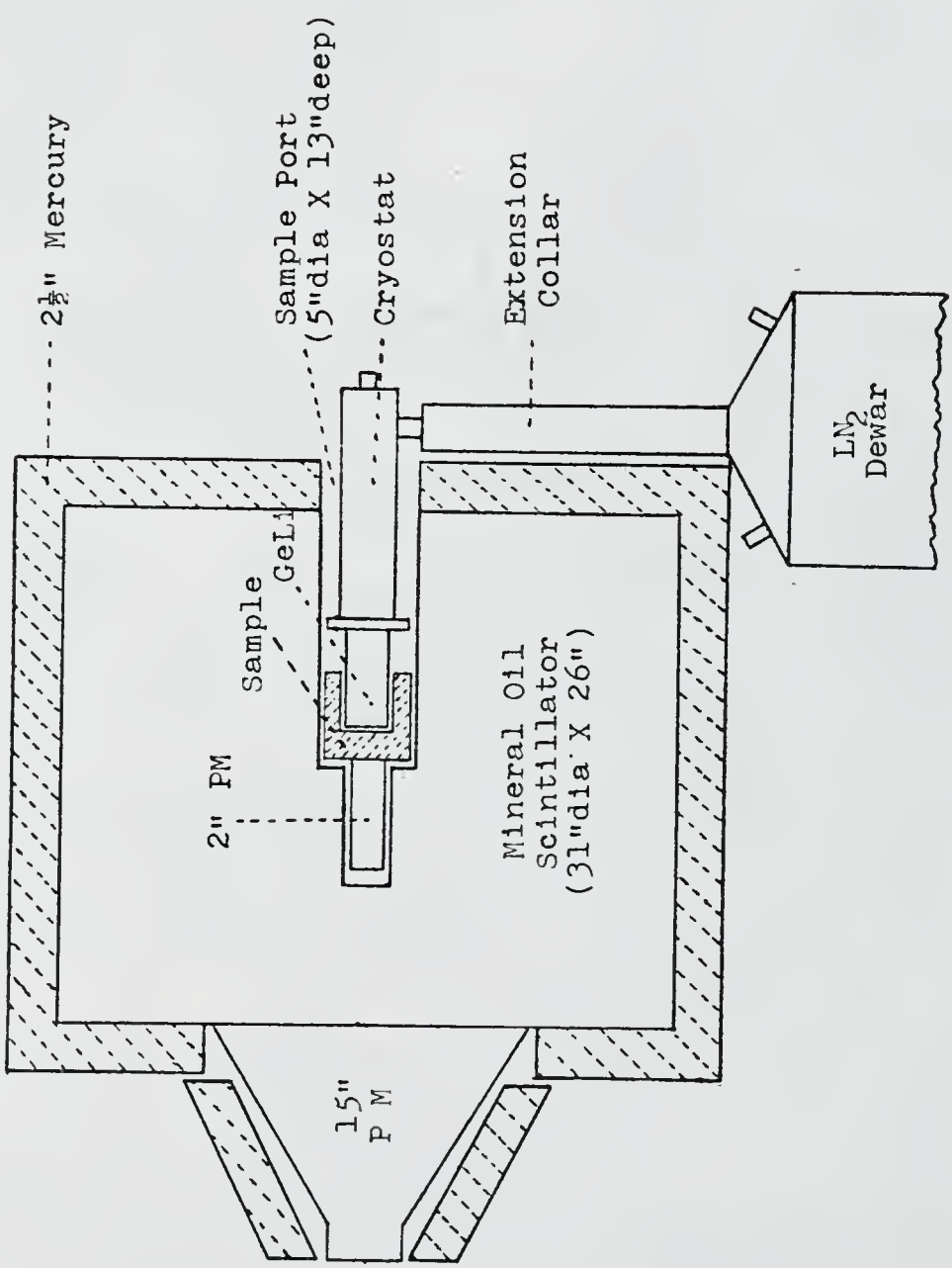

Fig. 2. Guarded Ge(Li) system configuration.

Fig. 3 Ge(Li) detector - side view.

Fig. 4 Ge(Li) detector - frontal view.

nitrogen container required for cooling of the crystal and a preamplifier mounted on the side. The standard Ge(Li) detector configuration prohibits its insertion into a large guard detector. Therefore to facilitate use of this detector, a 10 inch long by 2.5 inch diameter plexiglass collar having 0.25 inch thick walls was used to raise the detector to a more accessible position (see Figure 5). Due to cooling requirements of the detector, this position could be maintained for only 24 hours without topping-up the liquid nitrogen. (In the standard position, the nitrogen container can cool the detector for approximately three weeks.)

B. Guard Detector

The single requirement of the guard detector is that it sense nearly 100% of all gamma photons entering it. This requires that each gamma photon go through at least one Compton scatter. Since the scatter cross section is typically much larger than the photoelectric cross section, Compton scatter dominates the total mass attenuation coefficient which is approximately equal (av. 0.1 cm^2/g)[13] for all available detectors within the energy range of interest. Thus, to obtain 95% detection the mass thickness must be 30 g/cm^2. For NaI(Tl) crystals this would require a detector depth of about 8 cm and for liquid or plastic scintillators about 30 cm.(Ge(Li) detector configuration limits its positioning into a solid guard detector to 30 cm deep.)

Fig. 5 Ge(Li) detector with extension collar.

Liquid scintillator was chosen for the guard detector because of its faster decay time over NaI(Tl) and its larger output and longer light mean free path than plastic scintillator.[13] The former lowers the energy detection limit and decreases dead time while the latter allows use of a larger volume detector, and thereby higher detection efficiency. Pilot Chemical's new high-efficiency (60% re anthracene) mineral oil scintillator was determined to have one of the longest mean free paths (5 meters) and the shortest decay times (2 ns).[14] The guard detector consists of 80 gallons of this scintillator in a 31 inch diameter by 26 inch long cylindrical tank with a Fairchild K2128 15 inch photomultiplier (see Figure 6) mounted on one face (see Figure 7) and a 5 inch diameter by 12 inch long sample port in the opposite face (see Figure 8). The inner surfaces of the tank are painted with white epoxy paint to increase photomultiplier light collection.

The Ge(Li) detector can then be positioned in the guard detector port as shown in Figure 9.

C. Sample Detector

The sample detector was designed in the shape of a Marinelli beaker (coaxial around the primary detector) to allow detection of large-volume low-concentration samples. Since addition of sample depth beyond 3.5 cm has little advantage due to scatter and absorption in the sample (50% attenuation path of 100 keV gamma photons in water), the sample container size was restricted to 1.5 litres giving

Fig. 6 Guard detector photomultiplier tube.

Fig. 7 Guard detector with photomultiplier mounted.

Fig. 8 Sample port mounted in guard detector.

Fig. 9 Ge(Li) detector positioned in sample port.

about 3.5 cm of depth around the primary detector (see Figure 10).

The sample container itself is made of 15-mil thick aluminum to minimize absorption (2% of incident 70 keV gamma photons), is coated with white reflective epoxy paint and is viewed on the end by an RCA 6655 2-inch diameter photomultiplier tube.

In order to act as a detector, the sample must be mixed with a liquid scintillator. Several different commercial scintillators allow addition of up to 40% water. These include Aquasol by New England Nuclear and Insta Gel by Packard Instruments. In addition, a mixture of p-xylene and Triton N-101 has been shown to accept 40% water.[15] However, only Aquasol was used due to its superior light transmission.

Two sample ports were constructed for use with and without the active sample container. Figure 11 shows the sample port for use without the active sample container and is constructed of 50 mil thick aluminum. Figure 12 shows the sample port for use with or without the active sample container and is constructed of 125 mil thick plexiglass. The former absorbs 6% of incident 70 keV gamma photons and the latter 2%.

D. Counting Room and Shielding

The counting room, surrounded by 24 inch thick low-activity poured concrete, measured 7.5 feet by 18 feet. The positioning of the guarded detector system in this counting room can be seen in Figures 13 and 14. The counting room also

Fig. 10 Sample container with photomultiplier mounted.

Fig. 11 Sample port for standard technique.

Fig. 12 Sample port for active sample technique.

Fig. 13 Counting room and entrance.

Fig. 14 Counting room.

houses a 4x4 inch NaI(Tl) system.

Gamma exposure as measured on a Nuclear Chicago model 2650 gamma survey meter was 0.01 mR/hr in the counting room and five times higher outside of the room.

Mercury was used to shield the guarded Ge(Li) system since it has a higher mass number, greater density, and lower activity than lead. Five thousand pounds of mercury in 2.5 inches thick double wall tanks (approximately equivalent to 4 inches of lead) surround the guard detector and its photomultiplier tube (see Figure 15). With the shield, the guard detector measures 36 inches diameter by 31 inches long.

Due to inherent activity in construction materials, the detectors, and the mercury, additional shielding is not significantly advantageous.

As protective measures against mercury toxicity, a ventilator system and seamless floor were installed in the counting room.

E. Electronics

The complete system electronics is block diagramed in Figure 16. Each of the detectors has its own preamplifier, linear amplifier, and threshold detectors which drive coincidence and anticoincidence gating. In addition, the Ge(Li) detector electronics include an ORTEC model 120-2B preamplifier (supplied with the detector), a model 485 linear amplifier, and a model 444 biased amplifier. Except for these, the ORTEC high voltage supply, and a Packard Model 115 400 channel multichannel analyzer (MCA) (shown in Figure 17) the electronics were

Fig. 15 Photomultiplier shielding.

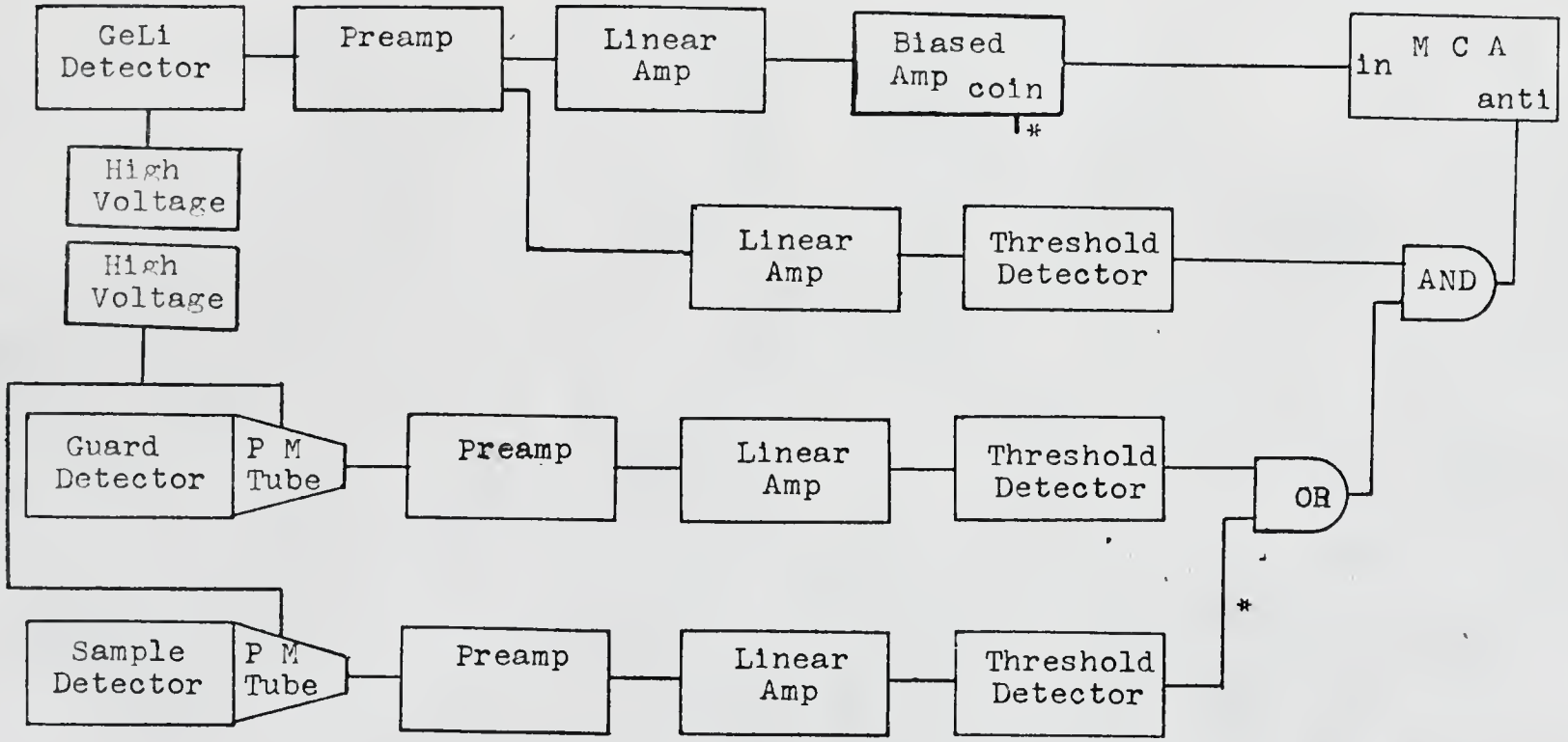

* For coincidence guarding connect to biased amplifier

Fig. 16. Guarded Ge(Li) system electronics.

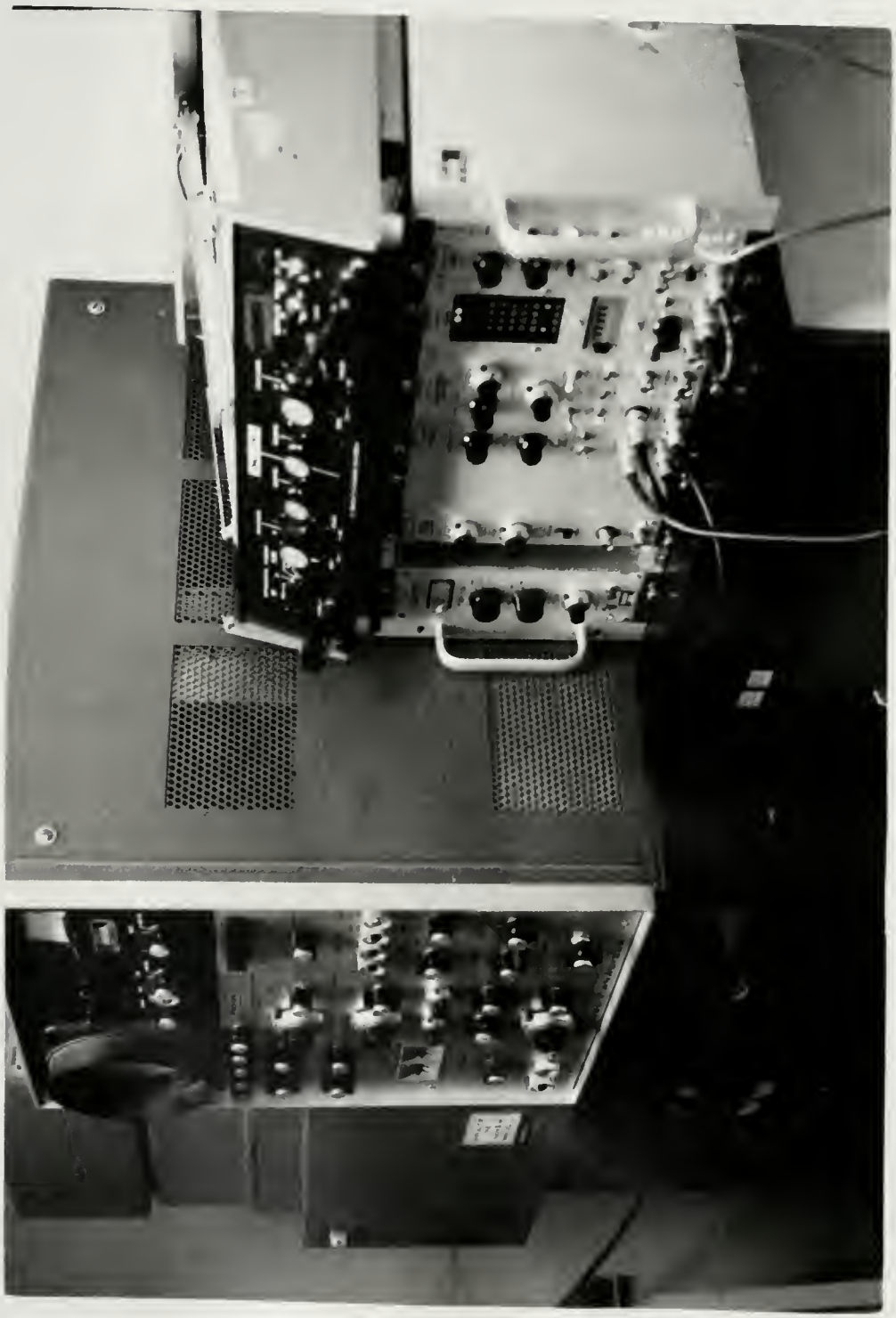

Fig. 17 Ge(Li) system analyser.

custom designed and built in the laboratory.

The signal from the Ge(Li) crystal after amplification in the 120-2B preamplifier is split, being amplified by the 485 linear amplifier and 444 biased amplifier before entering the MCA, and being amplified, sensed by a threshold detector, and then given control of the gate leading to the anticoincidence input of the MCA. Similarly, the guard detector and sample detector have their own identical preamplifiers, linear amplifiers, and threshold detectors. In the sample-guard mode, these two threshold signals are combined by an OR gate which feeds the Ge(Li) AND gate controlling input to the MCA anticoincidence input. In the coincidence sample mode, only the guard threshold feeds the Ge(Li) AND gate while the sample threshold controls the coincidence input of the biased amplifier.

The effect of this circuitry for the sample-guard mode is to send an anticoincidence control pulse to the anticoincidence input of the MCA only when the Ge(Li) detector yields a signal above its noise level and the guard detector or the sample detector yields a signal above its respective noise levels. The effect for the coincidence sample mode is to allow amplification of the Ge(Li) signal only when the sample detector yields a signal above its noise level and to send an anticoincident pulse to the anticoincidence input of the MCA only when the Ge(Li) detector and guard detector yield signals above their respective noise levels.

The circuit diagrams for the electrons of the three detectors, the coincidence units, control pulse generators,

and cable drivers are given in Appendix A.

CHAPTER IV

NaI(Tl) SYSTEM

In order to better show the advantages of a guarded Ge(Li) system, comparison is made with a NaI(Tl) system. In this chapter both the NaI(Tl) configuration and its associated electronics are presented.

A. Configuration

The NaI(Tl) system used as a standard for comparison consists of a Harshaw 4x4 inch NaI(Tl) crystal viewed by a photomultiplier tube and positioned in the center of a 2 foot cubic, 2 inch thick lead shield lined with Cu and Cd (see Figure 18). The top side of the shield is supported on rollers to allow access to the detector crystal (see Figure 19). The shield and detector system occupies the rear corner of the low level counting room as shown in Figure 20.

The NaI(Tl) detector is customarily used to count samples in both 1.0 litre and 3.5 litre Marinelli beakers. In addition, samples in 1.0 litre "ice cream" containers and flat samples are frequently counted on this crystal.

B. Electronics

The electronics consists of a Power Designs Pacific model HV-1565 high voltage power supply, Nuclear Data models

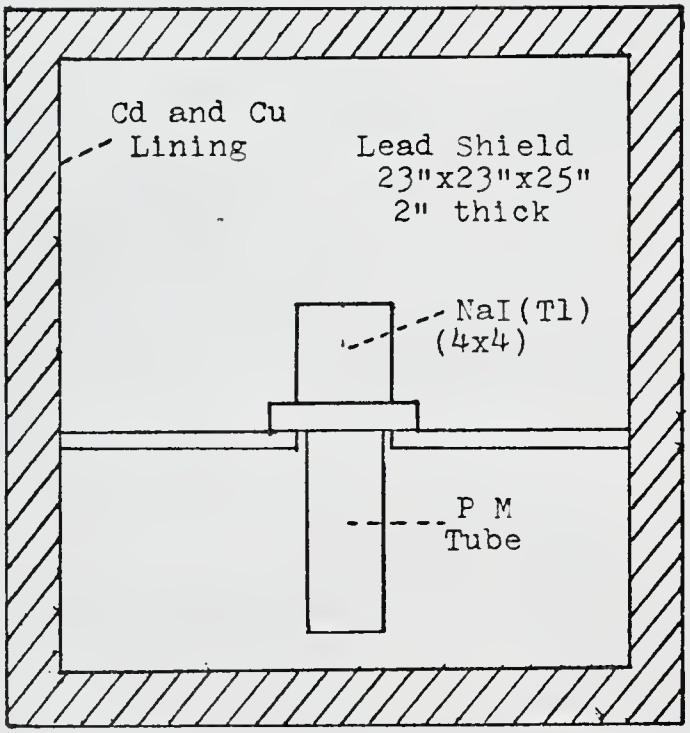

Fig. 18. NaI(Tl) detector configuration.

Fig. 19 NaI(Tl) crystal in lead shield.

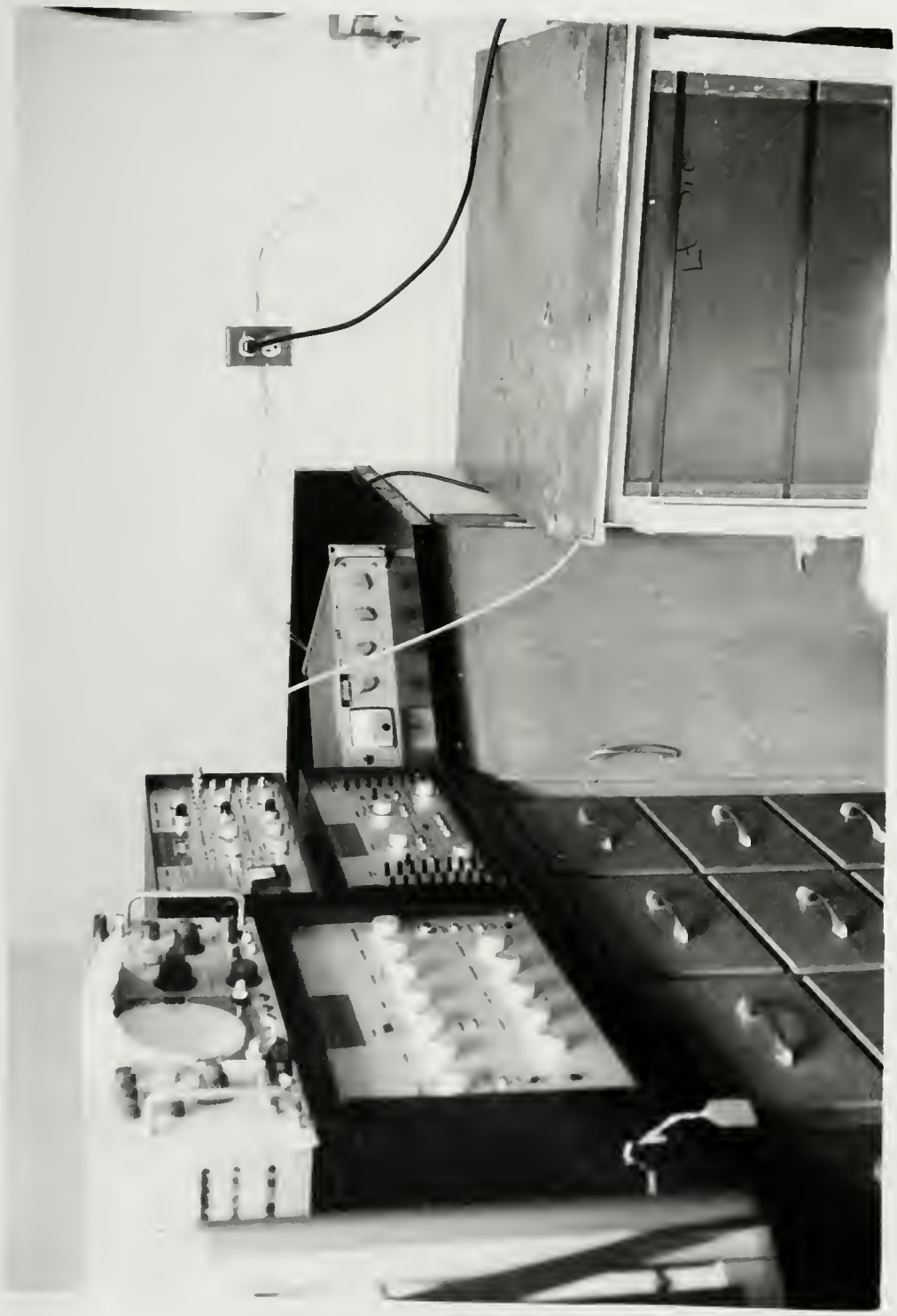

Fig. 20 NaI(Tl) system in counting room.

ND-180F analog to digital converter, ND-180M 512 channel memory unit, and ND-180R readout control unit, a Tally Corporation model 1506 paper punch, a Tektronix model RM503 oscilloscope, a Nuclear Data model ND-316 autofinger mounted on an IBM selectric typewriter, and a Dohrmann Instruments model 299 chart recorder. The system block diagram is shown in Figure 21.

The signal after collection by the photomultiplier tube is amplified, digitized and recorded in the appropriate memory channel. Upon command, the memory can either be displayed on the oscilloscope, plotted, or paper punched. The latter allows computer analysis of the data.

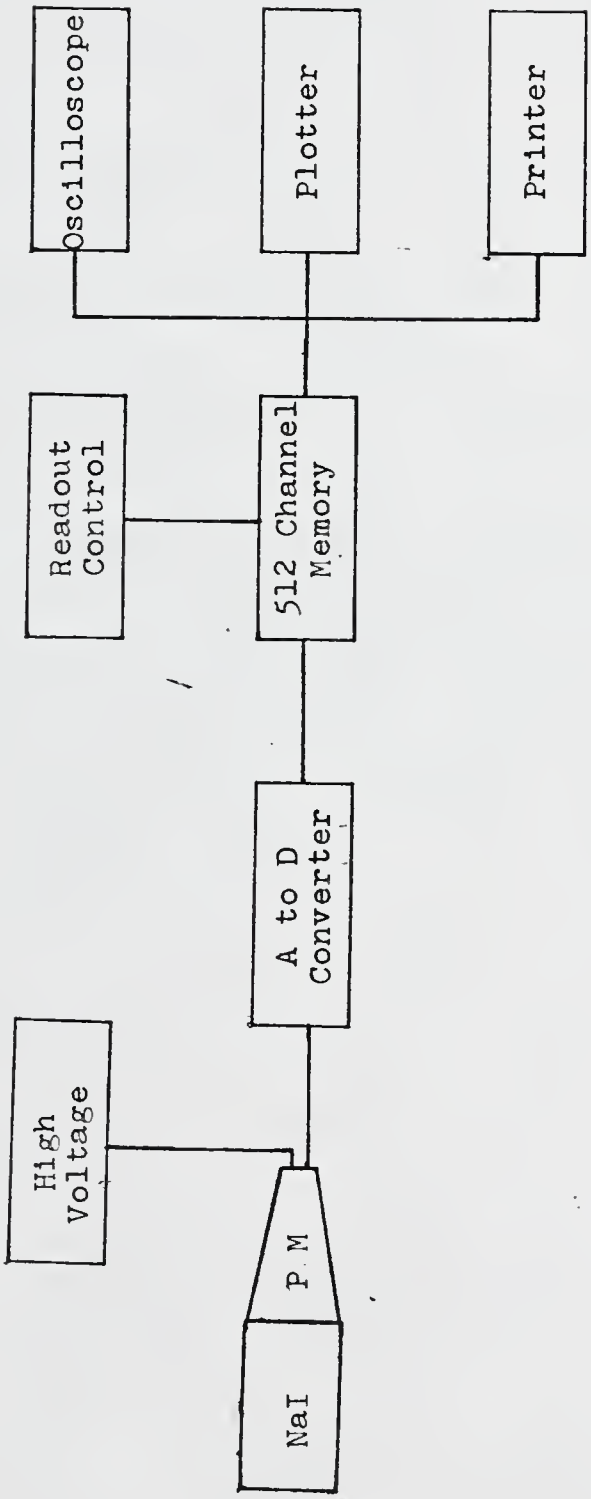

Fig. 21. NaI(Tl) system electronics.

CHAPTER V

NaI(Tl) PERFORMANCE

In this chapter the optimum performance of the 4x4 inch NaI(Tl) system in the low-level counting room as described in Chapter IV is stated. Included are system background, efficiency, minimum detectable activity, peak-to-Compton ratios, and ability to analyze complex spectrum.

A. Detector Background

The 4x4 inch NaI(Tl) crystal background count-rate was determined in the absence of a sample and with the shield in place. Since standard counting procedure in this laboratory uses 40-minute counts, a 40-minute background was accumulated and is plotted in Figure 22. Only traces of the 0.35 MeV RaB and the 1.46 MeV ^{40}K photopeaks are visible in the spectrum. Table 1 lists the background count-rate grouped in various energy ranges and shows a cumulative background count-rate of just over 500 cpm for the 70 to 2500 keV range.

B. Efficiency

The absolute efficiency of the 4x4 inch NaI(Tl) crystal was measured for both point sources (1.0 cm from the crystal) and 3.5 litre sources with calibrated sources obtained from

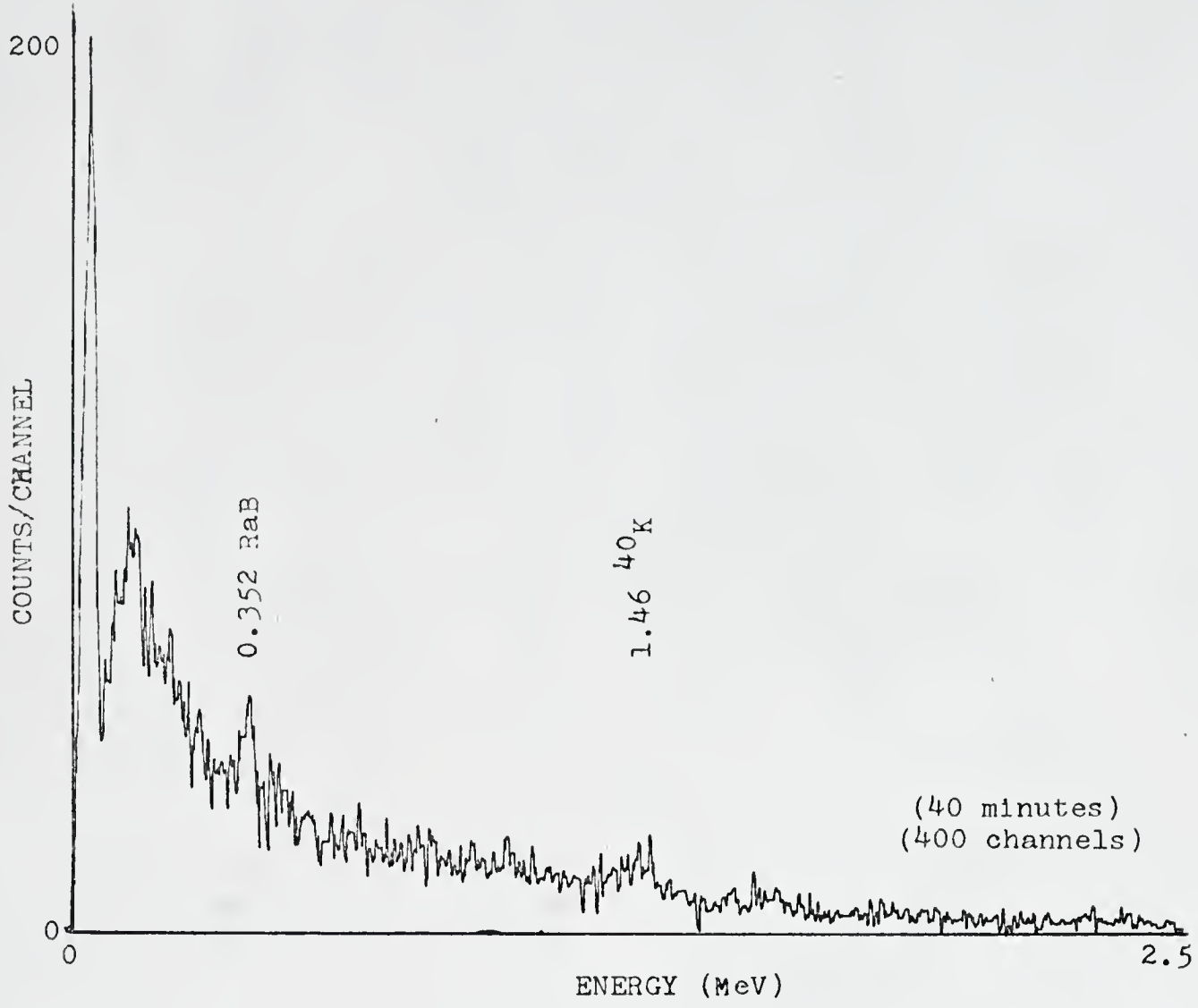

Fig.22. Background for NaI(Tl).

Table 1

Background Count Rate for the NaI(Tl) System

Energy (keV)	Count rate (cpm)	Energy (keV)	Count rate (cpm)
70-200	104	70-2500	546
200-400	158	200-2500	442
400-600	88	400-2500	359
600-800	50	1000-2500	107
800-1000	38		
1000-1500	65		
1500-2000	29		
2000-2500	13		

Baird Atomic and the Public Health Service. The plots of photopeak (full width at tenth maximum) efficiency vs. energy are shown in Figure 23 and include data from the Public Health Service [16] and previous data taken on this system. [17] The data yields essentially straight lines on log-log paper, showing increasing efficiency with decreasing energy down to a point where detector window absorption becomes significant. These data also show that the 3.5 litre sample efficiency is typically 1/3 of that for the point source, the difference being attributed to differences in the average source-to-detector distance.

C. Minimum Detectable Activity

The theoretical minimum detectable activity depends upon the background count and photopeak efficiency. It was determined for the 4x4 inch NaI(Tl) detector by requiring a 95% detection certainty. This means that the theoretical minimum detectable activity equals two times the standard deviation in net count (gross minus background) under the photopeak energy spread, corrected for detector efficiency. For a 40-minute count, the minimum detectable count rate in cpm equals

$$\frac{2}{40}\sqrt{(\text{gross count} + \text{background count})}$$

which yields a minimum detectable activity in dpm of

$$\frac{2\sqrt{2 \times \text{background count (under photopeak)}}}{40\ (\text{efficiency})} .$$

Using the measured photopeak efficiency and background

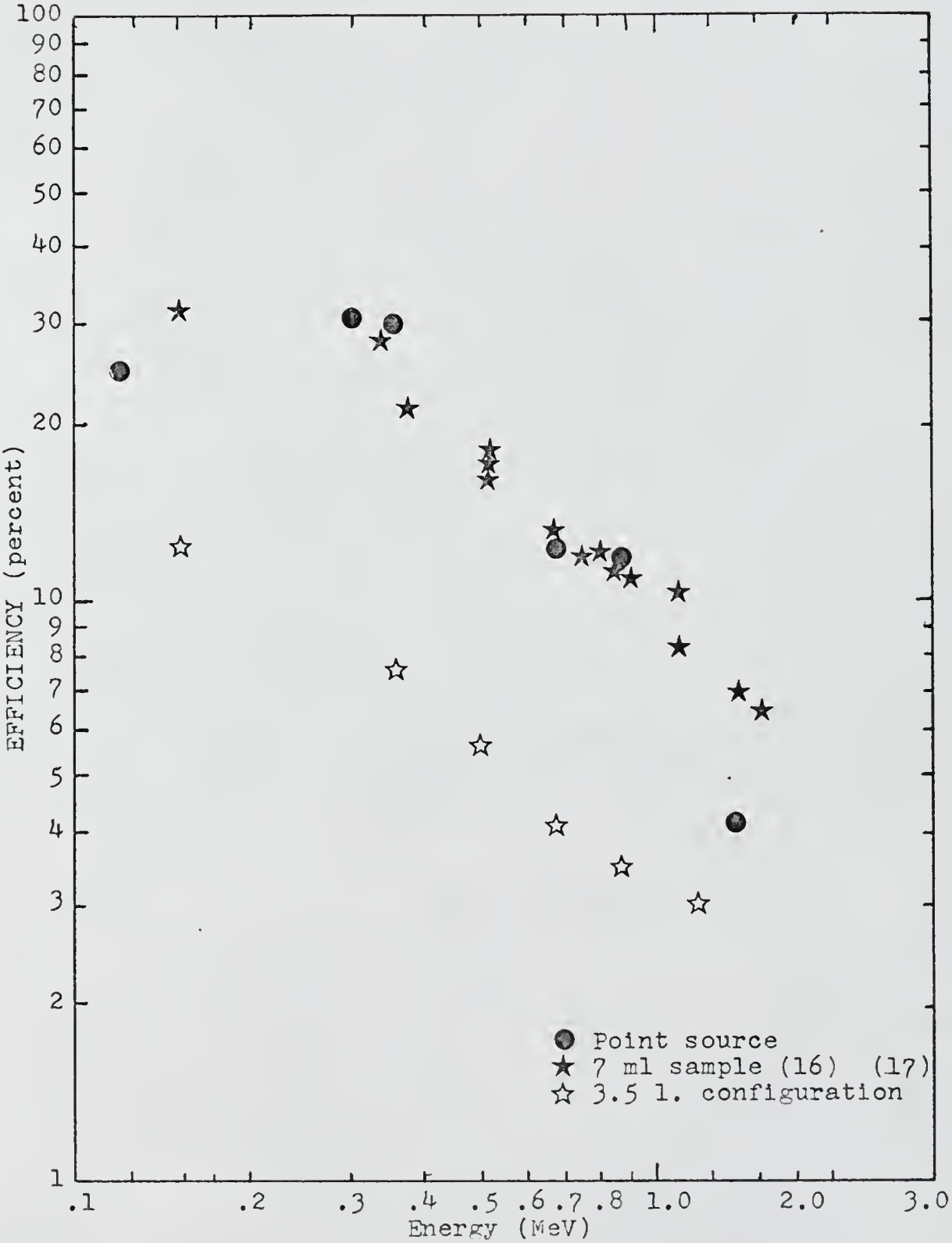

Fig.23. NaI(Tl) photopeak efficiency.

data, the theoretical minimum detectable activity was calculated for nine radionuclides and photopeak energies. Figure 24 shows a plot of minimum detectable activity in gamma photopeak dpm vs. energy. In addition, the minimum detectable activity in pCi and the minimum detectable concentration in pCi/l for several radionuclides of interest are listed in Table 2.

D. Peak-to-Compton Ratio

The peak-to-Compton ratio of a detector is important since it is an indication of the amount of interference between radionuclides in the complex spectrum. Figure 25 shows the peak and Compton relationship in a typical point-source spectrum. Statistical variation in large Compton plateaus greatly increases the minimum detectable activity in that energy range. This uncertainty increases with large-volume samples due to Compton scatter within the sample before detection. Also in complex spectra , addition of Compton plateaus at the lower energies becomes very significant.

The peak-to-Compton ratio for the 4x4 inch NaI(Tl) detector was measured and plotted in Figure 26 for both point sources and 3.5-litre sources. The degradation in peak-to-Compton ratio for the large sample can be readily seen to increase at lower energies.

E. Complex Spectrum

Figure 27 shows a complex spectrum for the 4x4 inch NaI(Tl). The complex spectrum of ^{226}Ra was used in order to

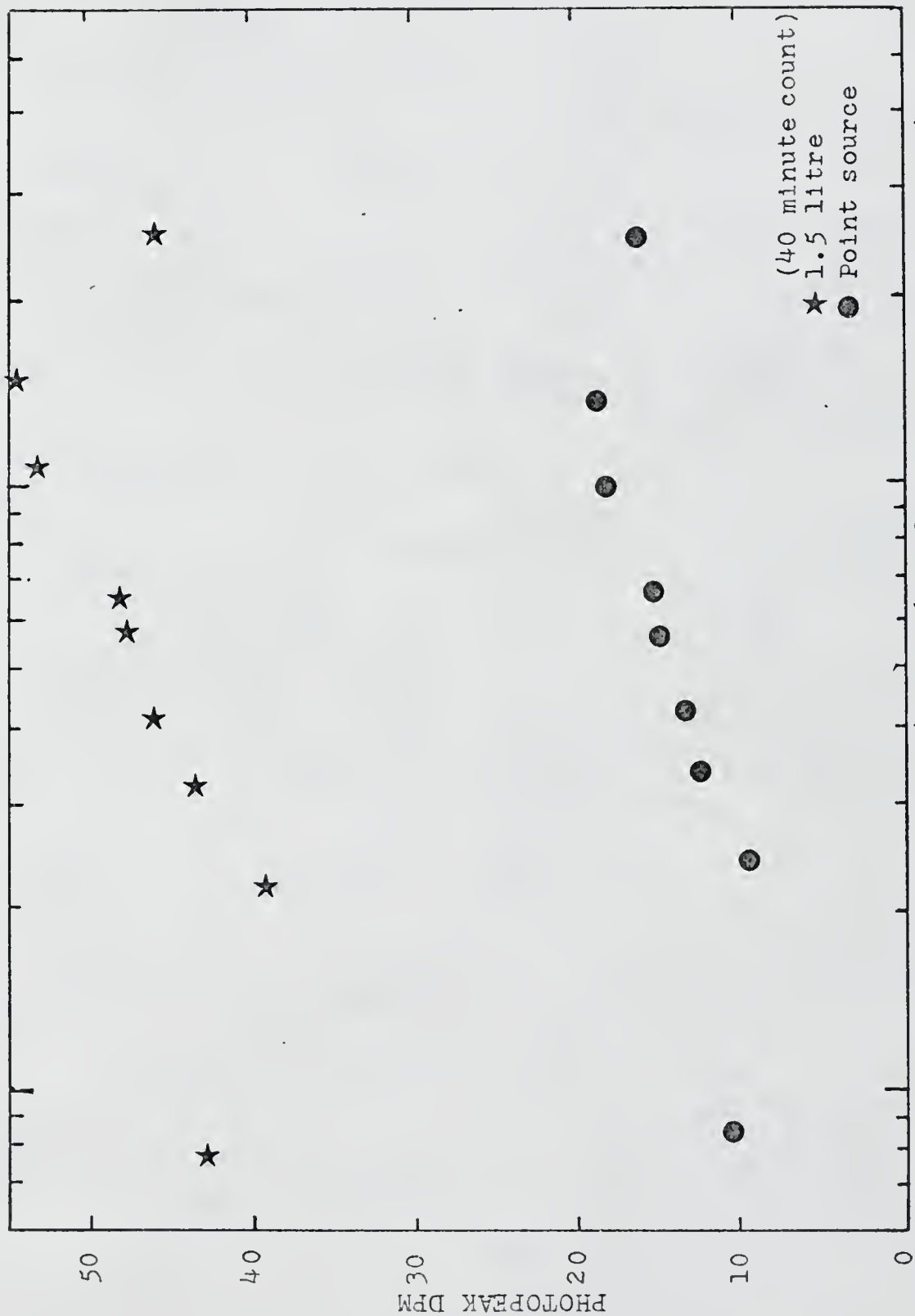

Fig.24. Minimum theoretical detectable activity for NaI(Tl).

Table 2

Theoretical Minimum Detectable Activities for the NaI(Tl) System

(40 min. count)

Standard (MeV)	Minimum Detectable Activity, pCi(point source)	Minimum Detectable[1] Activity, pCi(3.5 l)	Minimum Detetable[1] Concentration, pCi/l(3.5 l)
^{226}Ra (1.764)	---	700	200
^{232}Th (0.908)	---	48	14
^{137}Cs (0.662)	8.5	36	10
^{95}Zr (0.724)	3.7	17	5
^{106}Ru (0.512)	34	120	34
^{131}I (0.364)	8.0	22	6.3
^{144}Ce (0.134)	45	170	48
^{65}Zn (1.115)	14.5	61	17
^{54}Mn (0.835)	7.3	24	6.8

[1] From "Environmental Surveillance for Radioactivity in the Vicinity of Crystal River Nuclear Power Plant:An Ecological Approach", quarterly progress report - Nov. 1, 1970 - Jan. 31, 1971, University of Florida.

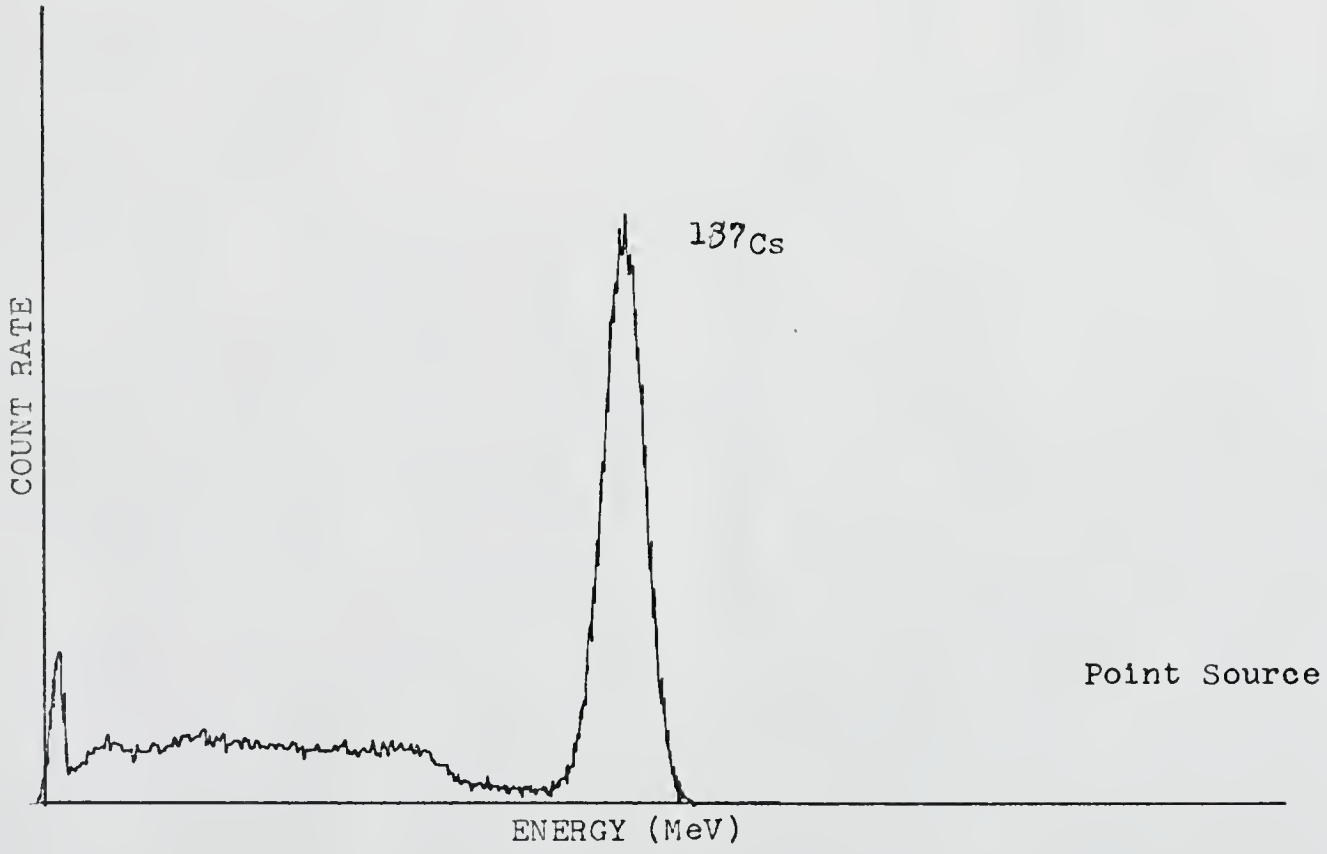

Fig.25. Peak and Compton spectrum for NaI(Tl).

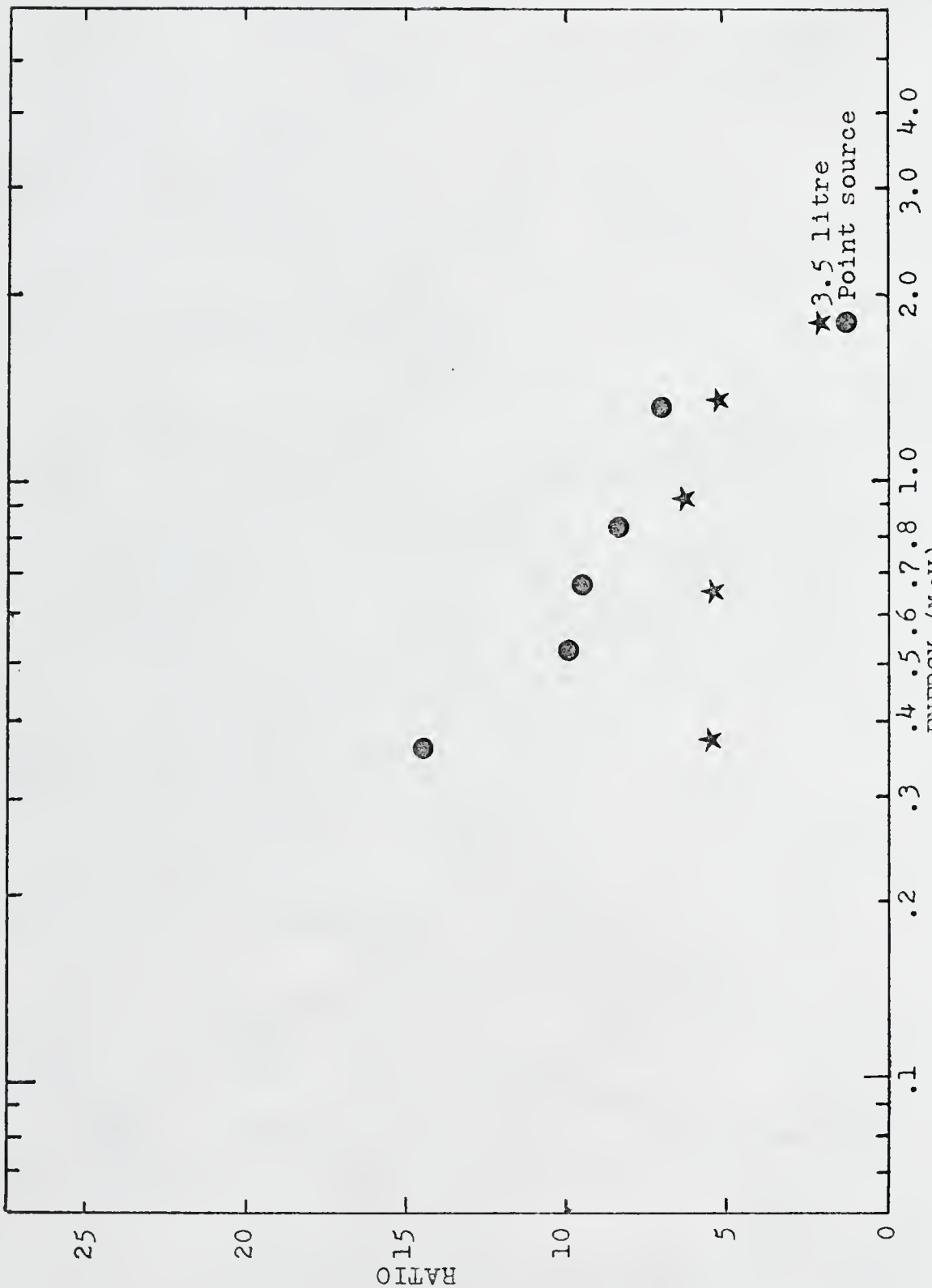

Fig.26. Peak-to-Compton ratio for NaI(Tl).

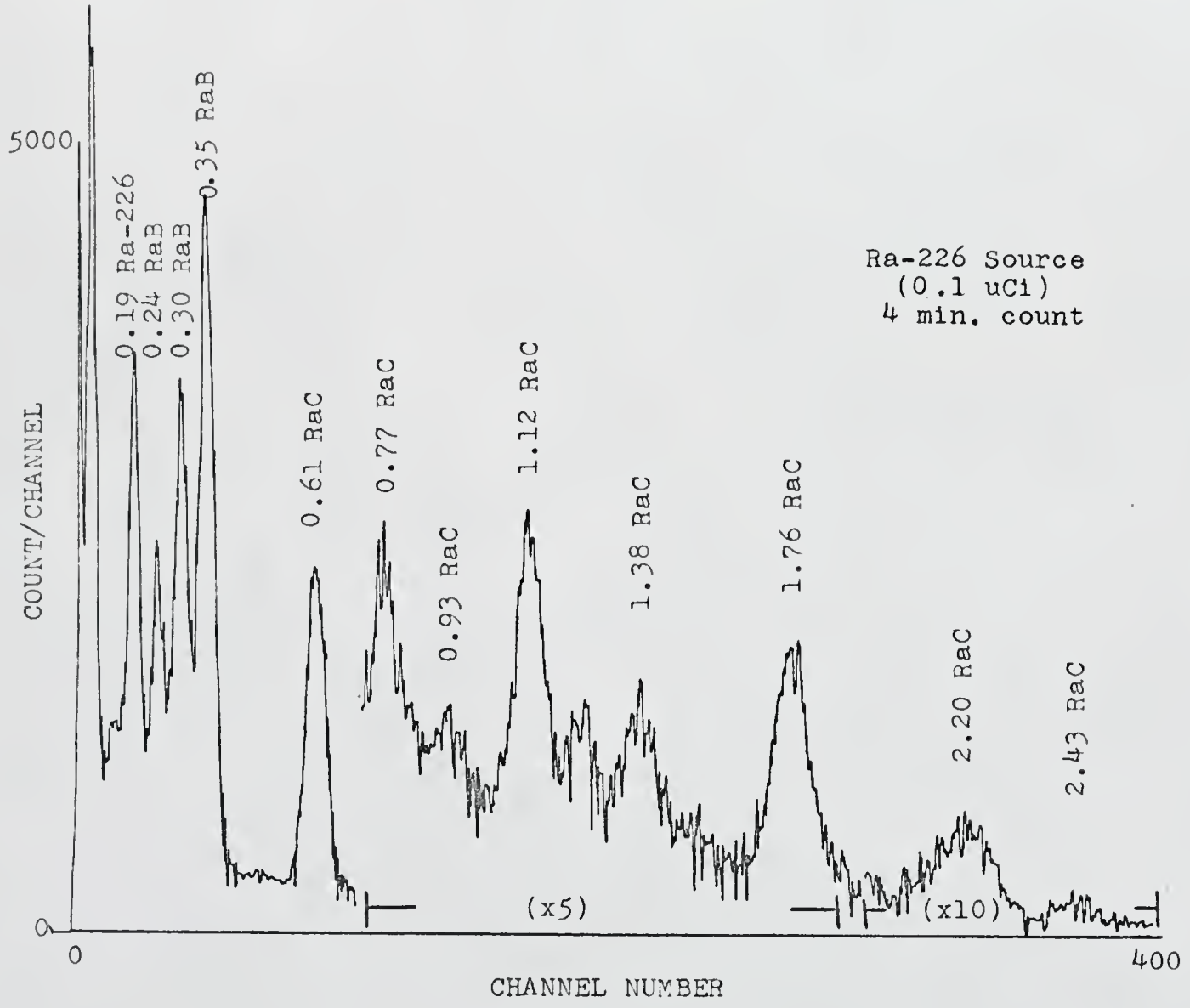

Fig. 27. Complex NaI(Tl) spectrum.

standardize comparison. It can be seen that both the poor resolution and the addition of Compton continuum raise the minimum detectable activity in the low-energy range of the spectrum to approximately the activity of the high-energy photopeak radionuclides in the spectrum.

CHAPTER VI

Ge(Li) SYSTEM PERFORMANCE

In this chapter the performance of the standard Ge(Li) system is presented. System background, efficiency, minimum detectable activity, peak-to-Compton ratios, and complex spectrum resolution are tabulated.

A. System Background

In order to show both shielding benefits and shielding problems, a 24-hour unshielded background in the low-level counting room was taken with the Ge(Li) spectrometer. The spectrum given in Figure 28 shows a complex collection of photopeaks from both radon and thoron daughters. Background with 2.5 inches of mercury shielding, given in Figure 29, shows a considerable reduction across the spectrum with fewer photopeaks being discernible. The background still contains small radon daughter photopeaks mainly due to their presence in the large air space between the shielding and the detector. Background with this air space filled with liquid is discussed in Chapter VIII. Integrated background, both shielded and unshielded, is tabulated in Table 3 for several energy ranges.

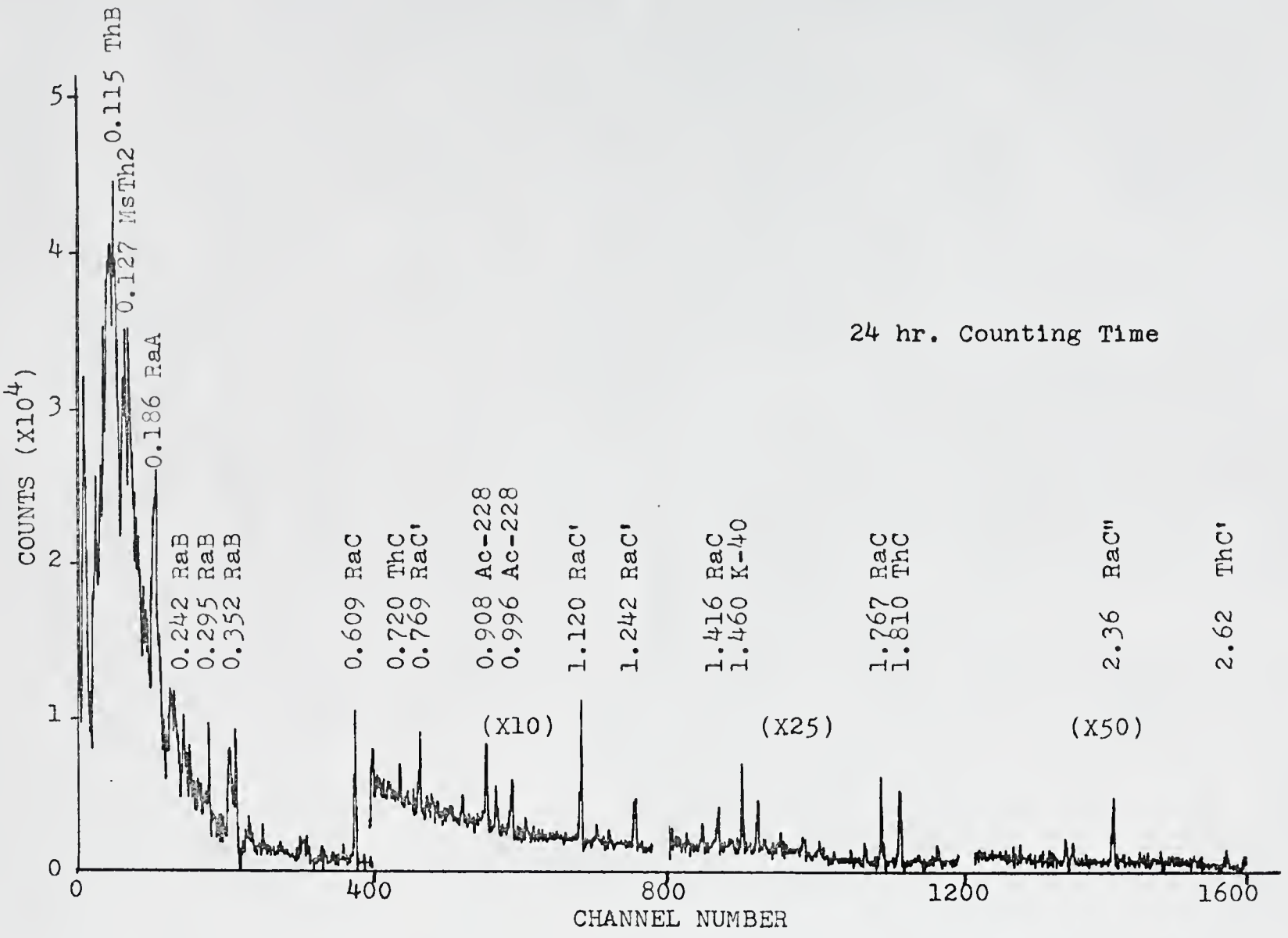

Fig. 28. Counting room background.

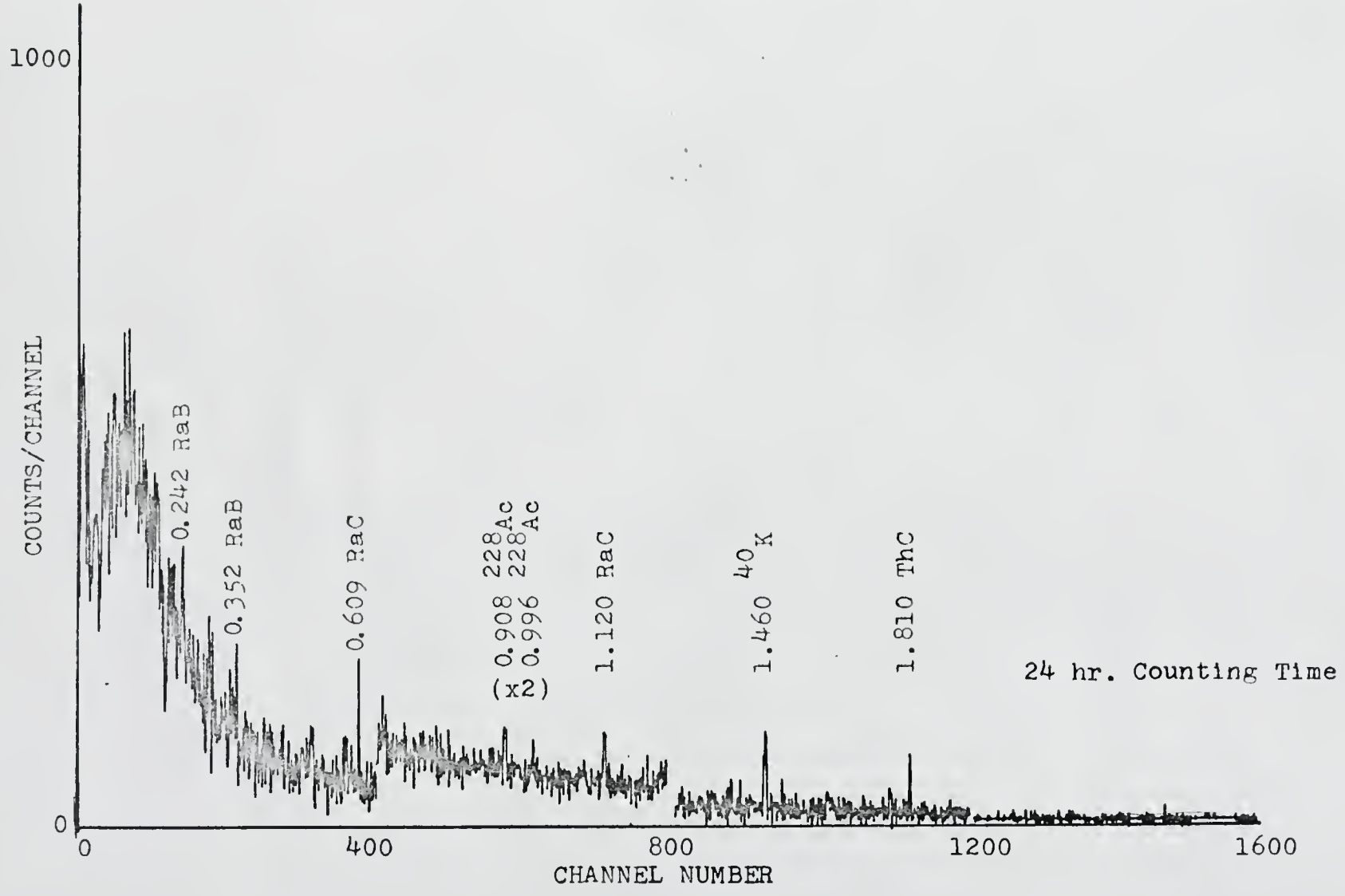

Fig.29. Ge(Li) background with Hg shielding.

Table 3

Background Count Rate for the Ge(Li) System

Energy Range (keV)	Count Rate-cpm	
	Unshielded	2.5 in. Hg
70-200	1108	87
200-400	221	12
400-600	77	5
600-800	37	3
800-1000	27	2
1000-1500	38	3
1500-2000	15	1.3
2000-2500	7	0.7
70-2500	1531	114
200-2500	423	27
400-2500	202	15
1000-2500	61	5

B. Efficiency

The efficiency of Ge(Li) detectors is much less than that of NaI(Tl) detectors, ranging up to only 20% as efficient as 3x3 NaI(Tl) for ^{60}Co. The Ge(Li) detector used for this system was rated only 6% efficient (re 3x3 inch NaI(Tl) - ^{60}Co source). To allow activity calibration, an absolute efficiency for the Ge(Li) detector was determined for both calibrated point sources and for 1.5-litre sources (configuration of the active-sample container). Both are plotted in Figure 30, and essentially are straight lines on log-log paper with efficiency increasing at decreasing energies. The 1.5-litre configuration is again about 1/3 as efficient as that for the point source (1 cm distance) due to the difference in geometry factors for the two configurations.

C. Minimum Detectable Activity

The theoretical minimum detectable activity was determined as in Chapter V. For a 40-minute count, it equals in dpm

$$2\sqrt{\frac{2 \times \text{Background count (under photopeak)}}{40 \times \text{efficiency (of photopeak)}}}$$

Figure 31 shows the theoretical minimum detectable photopeak activity for the 34 cc Ge(Li) detector with 2.5 inches of mercury shielding and shows a slight increasing sensitivity at lower energies. In addition, the theoretical minimum detectable activity in pCi and theoretical minimum detectable concentration in pCi/l are tabulated in Table 4 for several radioisotopes of interest.

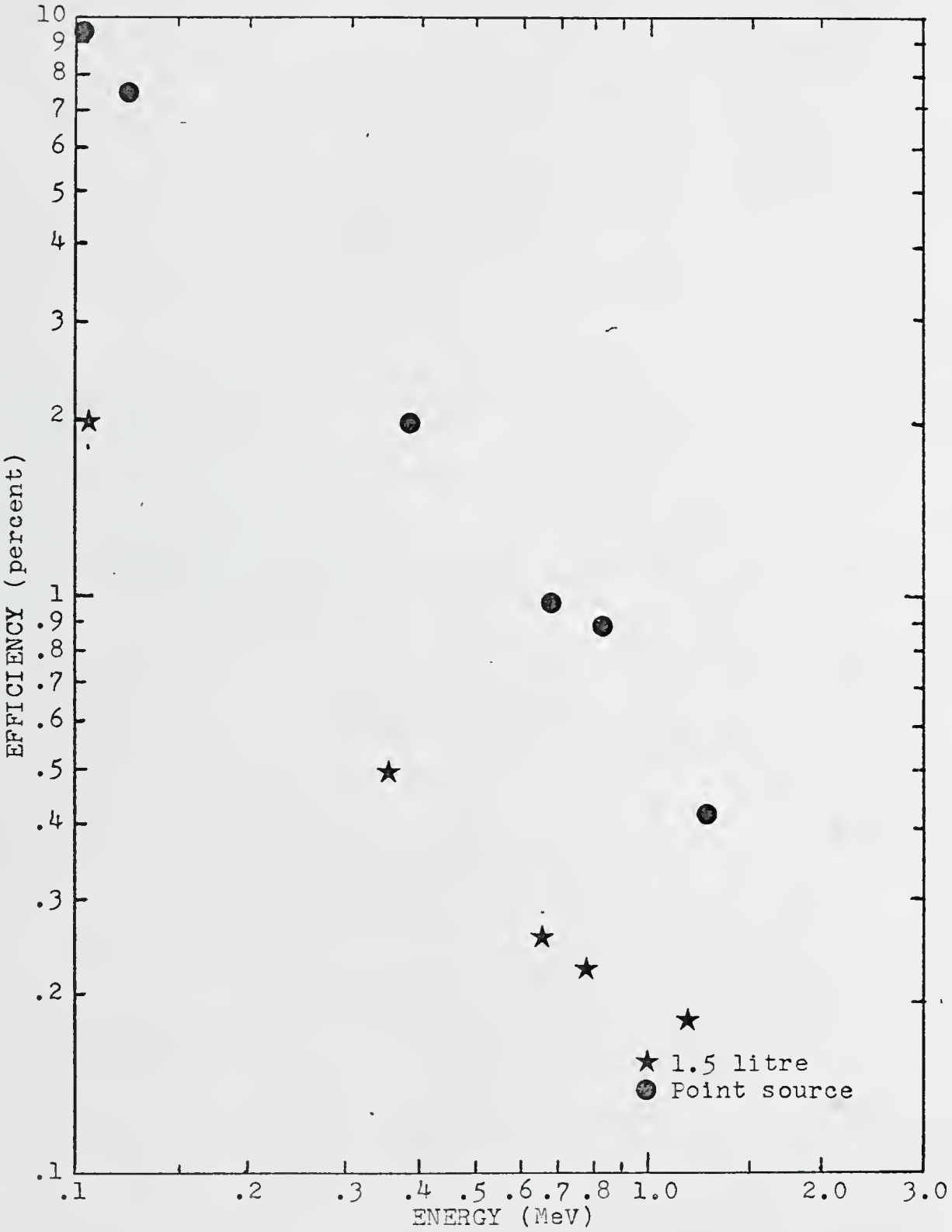

Fig.30. Ge(Li) photopeak efficiency.

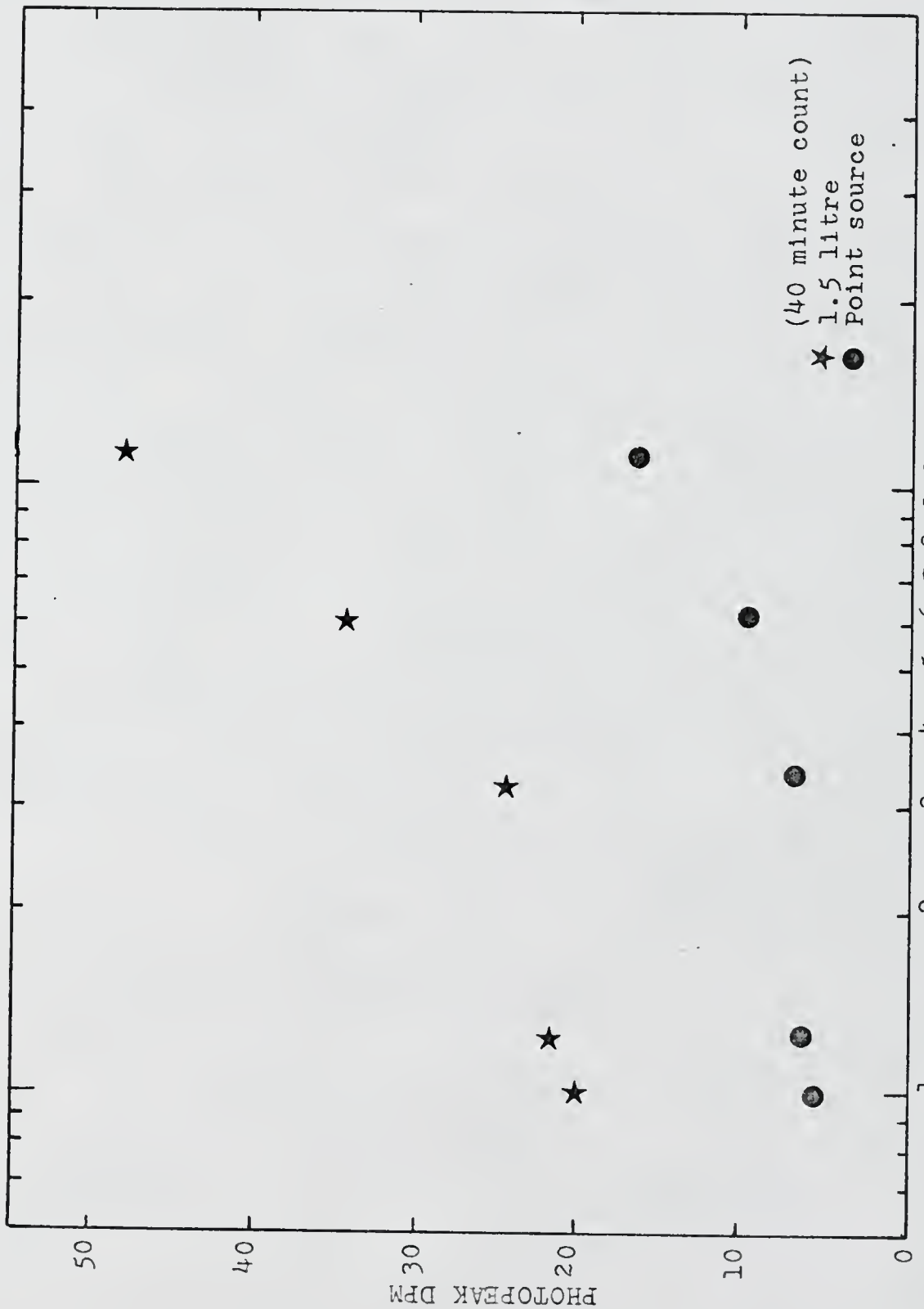

Fig. 31. Minimum theoretical detectable activity for Ge(Li).

Table 4

Theoretical Minimum Detectable Activities for the Ge(Li) System

Standard		Minimum Detectable Activity, pCi (point source)		Minimum Detectable Activity, pCi (1.5 l)		Minimum Detectable Concentration, pCi/l (1.5 l)	
	(MeV)	24 hr.	40 min.	24 hr.	40 min.	24 hr.	40 min.
^{40}K	(1.460)	45	60	130	180	85	120
^{226}Ra	(0.352)	10	10	34	34	22	22
^{232}Th	(0.908)	3.7	22	11	66	7.3	44
^{137}Cs	(0.662)	0.9	5.3	3.0	18	2.0	12
^{95}Zr	(0.724)	1.5	9.0	4.7	28	3.1	18.6
^{106}Ru	(0.622)	6.0	36	20	120	13	80
^{131}I	(0.364)	0.7	4.3	2.9	17	1.9	11
^{144}Ce	(0.134)	4.5	27	23	136	15	90
^{65}An	(1.115)	3.3	20	10	60	6.7	40
^{54}Mn	(0.835)	1.1	7	3.3	20	2.3	14

D. Peak-to-Compton Ratio

Due to the high resolution of Ge(Li) detectors, their peak-to-Compton ratios are typically several times larger than those for NaI(Tl). The peak-to-Compton ratio for several radionuclide photopeaks was determined for the 34 cc Ge(Li) detector and is plotted in Figure 32. Both point-source data and 1.5-litre data are shown. Again it can be seen that the peak-to-Compton ratios for the large-volume sources are much less than for the point sources, being particularly worse at low energies.

E. Complex Spectra

To demonstrate the usefulness of the Ge(Li) detector for analysis of complex spectra, the complex spectrum for ^{226}Ra is shown in Figure 33. It can be seen that the Compton continuum contributes most to the increase in the practical minimum detectable activity and not the photopeaks which are now only 3 keV wide. Thus the minimum detectable activity at low energies is comparable to the Compton continuum and can be predicted by the cumulative activity of all radionuclide photopeaks of higher energies divided by the average peak-to-Compton ratio.

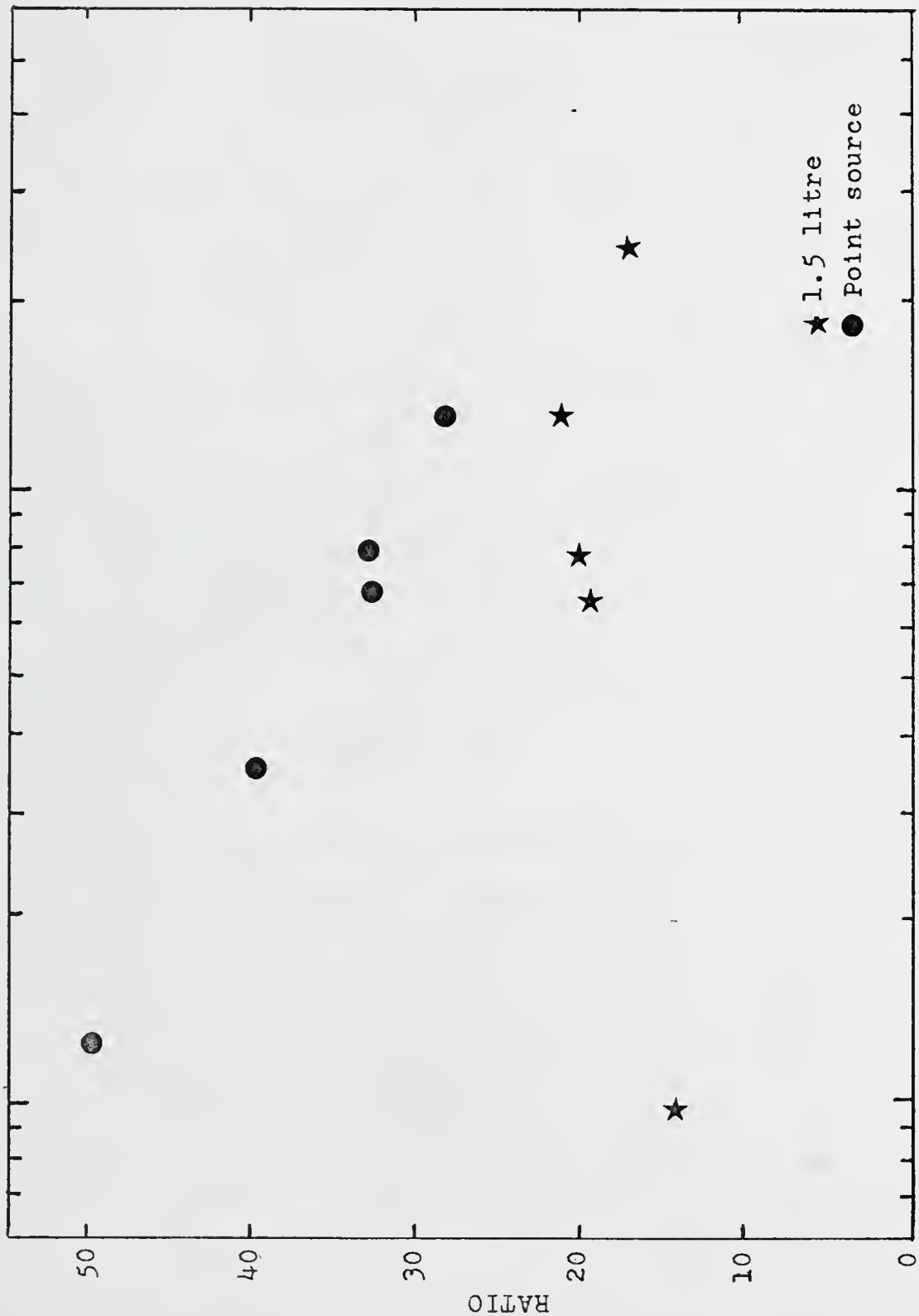

Fig.32. Peak to Compton ratio for Ge(Li).

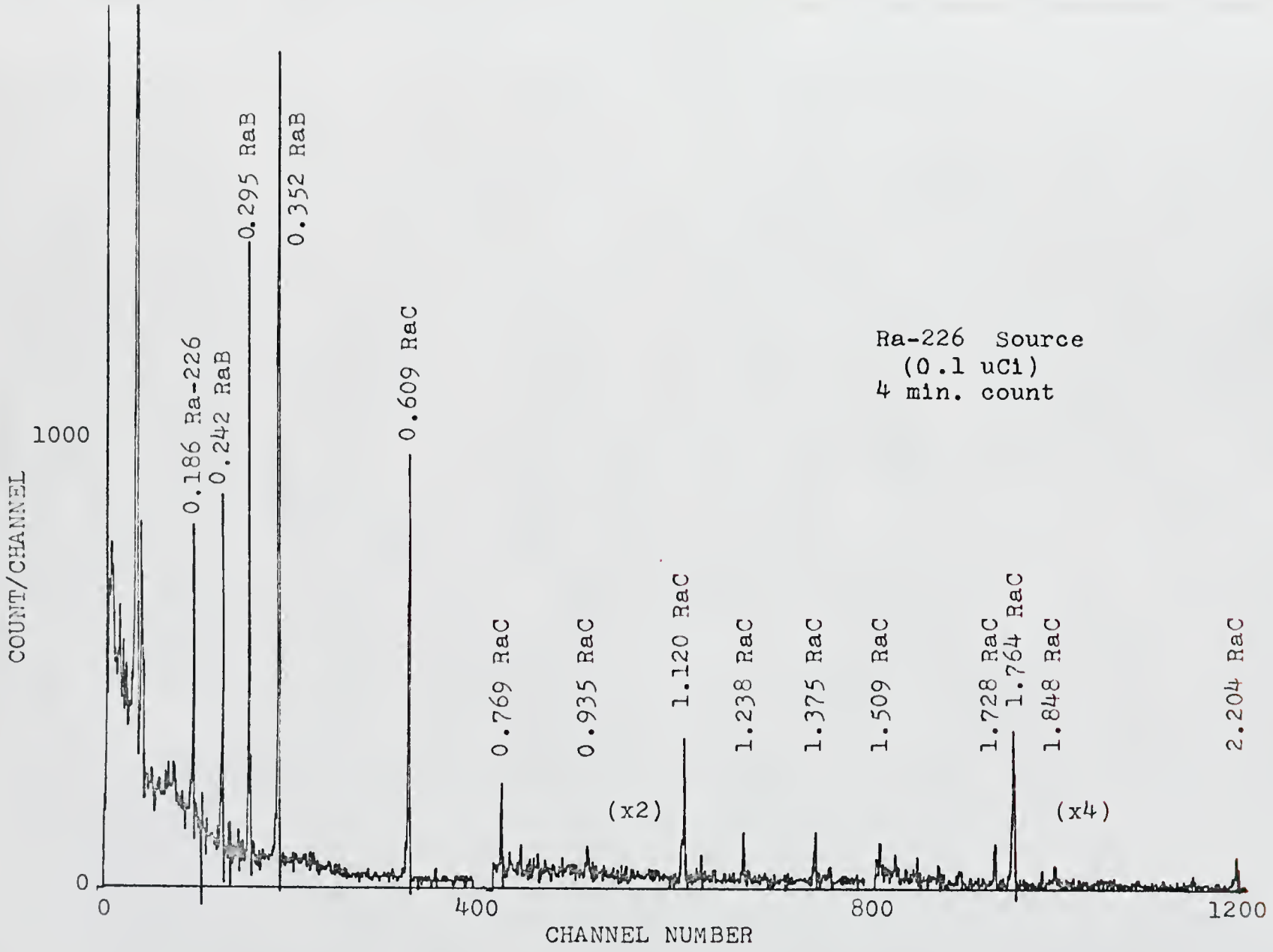

Fig.33. Unguarded complex Ge(Li) spectrum.

CHAPTER VII

GUARDED SYSTEM PERFORMANCE

In this chapter the performance of the anticoincidence guarded Ge(Li) spectrometer is presented. As in Chapter VI, the system background, peak-to-Compton ratio, and minimum detectable activity are specified. In addition, factors determining guard-detector efficiency and reduction in photopeak efficiency are explained.

A. System Background

In the guarded mode, gamma-ray spectrum background is reduced due to the additional passive shielding of the liquid scintillator, the removal of Compton scattered events in the guard which are detected in the Ge(Li) crystal, and the removal of Compton scattered events in the Ge(Li) crystal which are detected in the guard.

Figure 34 shows a 24-hour background spectrum with the guard off. Comparison of this with Figure 29 (mercury shielded background) shows a decrease in the background at high energies but an increase in the background at very low energies (200 keV) when the liquid scintillator is present. This difference is due to additional energy removal in Compton scatter by the low-mass-number liquid, thus reducing the

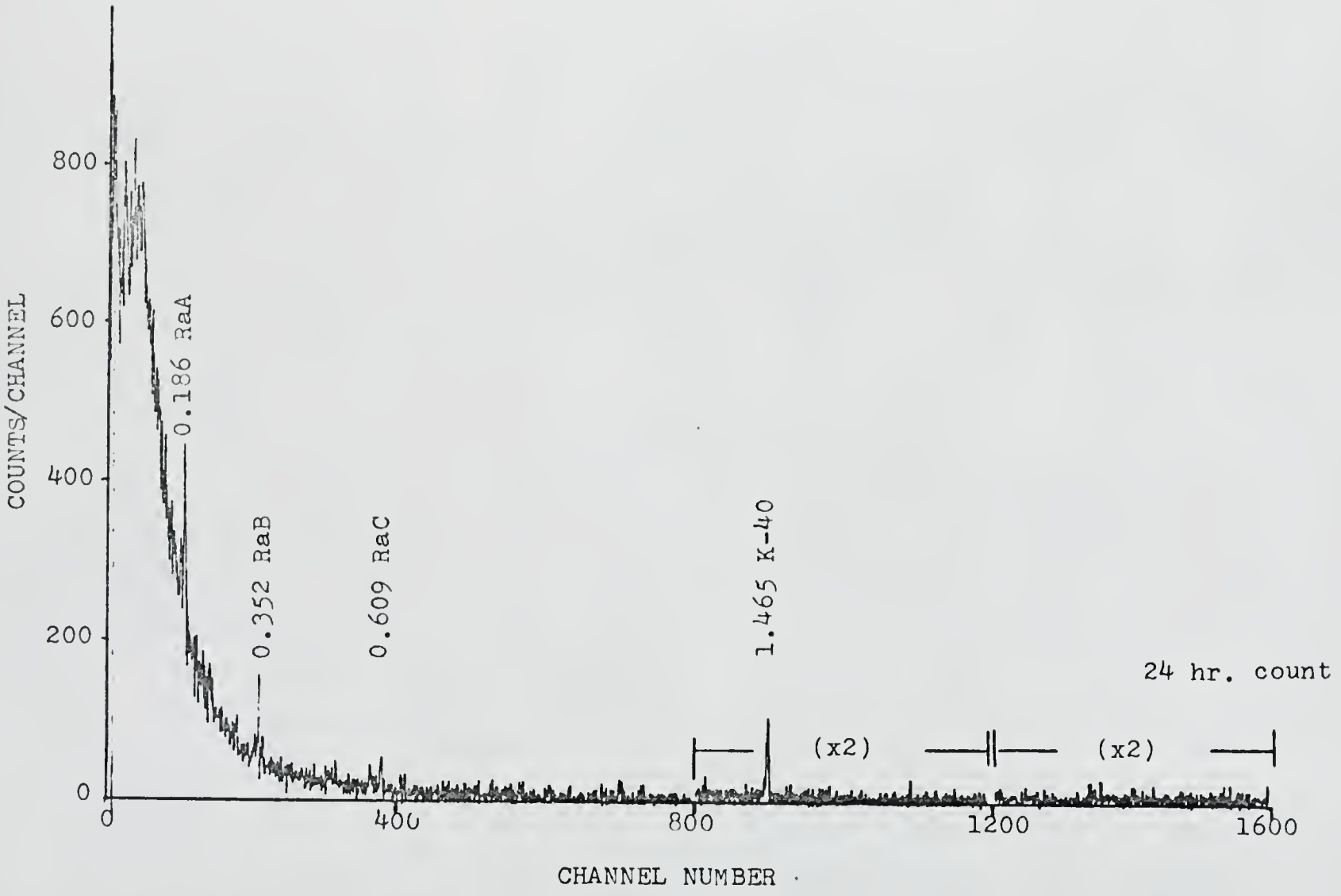

Fig.34. Unguarded Ge(Li) background.

energy of the background gamma photons. Figure 35 shows the effect of anticoincidence guarding on the background spectrum. A comparison of background is tabulated in Table 5 and in general shows a guarded background reduction of approximately 6 times over the unguarded for all energies. The photopeaks remaining in the spectrum are due to the unshielded 3% solid angle geometry of the sample port and the activity within the detector system. The ^{40}K photopeak in the spectrum corresponds to a point-source activity of 45 pCi and the ^{226}Ra daughter photopeaks correspond to an activity of 10 pCi. Thus, this sets the lower limit on the detectable activity for these two radionuclides.

B. Guard Detector Efficiency

The main purpose of the guard is to detect Ge(Li) crystal scattered gamma photons. Interaction in the guard detector may deposit only part of the photon's energy. Thus for the highest detection efficiency, the threshold of detection for the guard should be as low as practical. This was determined by allowing a photopeak reduction of 10% due to unrelated chance pulse counts in the guard detector system and corresponds to a background count rate of 2,400,000 cpm. Appendix B gives the background spectrum of the guard system and shows the threshold corresponding to 2,400,000 cpm to be deep in the noise region of the photomultiplier tube.

With the guard threshold set at this point (approximately 15 keV) its efficiency was determined and plotted in Figure 36.

Fig. 35. Guarded Ge(Li) background.

Table 5

Background Count Rate for the Guarded Ge(Li) System

Energy Range (keV)	Count Rate - cpm 2.5 in. Hg Unshielded	Guarded
70-200	1108	87	15
200-400	221	12	2.7
400-600	77	5.3	1.0
600-800	37	3.0	0.45
800-1000	27	2.0	0.34
1000-1500	38	3.0	0.54
1500-2000	15	1.3	0.17
2000-2500	7.3	0.7	0.13
70-2500	1531	114	21
200-2500	423	27	5.3
400-2500	202	15	2.6
1000-2500	61	5.0	0.84

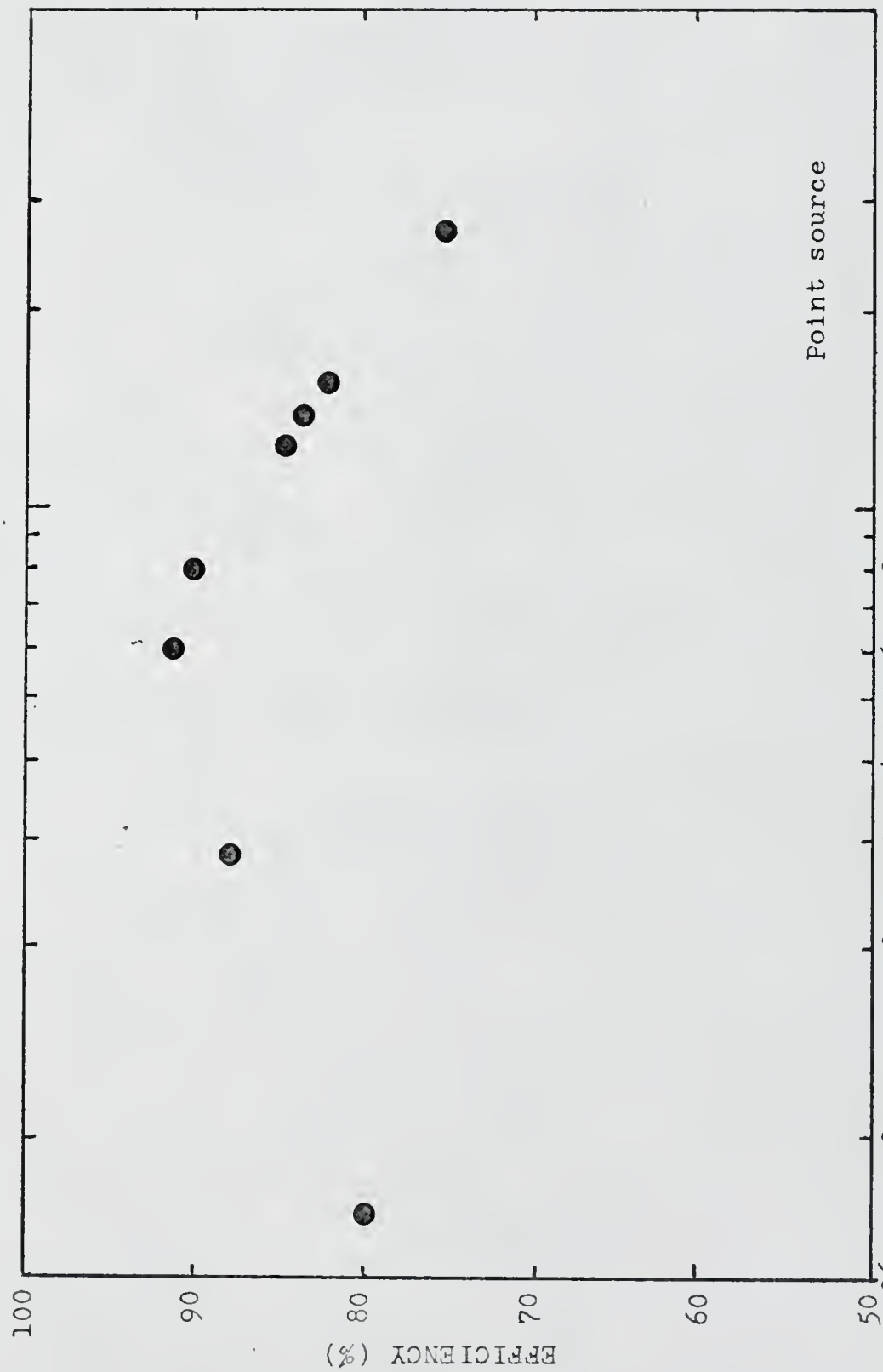

Fig. 36. Guard-detector efficiency.

Because of the high background count, the efficiency was calculated by first measuring the photopeak reduction for one photopeak of a cascaded decay (2 photons) radionuclide (e.g. ^{24}Na, ^{60}Co, ^{133}Ba, and ^{134}Cs). After deadtime correction the ratio of the guarded to unguarded count for one photopeak gives the undetected fraction of the other gamma photon (^{133}Ba and ^{134}Cs having complex cascade decay required some approximations).

The plot of efficiency shows a loss of efficiency with decreasing energy below 500 keV and a loss of efficiency with increasing energy above 700 keV. Losses in efficiency can be explained with a 3% energy independent geometry loss by the sample port, low energy loss due to a 15 keV detection threshold (loss $\simeq$ E(keV)/15, see Appendix C) and the decrease in attenuation coefficient for high-energy gamma photons.

The reduction in Compton continuum is directly dependent upon the guard detector efficiency except at low energies where the Ge(Li) detector mounts and casing absorb some of the crystal scattered gamma photons.

C. Photopeak Reduction

Since for highest Compton suppression the guard detector threshold must be set as low as possible (deep in the noise region), an acceptable photopeak reduction was arbitrarily chosen as 10%. A 10% reduction while not substantially affecting counting statistics or efficiency does greatly increase the allowable guard detector background and thus allows significant lowering of the threshold setting.

The guard detector background count rate which gives 10% chance coincidence is 40,000 counts per second.

D. Minimum Detectable Activity

The minimum theoretical detectable activity was determined as in Chapter VI. However, due to reduction in background count for the guarded spectrum, 40-minute counts gave backgrounds below 1 count per channel. When this occurred, Poisson statistics were used in determination of the minimum detectable activity (3 is the minimum photopeak count for 95% confidence in the extreme of zero bkg.).[18] Figure 37 gives the calculated minimum theoretical detectable activity in terms of gamma photopeak decay for both point sources and 1.5-litre sources as a function of energy. In addition Table 6 gives the theoretical minimum detectable activity, and minimum detectable concentration for several radionuclides for both 40 minute and 24 hour counts.

E. Peak-to-Compton Ratio

The peak-to-Compton ratios for the anticoincidence guarded 34 cc. Ge(Li) was determined as in Chapter VI for the unguarded Ge(Li). The guarded peak-to-Compton edge ratio was 9 times higher for ^{65}Zn and 8 times higher for ^{137}Cs. Figure 38 shows the guarded peak-to-Compton ratios as a function of energy for both point sources and 1.5-litre water sources. The peak-to-Compton ratio can be seen to be quite constant above 200 keV. The low-energy fall-off is

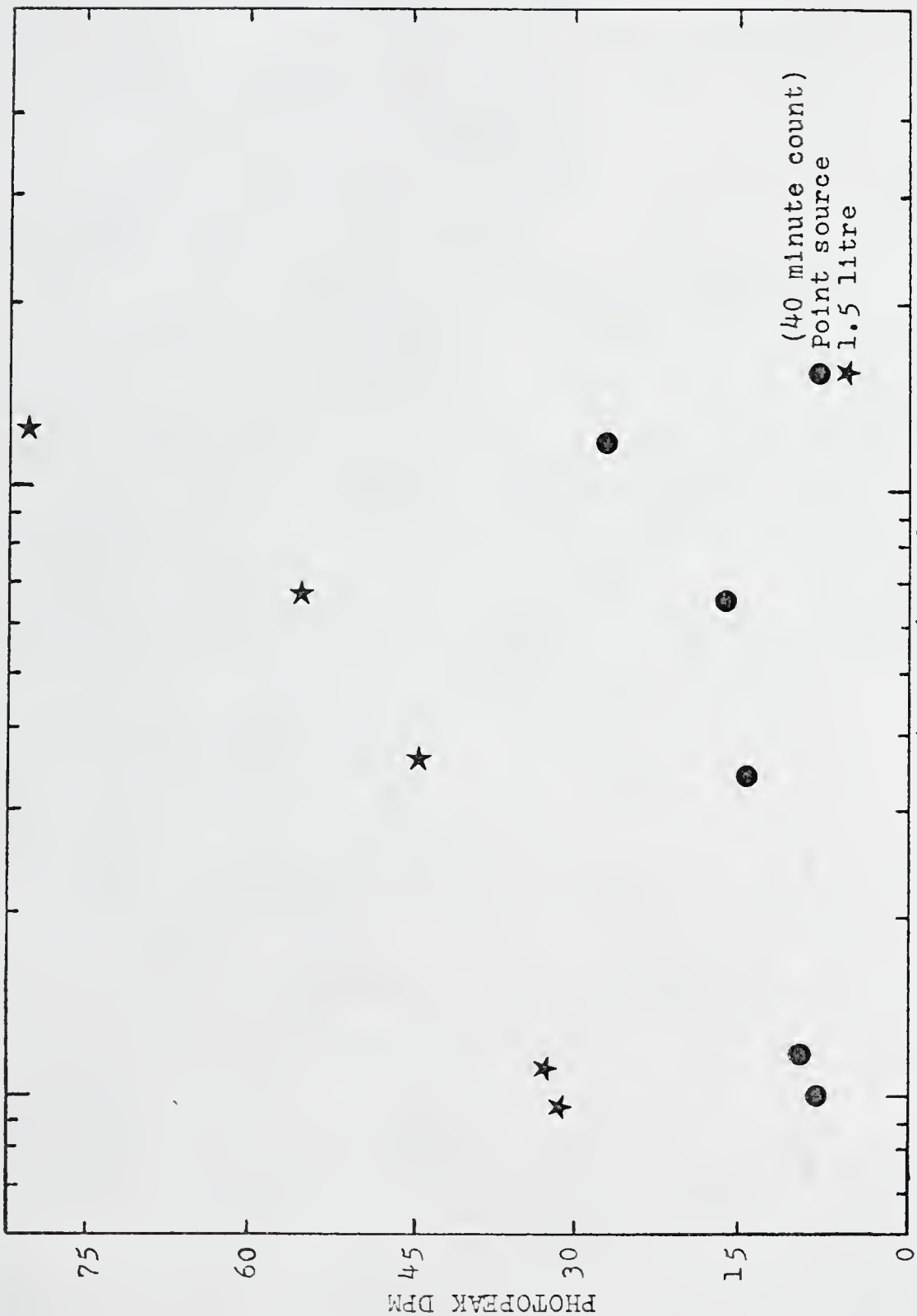

Fig. 37. Minimum theoretical detectable activity for guarded Ge(Li).

Table 6

Theoretical Minimum Detectable Activities for the Guarded Ge(Li) System

Standard	(MeV)	Minimum Detectable Activity, pCi (point source)		Minimum Detectable Activity, pCi (1.5 l)		Minimum Detectable Concentration, pCi/ l (1.5 l)	
		24 hr.	40 min.	24 hr.	40 min.	24 hr.	40 min.
^{40}K	(1.460)	45*	45*	130*	130*	90*	90*
^{226}Ra	(0.352)	10*	10*	34*	34*	22*	22*
^{232}Th	(0.908)	1.5	14	4.5	43	3.0	29
^{137}Cs	(0.662)	0.4	4.4	1.3	15	0.9	10
^{95}Zr	(0.724)	0.6	6	2.4	21	1.6	14
^{106}Ru	(0.622)	4.0	32	16	120	11	84
^{131}I	(0.364)	0.6	3.5	2.2	13	1.4	8.8
^{144}Ce	(0.134)	1.6	10	6.6	40	4.4	27
^{65}Zn	(1.115)	0.8	6.0	2.9	22	2.0	14
^{54}Mn	(0.835)	0.5	3	1.2	10	0.8	6.7

*Background levels

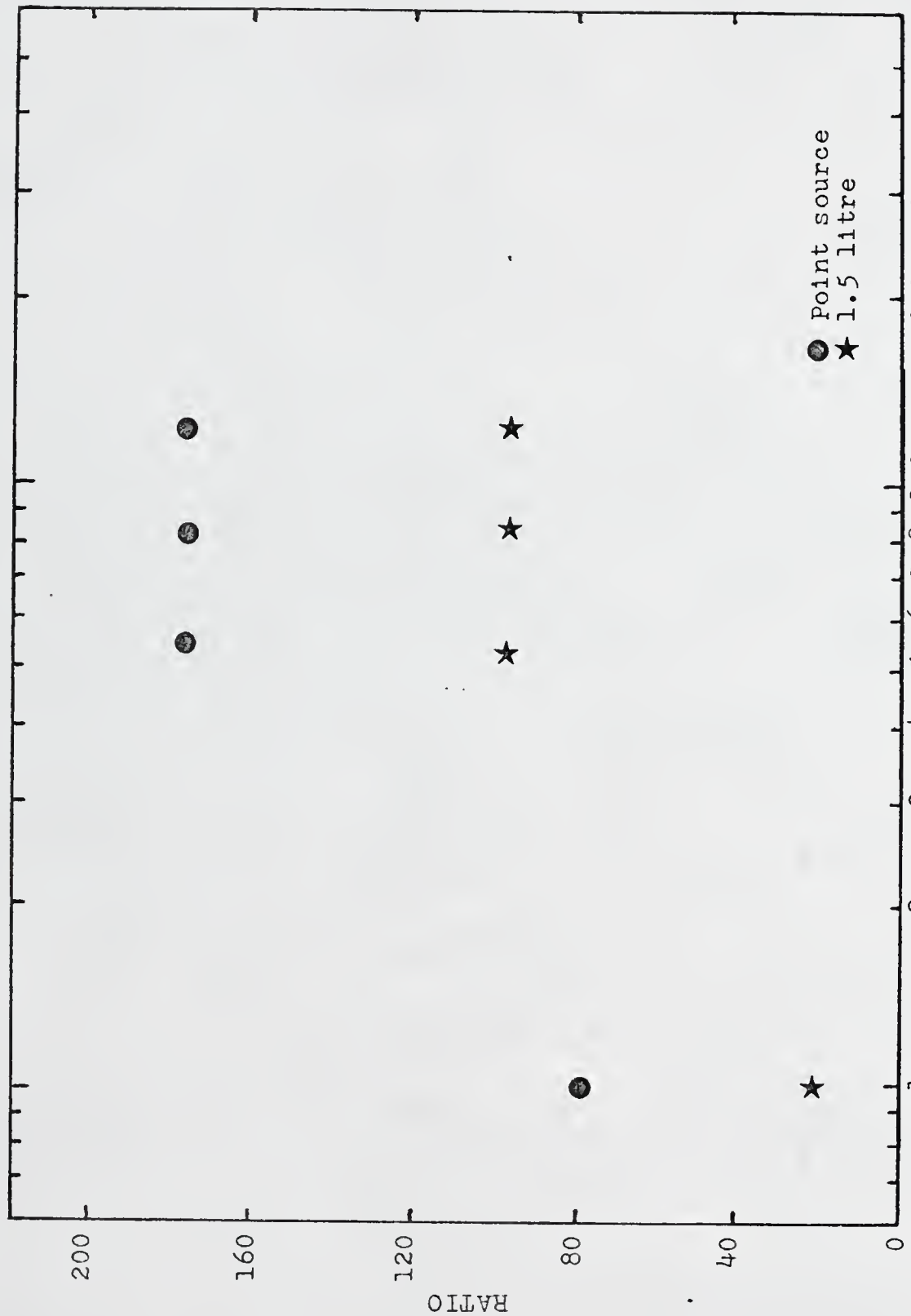

Fig. 38. Peak-to-Compton ratio for guarded Ge(Li).

due to both loss of efficiency in the guard system and absorption in the Ge(Li) crystal casing.

F. Complex Spectrum

The usefulness of the anticoincidence guarded Ge(Li) detector for a complex spectrum is shown in Figure 39. Radium^{-226} was used to show both the separation of the many photopeaks and the small amount of Compton continuum present. It can be seen that the minimum detectable activity doesn't significantly increase for complex spectra.

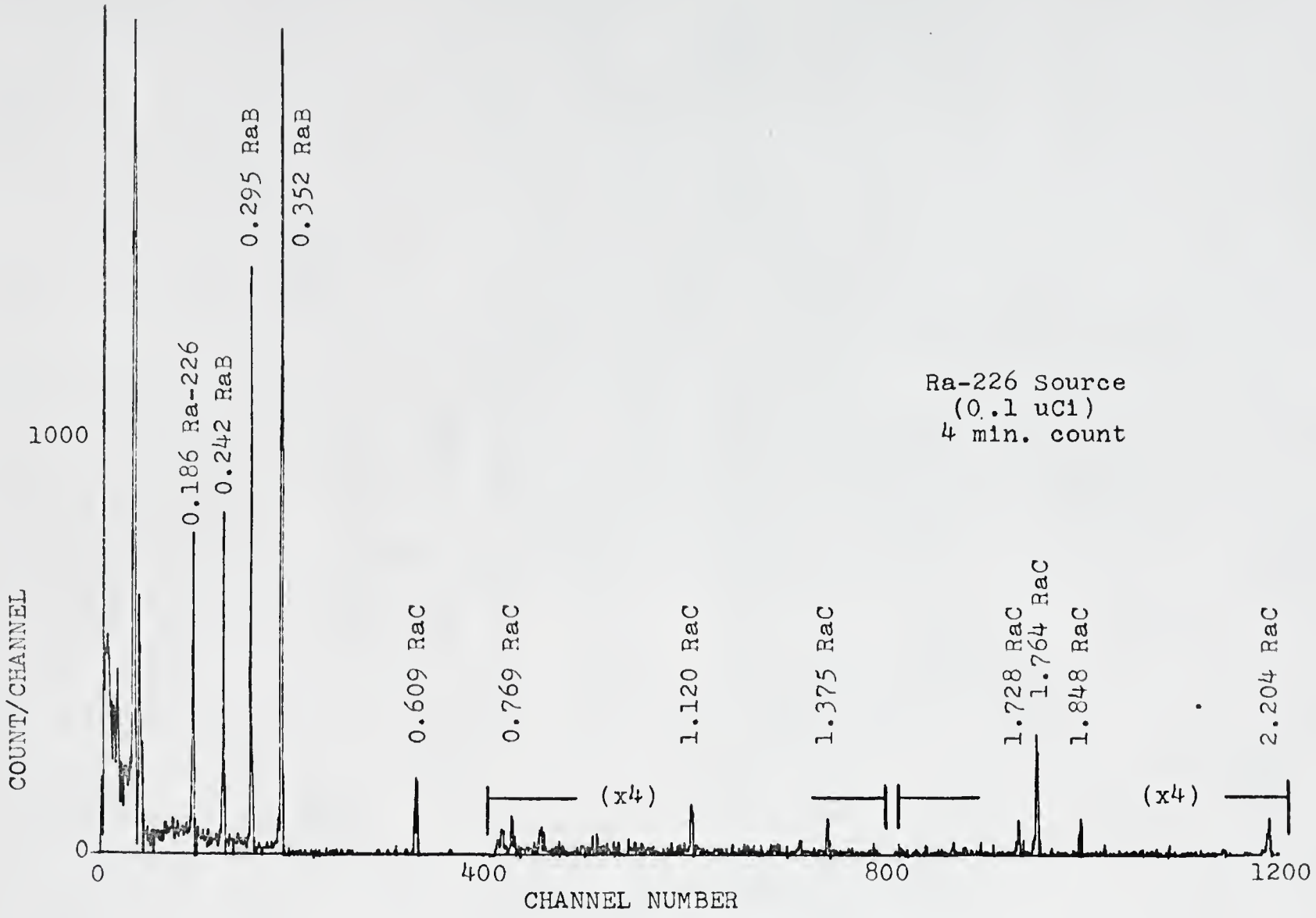

Fig.39. Guarded complex Ge(Li) spectrum.

CHAPTER VIII

ACTIVE-SAMPLE SYSTEM

In this chapter the performance of the anticoincidence guarded system with active-sample guarding is presented. Since the active-sample technique uses the same geometry as the 1.5 litre samples reported in Chapter VII, only differences in performance are presented. These include efficiency, peak-to-Compton ratios, minimum detectable activity, and separation of decay modes.

A. Efficiency

The efficiency of the active sample geometry is the same as that reported in Figure 30 for the 1.5-litre samples. Again, as with the standard anticoincidence guarding, random coincidence reduces the photopeak count. The guard again is set for a 40,000 count per second background while the sample detector is set for a 30,000 count per second background. The combined guarded background yields a 15% photopeak reduction as compared to a 10% reduction with guard shielding only.

B. Minimum Detectable Activity

The single radionuclide minimum detectable activity for the active sample technique is improved only at energies below

500 keV and then by only about 15% due to a 30% improvement in background suppression. The minimum theoretical detectable activities, determined as in Chapter V, are plotted in Figure 40 as a function of photopeak energy. In addition, the minimum theoretical detectable activities and concentrations for several radionuclides are tabulated in Table 7 for both 40-minute counts and 24-hour counts. The increase in the minimum detectable concentration is due to the required dilution of the sample with liquid scintillator.

C. Peak-to-Compton Ratio

The peak-to-Compton ratio for the active-sample technique is shown in Figure 41 as a function of energy. The peak-to-Compton ratios are restored to 95% of their point-source ratios at high energies but only restored to 50% at energies below 100 keV. However improvement in peak-to-Compton ratio is still approximately 2-fold across the spectrum.

D. Separation of Decay Modes

In addition to improving peak-to-Compton ratio, the active-sample technique removes all short-lived β^+ and β^- decay excited-daughter radiations from the spectrum. By requiring coincidence between the sample-detector and the Ge(Li) detector, these short-lived states can be left in the spectrum while removing all electron capture and metastable states. Figure 42 shows this division of states; however to show the effect with available radionuclides (positron

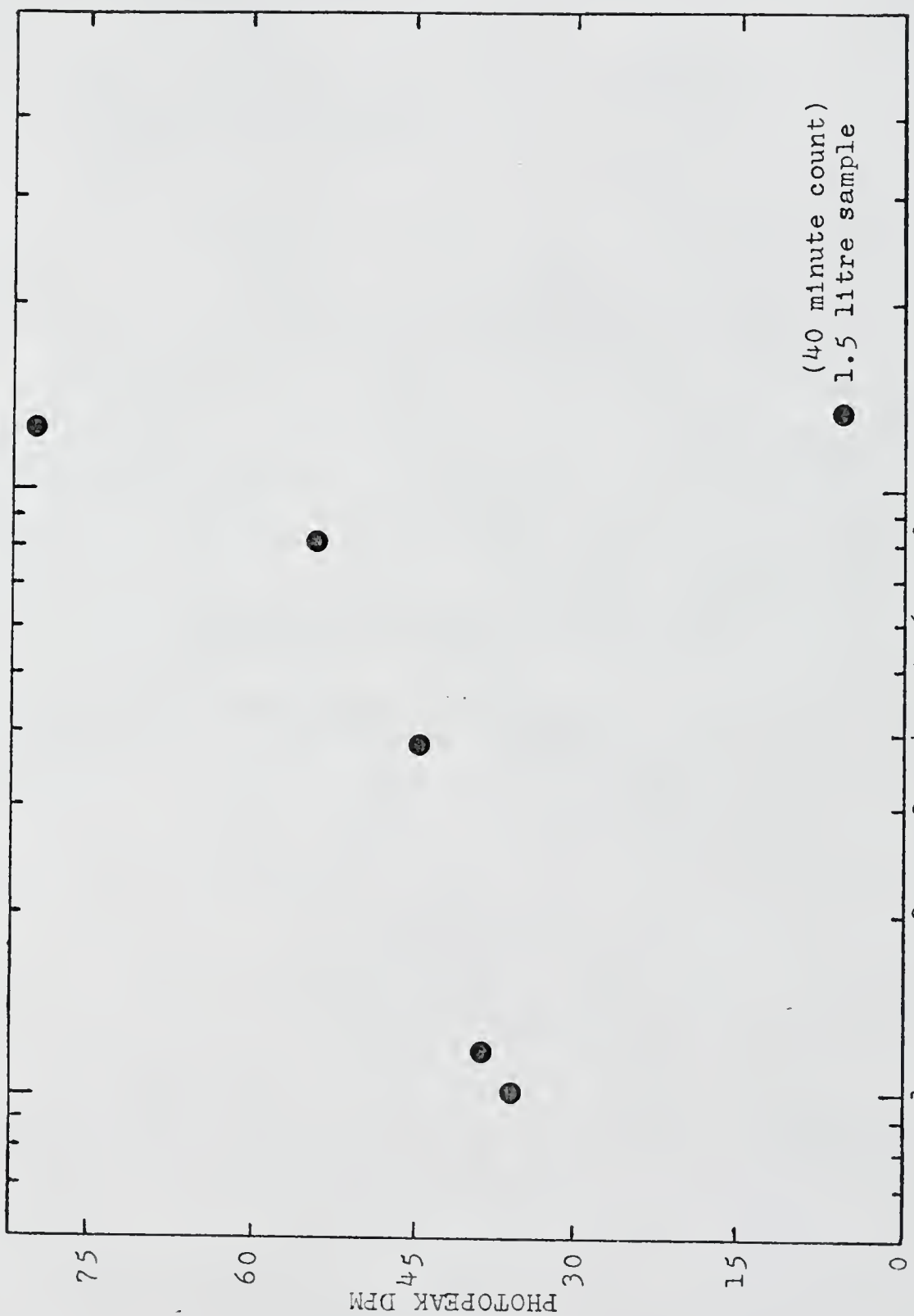

Fig. 40. Active-sample minimum theoretical detectable activity for Ge(Li).

Table 7

Theoretical Minimum Detectable Activities for Active Sample Ge(Li) System

Standard (MeV)		Minimum Detectable Activity, pCi (1.5 l)		Minimum Detectable Concentration, pCi/l (1.5 l)	
		24 hr.	40 min.	24 hr.	40 min.
^{40}K	(1.460)	130*	130*	330*	330*
^{226}Ra	(0.357)	34*	34*	85*	85*
^{137}Cs	(0.662)	1.3	15	3.2	38
^{232}Th	(0.908)	4.5	40	9.2	100
^{95}Zr	(0.724)	2.4	21	6.0	53
^{106}Ru	(0.622)	16	120	40	300
^{131}I	(0.364)	2.2	13	5.5	32
^{144}Ce	(0.134)	6.6	40	16	100
^{65}Zn	(1.115)	2.9	22	7.2	54
^{54}Mn	(0.835)	1.2	10	3.0	25

*Background levels

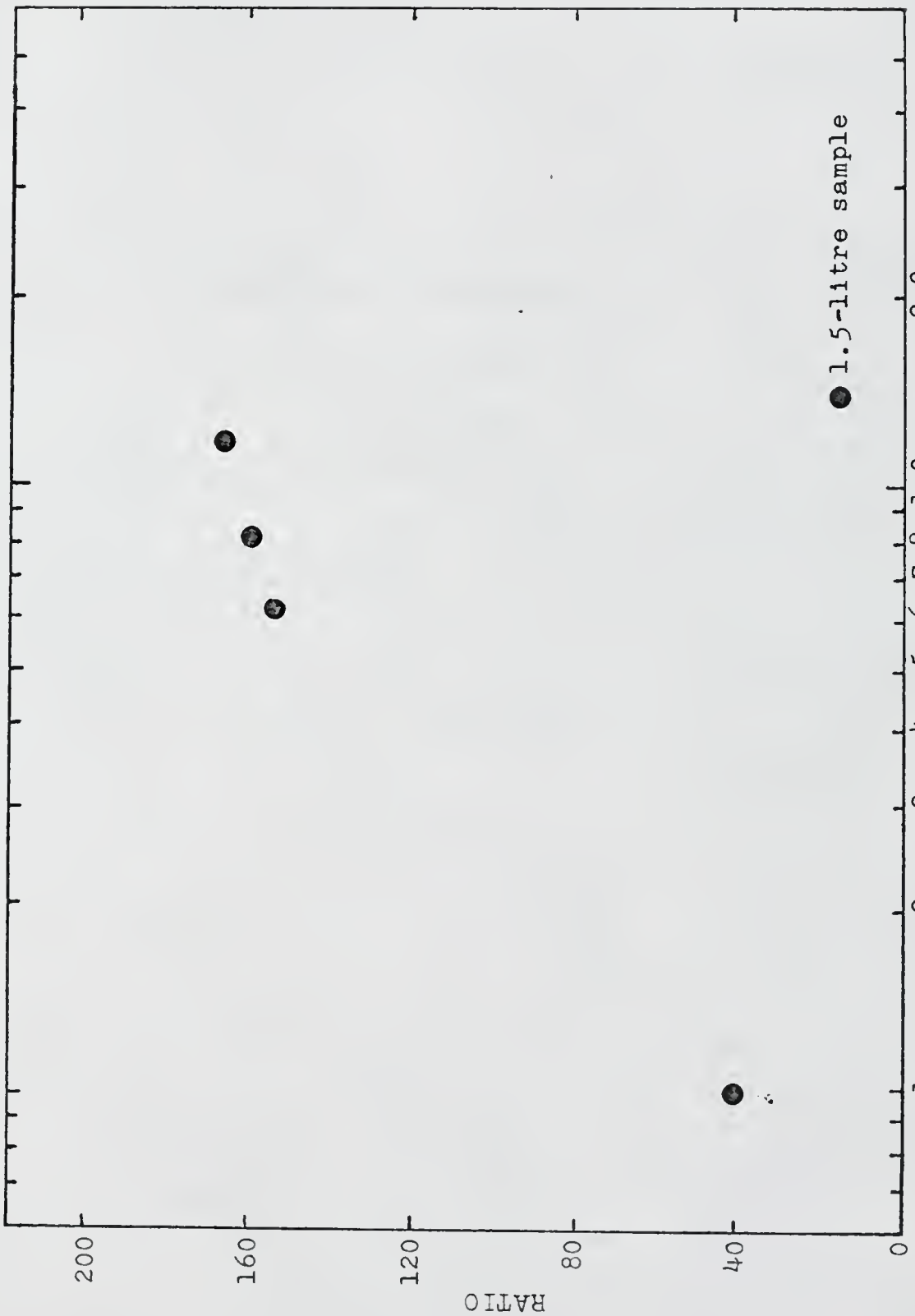

Fig. 41. Active-sample peak-to-Compton ratio.

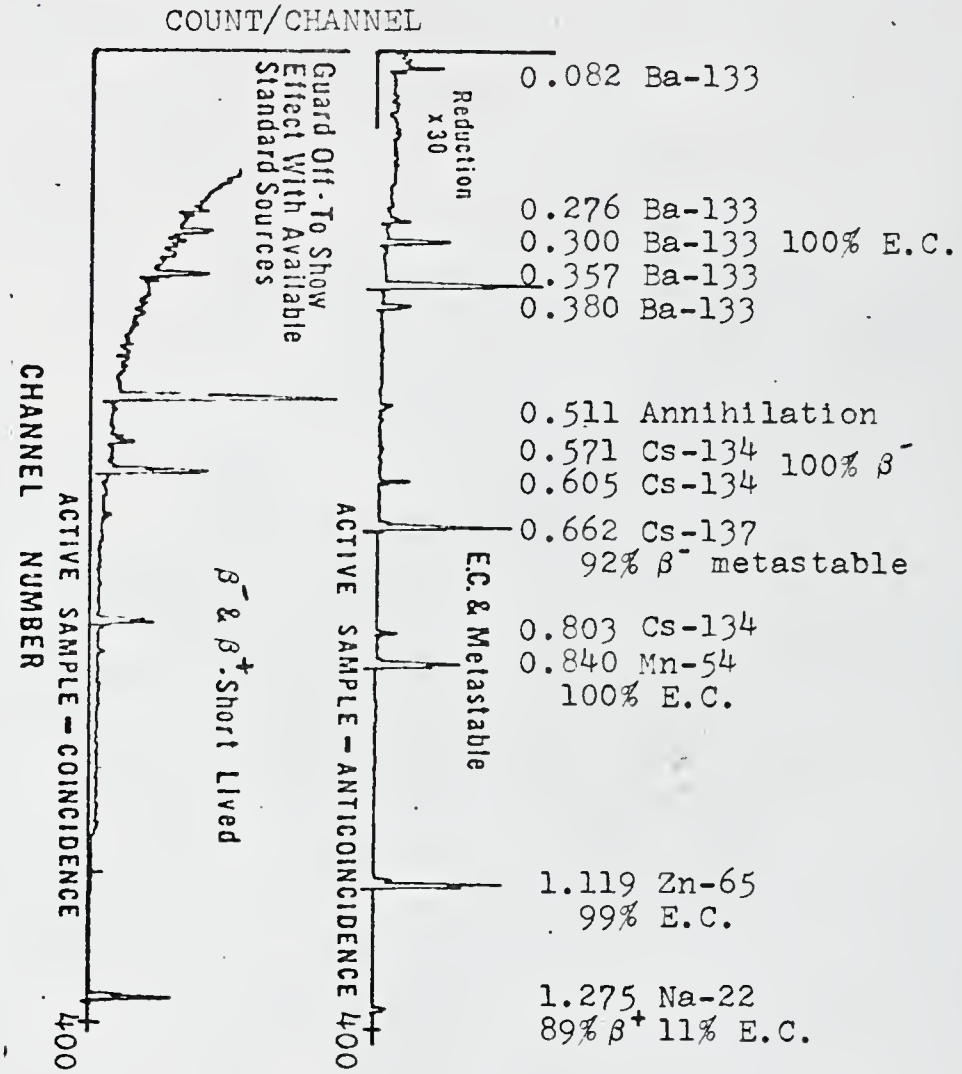

Fig. 42. Separation of decay modes.

and cascade decay), the guard was disconnected for the coincidence mode.

CHAPTER IX

COMPARISON OF SYSTEMS ON ENVIRONMENTAL SAMPLES

In this chapter the spectra produced with the various systems described previously are compared for their ability to identify radionuclides. Included are prepared samples and actual environmental samples in various forms.

A. Standard Samples

To show the advantages of the active-sample technique for water samples, two standards were prepared. The first, containing only ^{65}Zn, was used to produce the spectra in Figure 43. The upper two spectra are from a guarded and unguarded point source; the guarded spectrum shows a Compton edge suppression of a factor of 8. The remaining three spectra are for a 1.5 litre source. The normal guarded spectrum shows a Compton tail suppression of a factor of 7 while the active-sample guarded spectrum shows a suppression of a factor of 23. This additional Compton tail suppression would permit recognition of a much smaller photopeak within this energy region.

The other standard contained 6 radionuclides having different decay modes. The spectra are shown in Figure 44. In addition to the suppression of annihilation radiation,

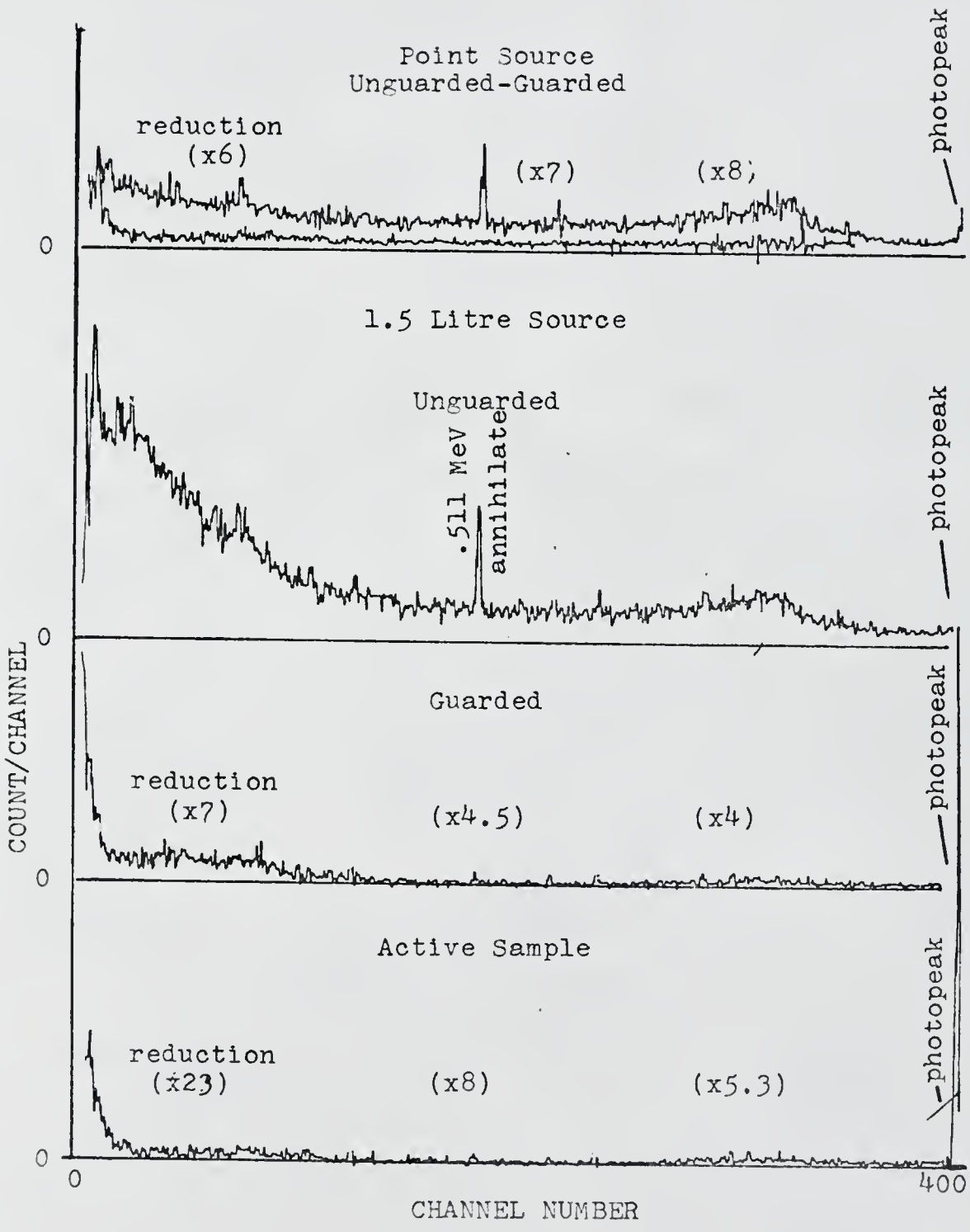

Fig. 43. Zn-65 source spectrum.

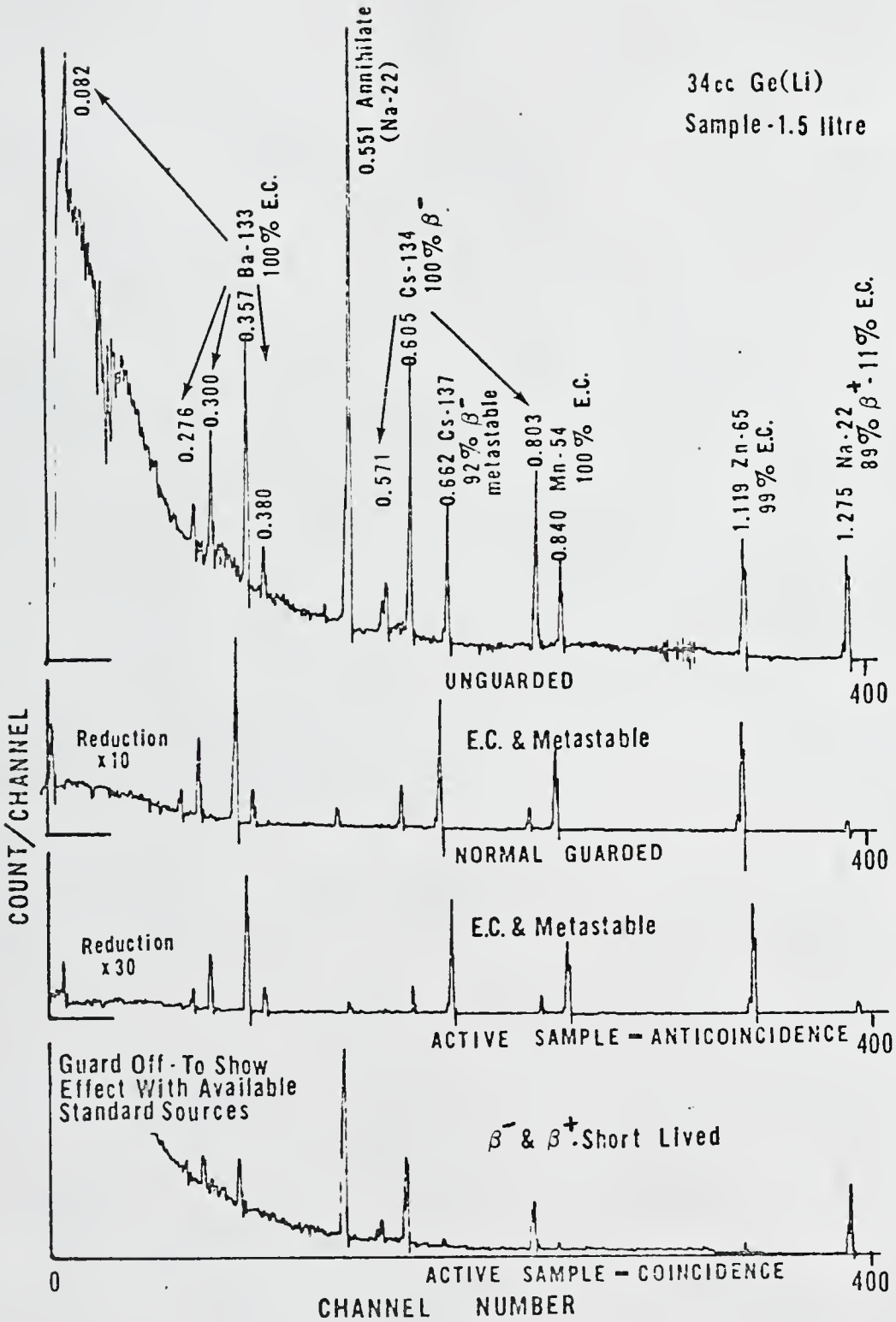

Fig. 44. Complex standard-sample spectrum.

cascade events, and the Compton tail in the normal guarded mode, the anticoincidence sample-guarded mode suppressed the Compton tail another factor of 3. Also the coincidence sample mode suppressed electron capture and metastable states while restoring the rest.

B. Air Sample

To demonstrate the usefulness of the normal guarded mode, an air sample was taken of 45,000 cubic feet of atmospheric air and allowed to decay for 3 days. Comparison of 40 minute count spectra for NaI(Tl), unguarded Ge(Li), and guarded Ge(Li) shows no identification of any radionuclide in either the NaI(Tl) or unguarded Ge(Li). However, data analysis on the guarded Ge(Li) spectrum indicates the presence of 100 pCi of ^{7}Be, 8 pCi of ^{103}Ru, and 12 pCi of ^{95}Nb (all activities determined from digital data - see Appendix D).

C. Water Samples

To demonstrate the advantages and disadvantages of the active-sample technique, two environmental water samples were counted on the various systems. The first sample was an environmental standard sample prepared by the Public Health Service and its spectra are shown in Figure 46. The NaI(Tl), unguarded Ge(Li) and guarded Ge(Li) spectra all show the presence of 200 pCi of ^{106}Ru and 200 pCi of ^{144}Ce although their presence in the guarded Ge(Li) is easiest recognized. The active-sample mode does not show their presence due to the dilution of the sample with scintillator.

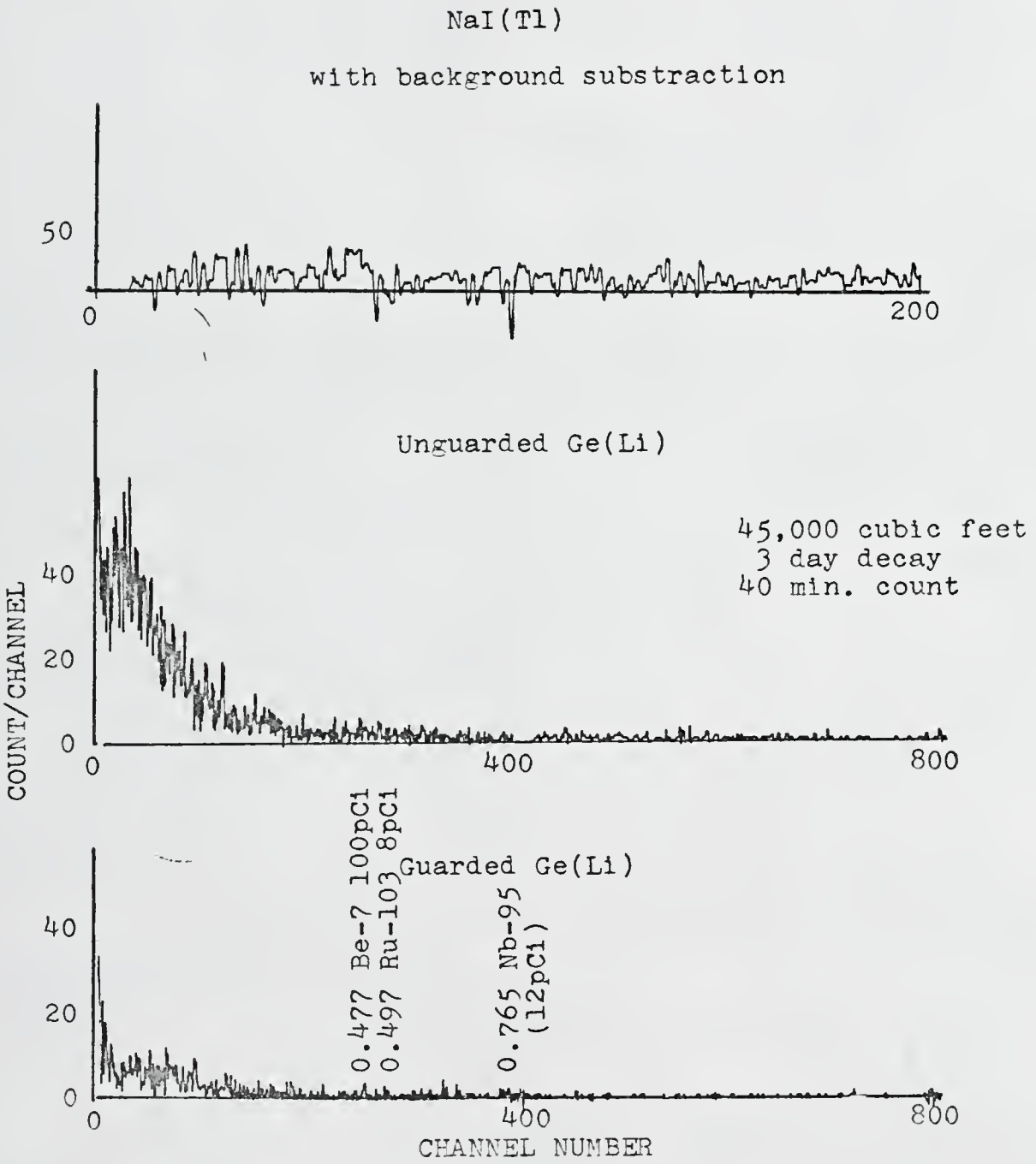

Fig. 45. Air sample spectrum.

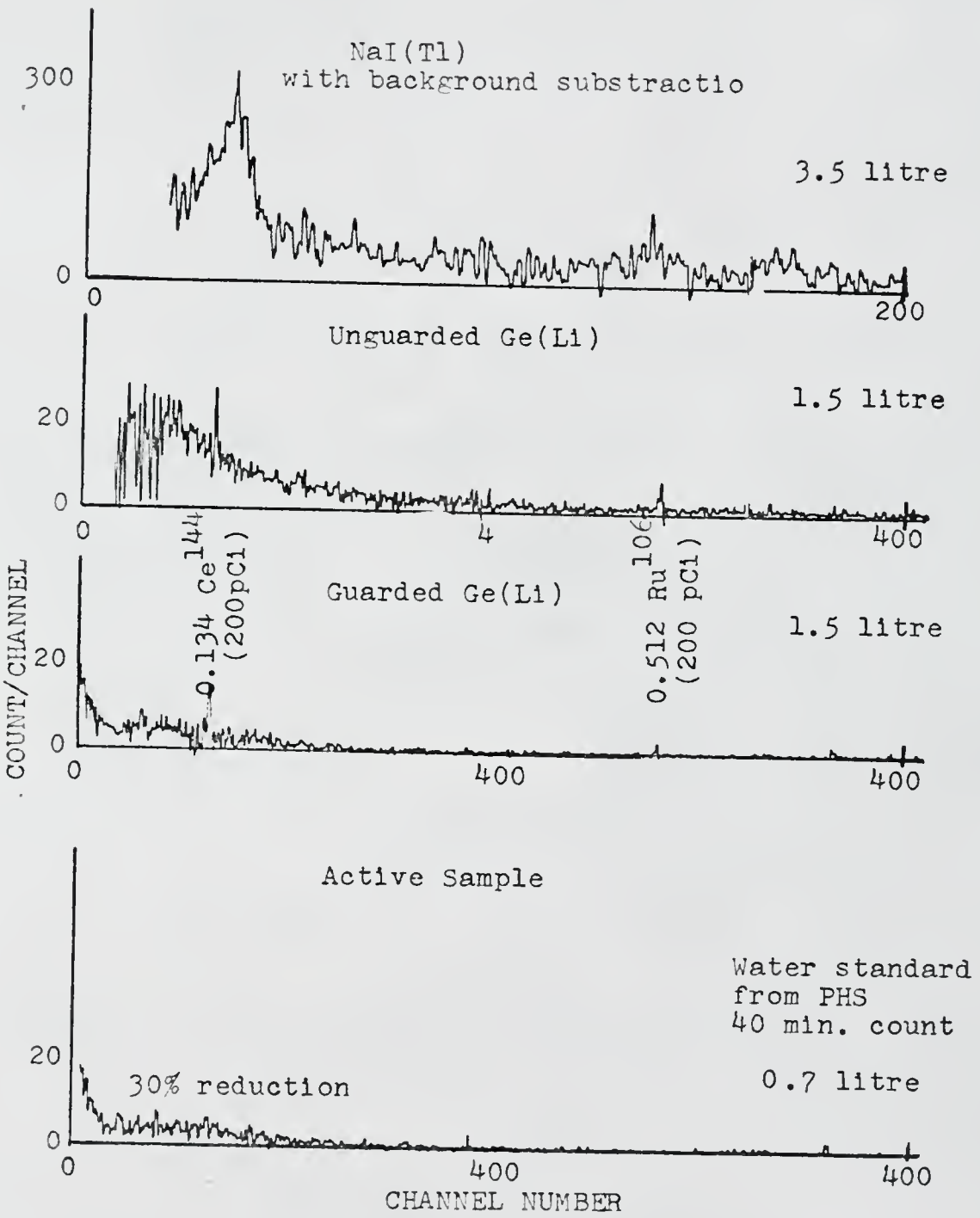

Fig. 46. Water standard spectrum.

The other environmental water sample was taken from the University of Florida Training Reactor coolant water. The spectra shown in Figure 47 indicates the presence of 20,000 pCi of activated ^{24}Na. The NaI(Tl) spectrum is completely swamped by the ^{24}Na, however the unguarded Ge(Li) clearly identifies the presence of 1,400 pCi of ^{99m}Tc, The guarded Ge(Li) spectrum also shows the presence of 700 pCi of ^{115}In and ^{115}Cd. The active sample mode spectrum, because of the removal of ^{24}Na (a short-lived β^-) and its Compton continuum, shows the presence of 13 pCi of ^{133}Ba and 90 pCi of ^{65}Zn (both contamination in the sample container). It should be noted that the ^{24}Na Compton continuum is less than the background in the active-sample spectrum and thus does not raise the minimum detectable activity in that region.

D. Solid Samples

To further show the usefulness of the guarded Ge(Li) system three environmental solid samples were analyzed. The first, whose spectra are shown in Figure 48, consists of an 800-gram soil sample taken from undisturbed top soil. All three spectra for this sample; the NaI(Tl), the unguarded Ge(Li), and the guarded Ge(Li) show the presence of 1200 pCi of ^{226}Ra and its daughter products, 500 pCi of ^{137}Cs, and 400 pCi of ^{40}K. The NaI(Tl) spectrum shows considerable interference between these radionuclides, especially between the 662 keV ^{137}Cs peak and the 609 keV RaC peak. The guarded Ge(Li) greatly reduces peak-to-peak interference and Compton-to-peak interference

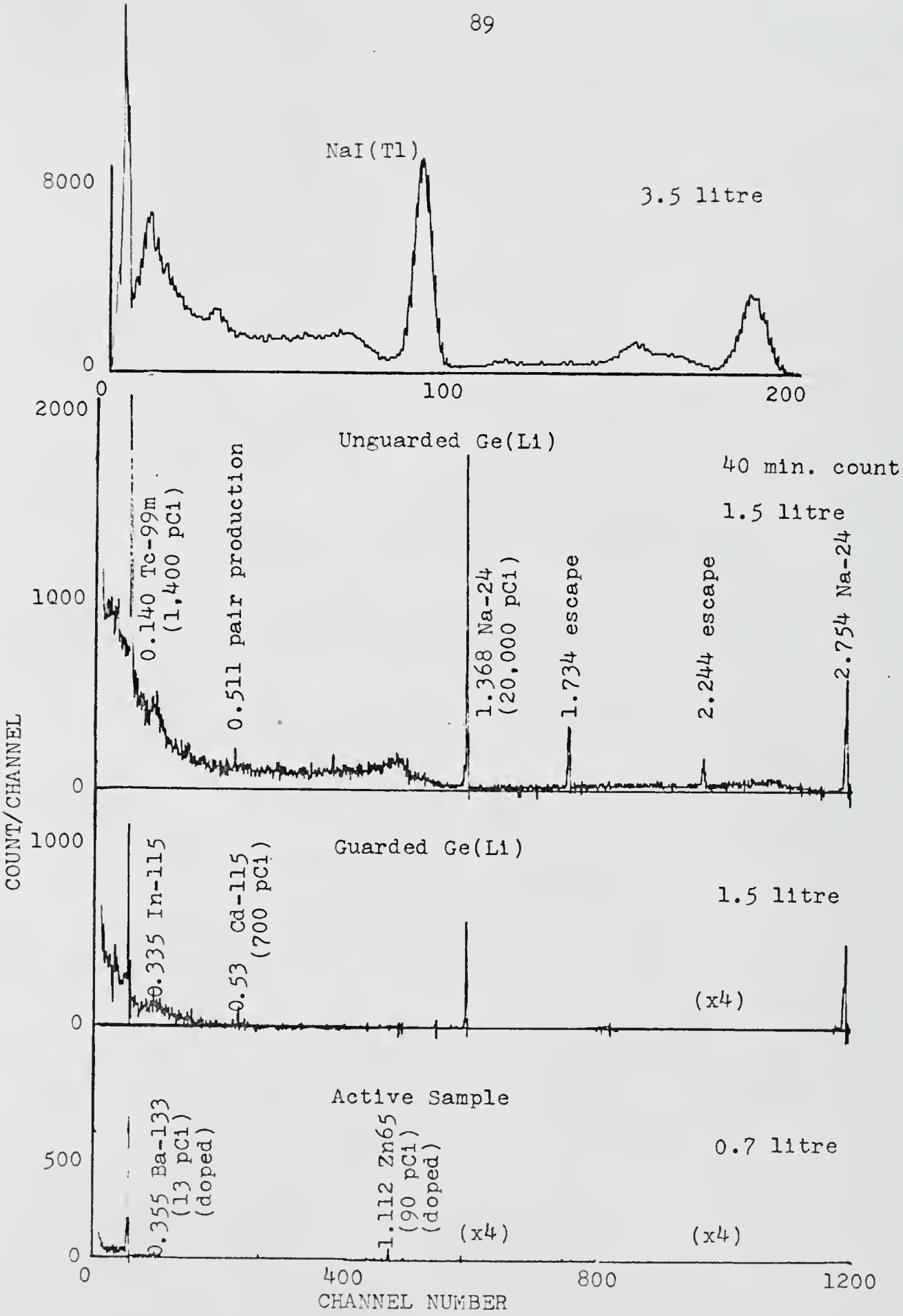

Fig. 47. UFTR primary coolant water spectrum.

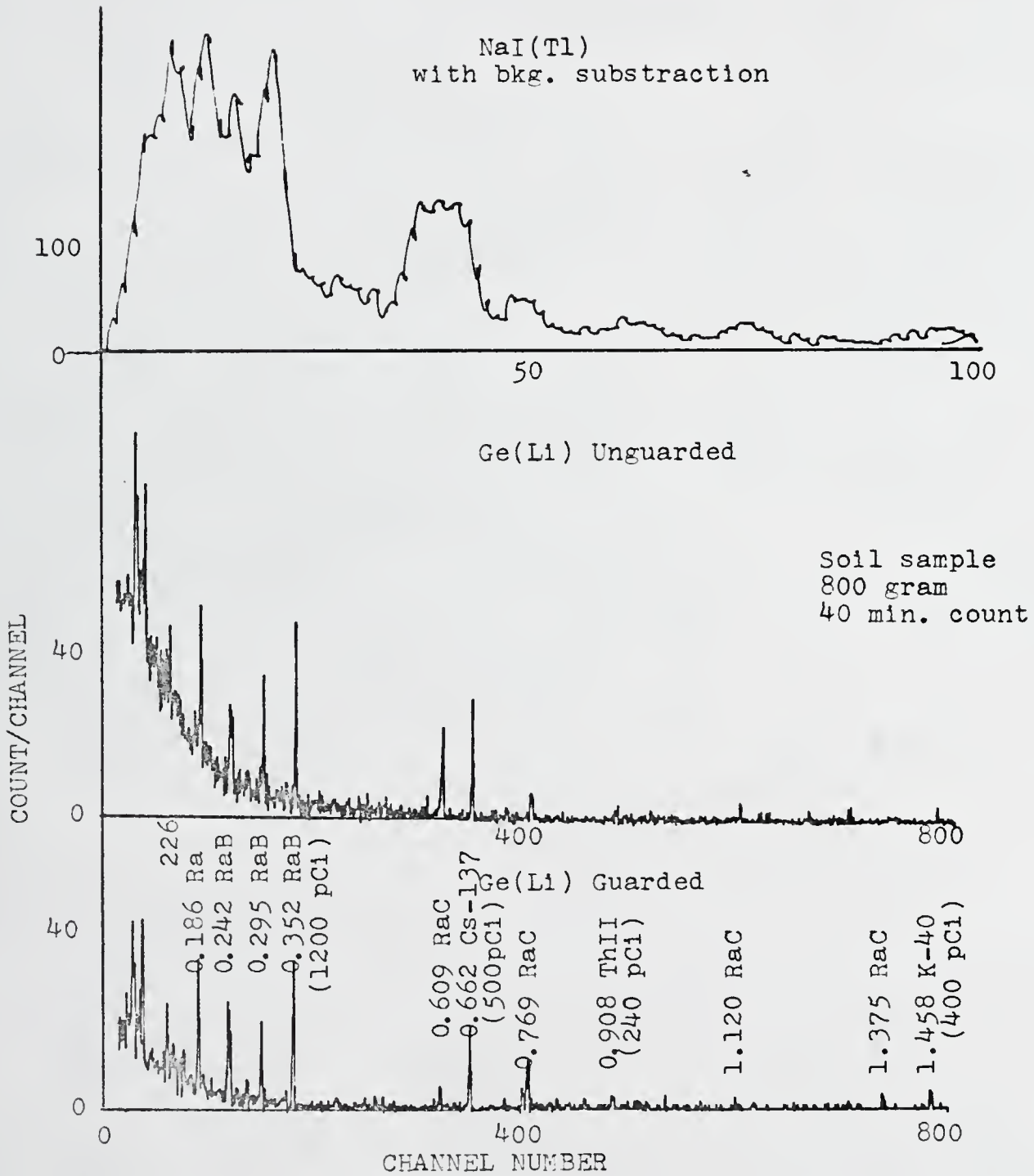

Fig.48. Soil sample spectrum.

making the identification of these radionuclides simpler.

The second sample consists of a 470-gram oyster sample taken from Crystal River. Its spectra, given in Figure 49, show no radionuclides visible in either the NaI(Tl) spectrum or the unguarded Ge(Li) spectrum. However the guarded Ge(Li) spectrum shows the presence of 200 pCi of ^{40}K, 18 pCi of ^{131}I and 150 pCi of ^{226}Ra.

The third solid sample consists of a 720-gram sample of seaweed taken from Crystal River. Its spectra shown in Figure 50, show the presence of 700 pCi of ^{40}K recognizable in all three spectra, and 320 pCi of ^{7}Be, 80 pCi of ^{232}Th and 250 pCi of ^{226}Ra recognizable only in the guarded spectrum.

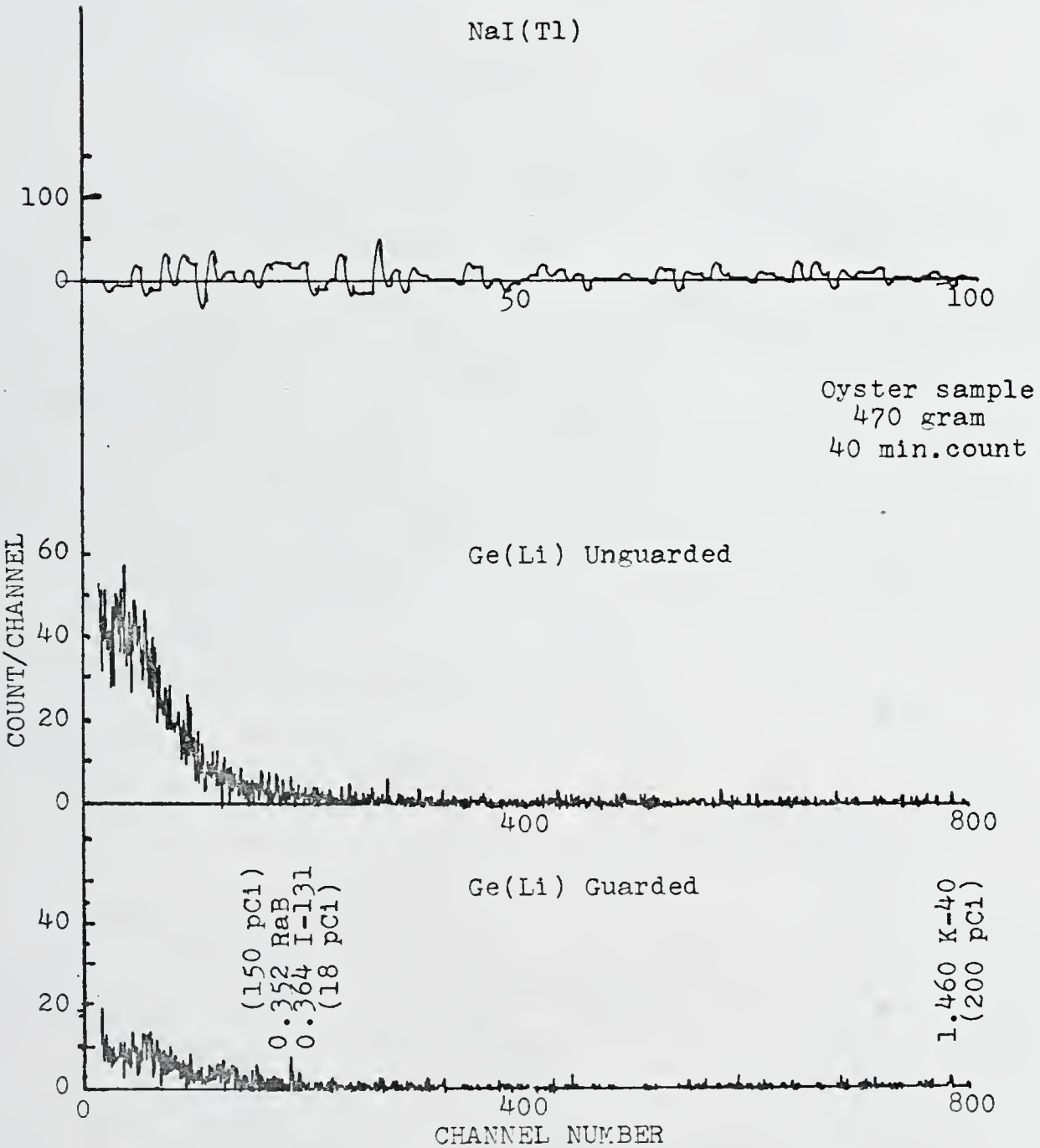

Fig. 49. Oyster sample spectrum.

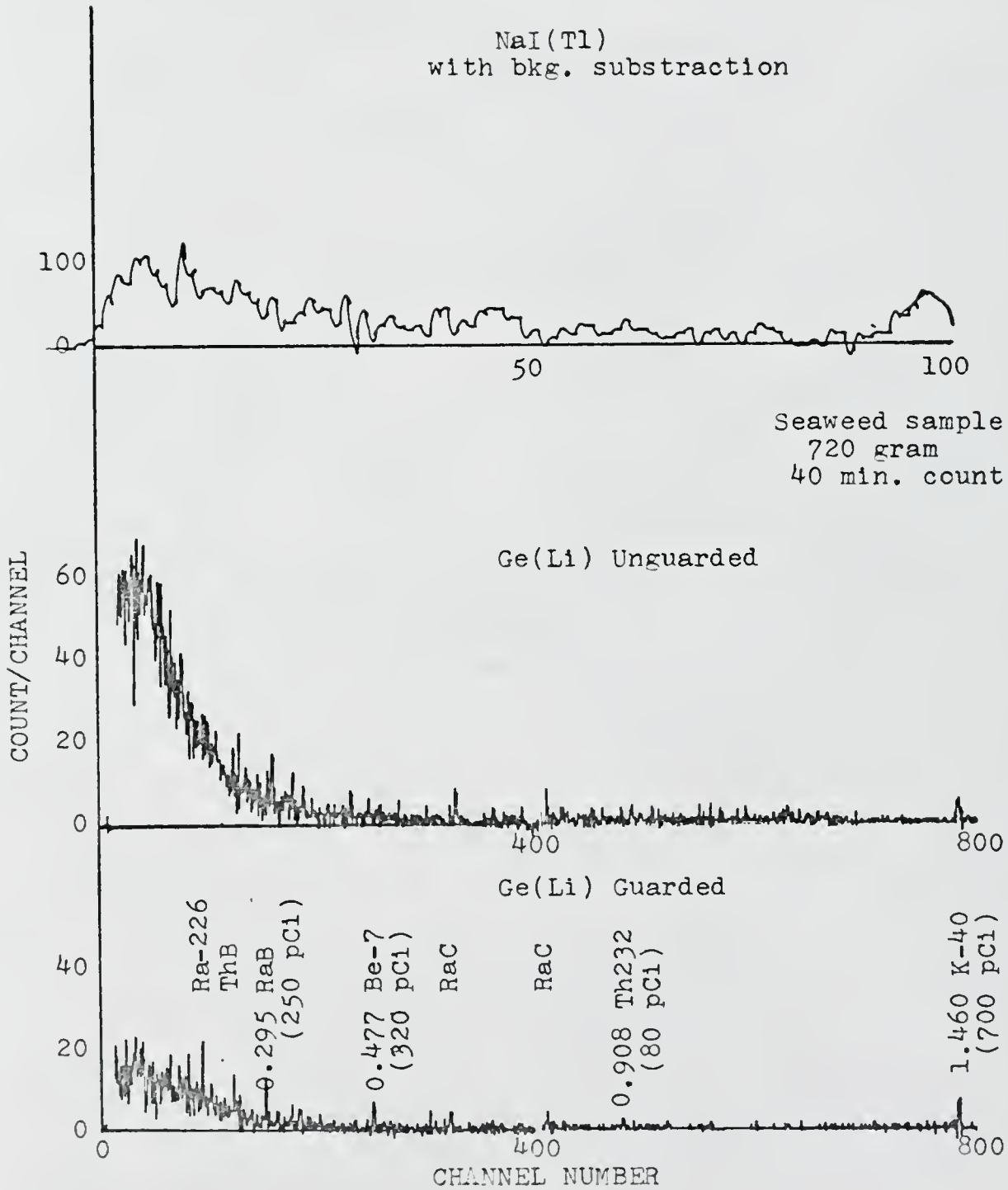

Fig.50. Seaweed sample spectrum.

CHAPTER X

EVALUATION OF DETECTION SYSTEMS

In this chapter the advantages of each system are enumerated. In addition, the relative usefulness of each system is explained.

A. NaI(Tl) System

The 4x4 inch NaI(Tl) system has the advantage of high detection efficiency (approaching the efficiency due to geometry factor alone below 400 keV) which allows less statistical error for short counting times due to the higher counting rate. The 4x4 inch NaI(Tl) system therefore has a lower single radionuclide theoretical minimum detectable activity than the unguarded, relatively low efficiency 34 cc. Ge(Li) system. However, due to the background reduction in the guarded 34 cc. Ge(Li) detector, the 4x4 inch NaI(Tl) system is superior for the detection of only a few radionuclides of low activity concentration (two adjacent radionuclide associated photopeaks appear as one in the NaI(Tl) and the NaI(Tl) system accepts larger samples).

The poor resolution of the NaI(Tl) detector lends itself to misidentification of photopeaks and the masking of photopeaks by the large Compton continuum of others. Thus, minimum detectable activity in the presence of a large amount

of high-energy gamma decay radionuclides is greatly increased. Therefore, in complex spectra the 4x4 inch NaI(Tl) detector may not have a lower minimum detectable activity than the unguarded 34 cc. Ge(Li).

B. Unguarded Ge(Li) System

The unguarded Ge(Li) system although having a higher minimum detectable activity than the NaI(Tl) allows the pin-point identification of photopeak energies to within 2 keV. This, along with its higher peak-to-Compton ratio, allows more reliable identification of radionuclides than the NaI(Tl), especially in complex spectra.

C. Guarded Ge(Li) System

The guarded 34 cc. Ge(Li) system has the advantages of a higher peak-to-Compton ratio (8 times better than the unguarded Ge(Li) and 16 times better than the NaI(Tl)) and a reduction of background (a factor of 6 over the unguarded Ge(Li)). This large background reduction gives a lower minimum detectable concentration by a factor of 2 and a lower minimum point-source minimum detectable activity by a factor of 4 over that for the 4x4 inch NaI(Tl) for long counting times, but approximately the same minimum detectable activity for 40 minute counts (due to the required change to Poisson statistics for low counts). In addition, the exceptionally high peak-to-Compton ratios allows the maintaining of this good minimum detectable activity in complex spectra.

However, due to the nature of anticoincidence guarding, cascade decay events and β^+ decay events are suppressed. Thus the usefulness for identification of such decay events is greatly reduced (50-fold for β^+ and 7-fold for cascade emitters).

D. Active-Sample System

The active-sample system restores the point-source peak-to-Compton ratio for large water samples. In complex spectra with the presence of large amounts of radionuclides, this additional Compton suppression improves the minimum detectable activity below 200 keV by a factor of 2 in spite of the required 2-fold dilution of the sample. In addition, the technique produces two simplified spectra which can aid in the identification of the radionuclides or selectively suppress interference due to either of the two classes of decay mentioned previously.

CHAPTER XI

CONCLUSIONS

Anticoincidence guarding of a 34 cc. Ge(Li) crystal has shown itself superior in its minimum detectable activity and minimum detectable concentration over an unguarded 4x4 inch NaI(Tl) detector for counting times as short as 40 minutes. For 24-hour counts, its minimum detectable point-source activity is roughly 4 times better than the unguarded 4x4 inch NaI(Tl). In addition the excellent peak-to-Compton ratio of the guarded Ge(Li) practically eliminates radionuclide spectral interference.

The active-sample technique, while showing only slight advantage in minimum detectable activity at low energies for typical environmental samples, shows particular promise in the selective removal of spectral counts of large quantities of certain radionuclides from the spectrum.. This removal process could be described as gamma-beta anticoincidence counting and gamma-beta coincidence counting.

Several improvements can be made in the guarded Ge(Li) system to further reduce its minimum detectable activity. First an increase in Ge (Li) detector efficiency would improve the minimum detectable activity by the square root of its relative improvement as would an increase in guard efficiency.

By employing a 20% efficient Ge(Li) detector, using beryllium instead of aluminum in the detector and sample port, reducing the sample port diameter to three inches, and using bi-alkali photocathodes in the guard detector photomultiplier tube (or cooling to 0°C to reduce phototube noise), an improvement in minimum detectable activity by a factor of 4 and an improvement in the peak-to-Compton ratio of the same factor could be achieved. Thus peak-to-Compton ratios could approach 800 and minimum detectable activities approach the 0.1 pCi level (for ^{137}Cs point source - 24 hour count).

APPENDICES

APPENDIX A

ELECTRONIC CIRCUITS

The active-sample anticoincidence guarded Ge(Li) spectrometer system required the design and construction of additional electronics including preamplifiers, threshold detectors, coincidence gate circuits and cable drivers. This appendix contains the circuit diagrams for the above required electronics. Figure 51 gives the circuit diagram for the sample-detector preamplifier, cable driver, threshold detector, and control pulse shaper. Figure 52 gives the circuit diagram for the guard-detector preamplifier, threshold detector, and control pulse shaper. Figure 53 gives the circuit diagram for the Ge(Li) detector timing preamplifier, threshold detector, and control pulse shaper. The coincidence and anticoincidence control circuits along with the pulse generators to drive the biased amplifier coincidence gate and the multichannel analyzer anticoincidence gate are given in Figure 54.

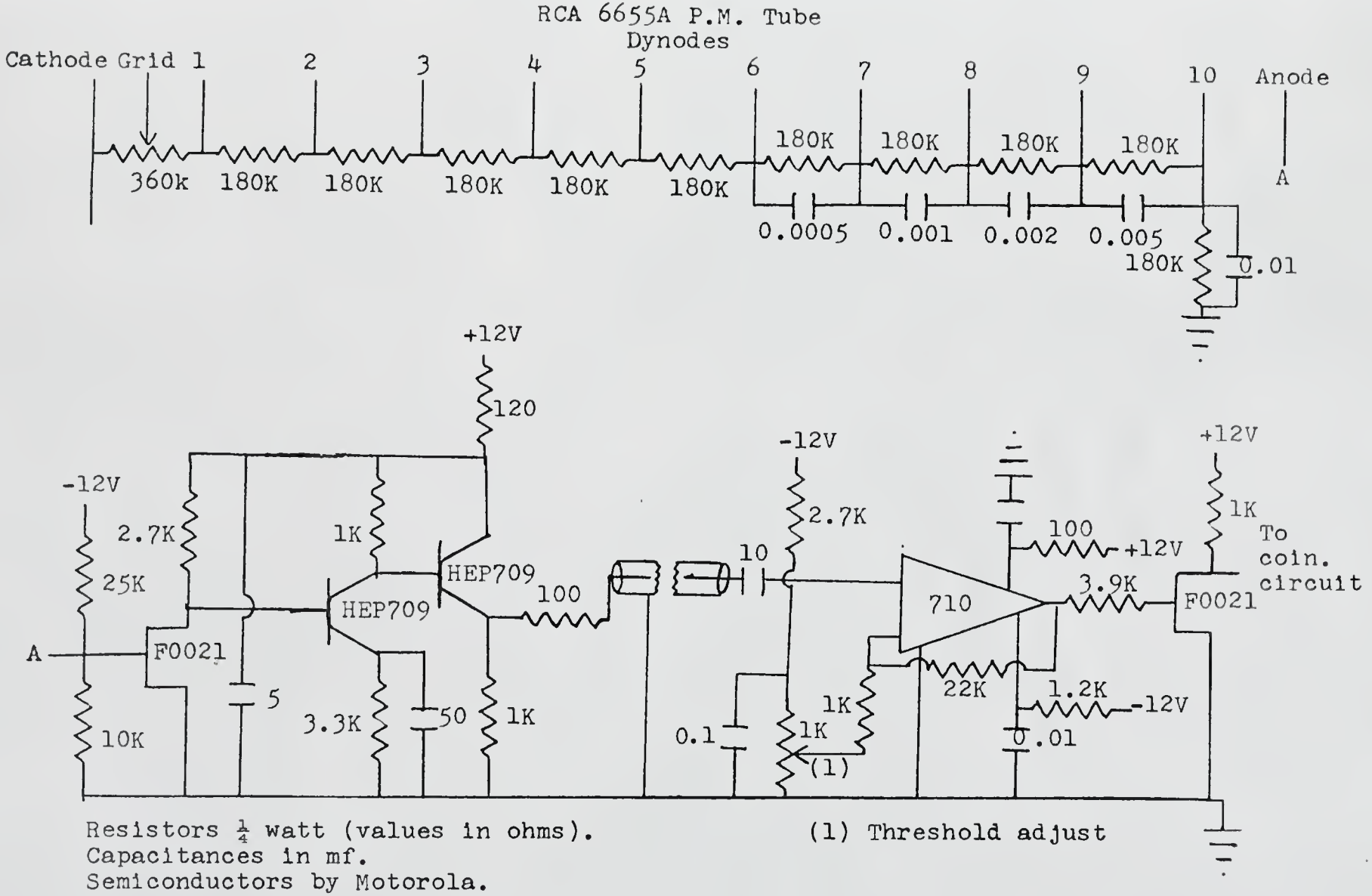

Resistors ¼ watt (values in ohms).
Capacitances in mf.
Semiconductors by Motorola.

(1) Threshold adjust

Fig. 51. Sample-detector electronics circuit.

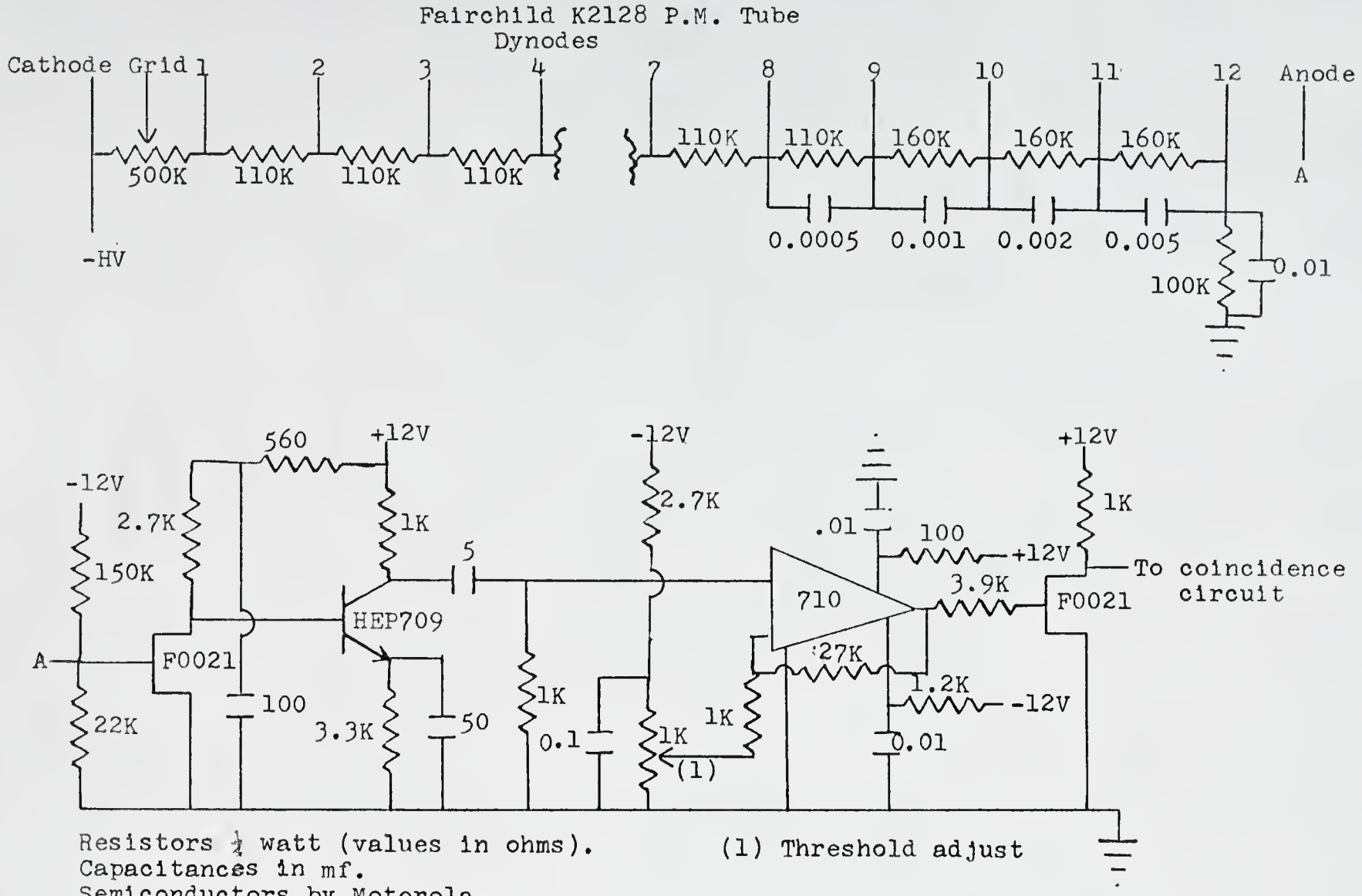

Fig. 52. Guard-detector electronics circuit.

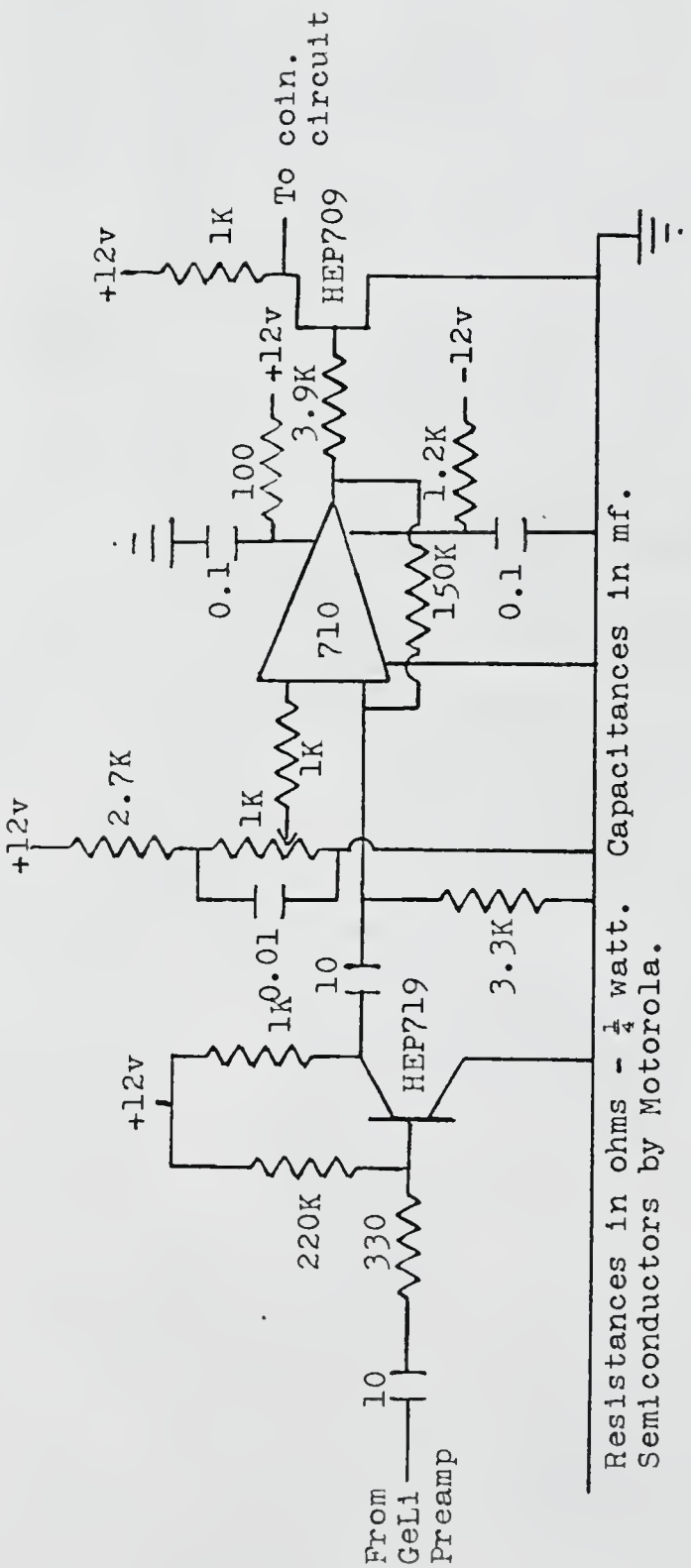

Fig. 53. Ge(Li) threshold electronics.

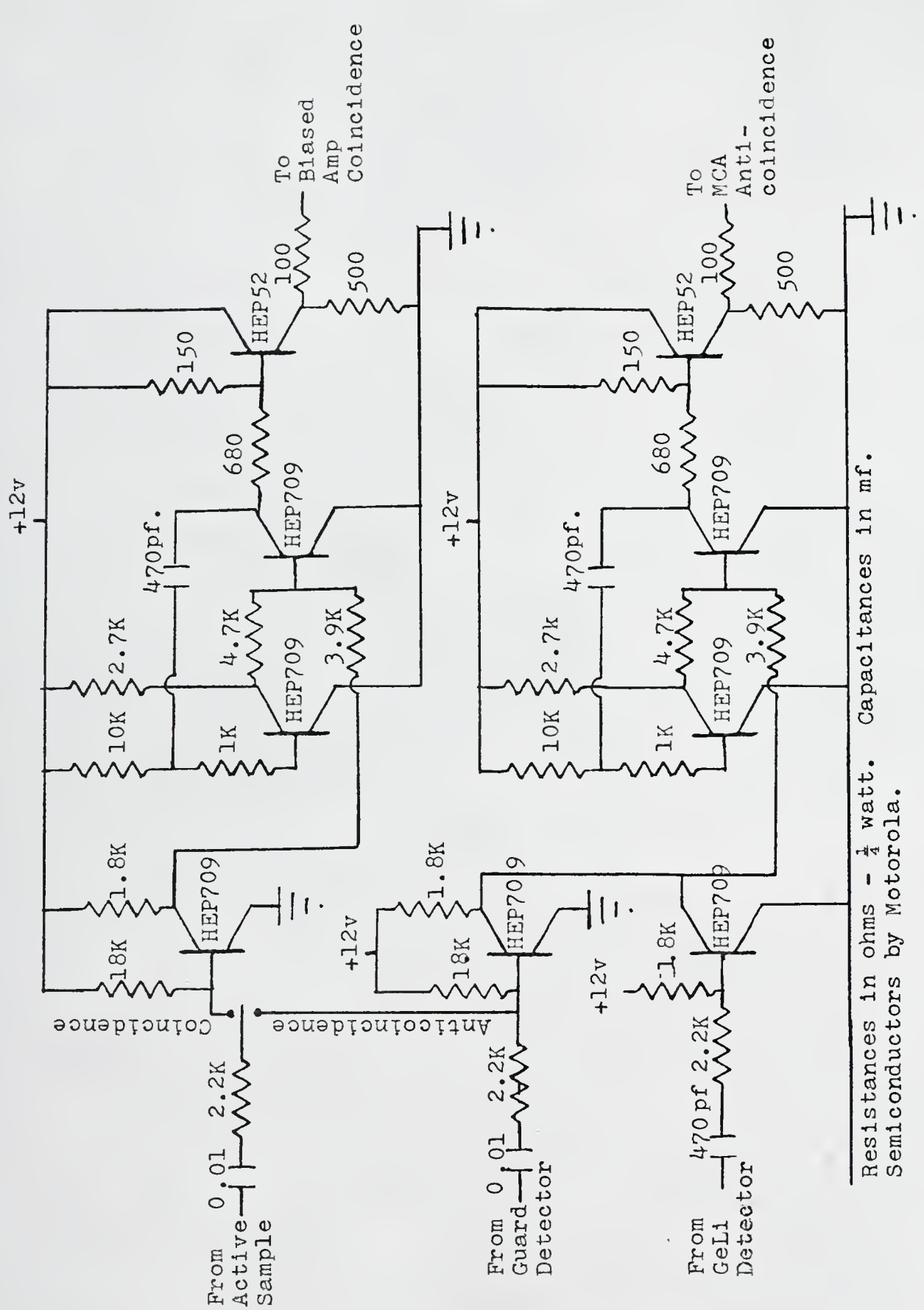

Fig. 54. System coincidence electronics.

APPENDIX B

GUARD DETECTOR CHARACTERISTICS

In this appendix the data leading to the determination of the guard detector energy threshold are presented. In addition the procedures used to determine this threshold are outlined.

Figure 55 shows two guard-detector gamma spectra taken with a ^{137}Cs point source. Since one spectrum was taken with the source positioned 8 inches from the phototube-end of the cylindrical guard detector and the other with the source positioned the same distance from the opposite end of the guard, the geometry factors are approximately the same and thus differences in the spectra are due to light absorption, reflection and collection. The similarity of the two spectra indicates very adequate light collection and very little position dependence throughout the guard.

Figure 56 shows the background spectrum of the guard with the guard detector threshold so marked. By requiring the integration of all channels above the threshold to yield 40,000 counts per second, the threshold channel could be determined.

Figure 57 shows an attempt to energy-calibrate the threshold with a point source ^{57}Co standard. By extrapolating the leading edge of the spectrum, an approximate channel

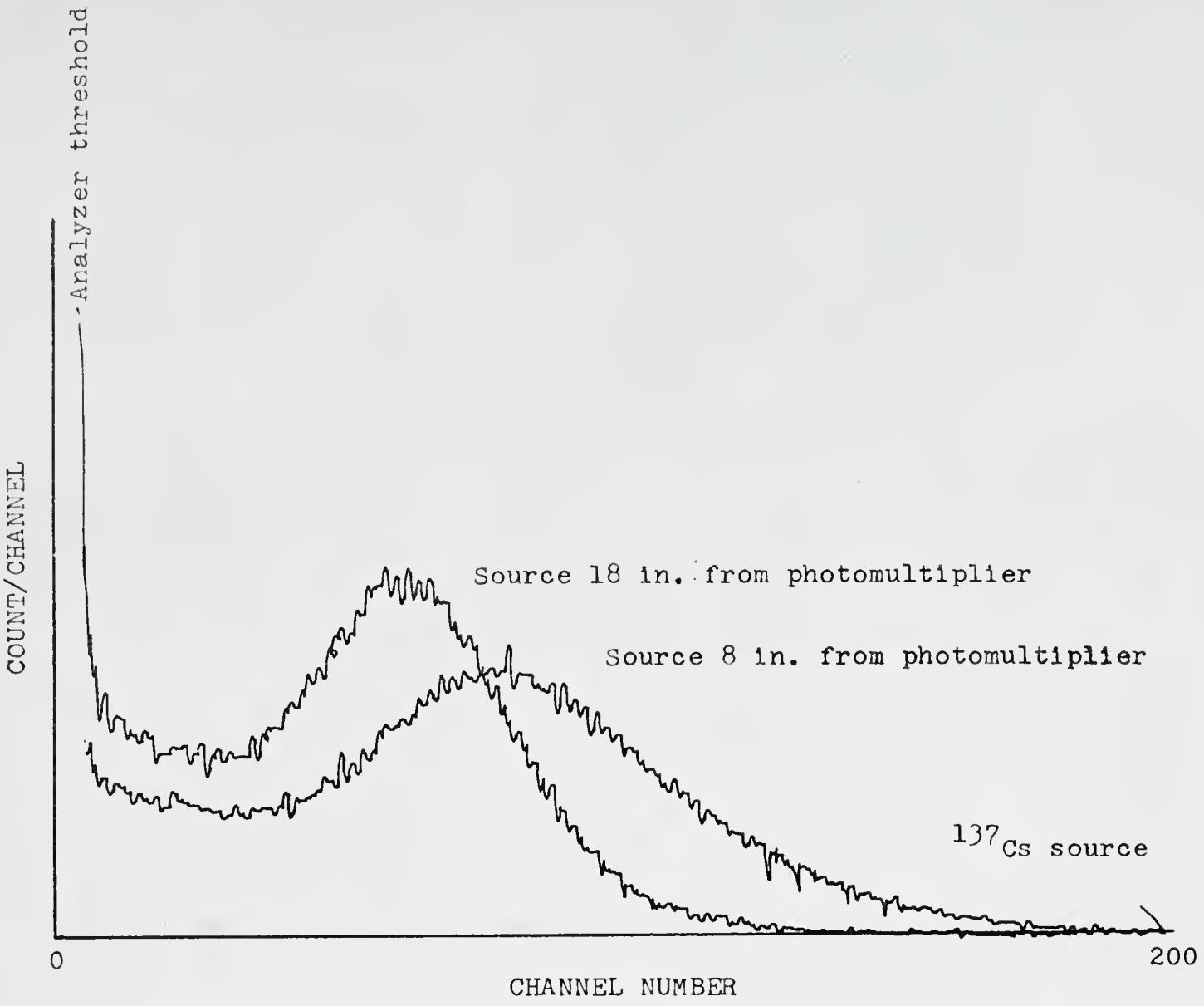

Fig. 55. Guard-detector light collection.

Fig. 56. Guard-detector background.

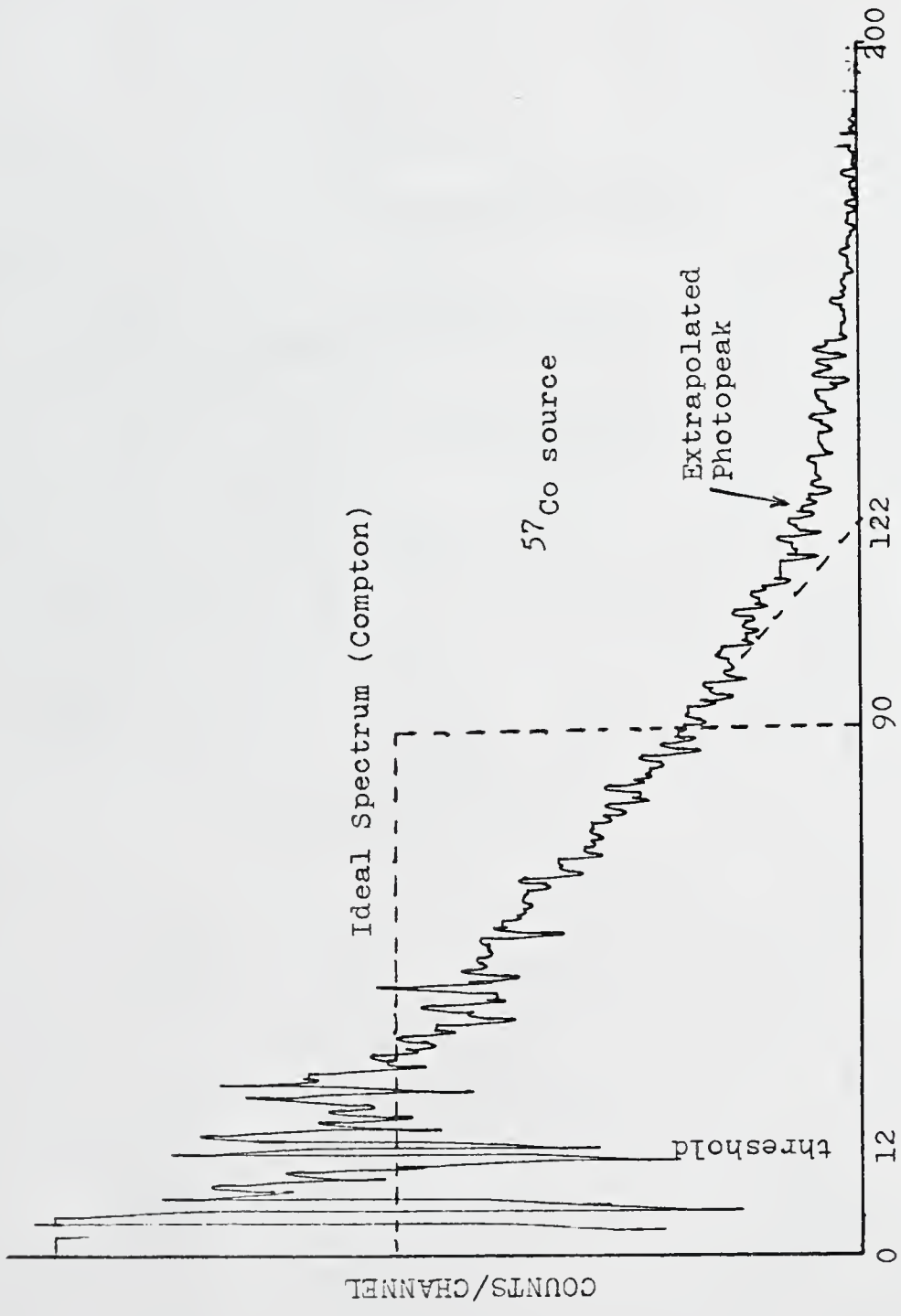

Fig. 57. Threshold calibration.

calibration of the photopeak energy is deduced. Comparison of the integration below the threshold to the total spectrum integration gives the fractional loss for ^{57}Co. The effective energy threshold of the guard detector is 15 keV and the effective fractional count loss is $^{15}/E(keV)$.

APPENDIX C

SPECTRUM ENERGY CALIBRATION

In this appendix the data used for the energy calibration of the analyzer display are presented. Included are the spectra of the standard radioisotopes used for calibration (see Figure 58) and the energy versus channel number calibration curve (see Figure 59). The slope of this calibration curve shows a 1.85 keV per channel energy division with no zero channel offset. The biased amplifier was used to produce an 800 channel spectrum in two runs with a 400 channel MCA.

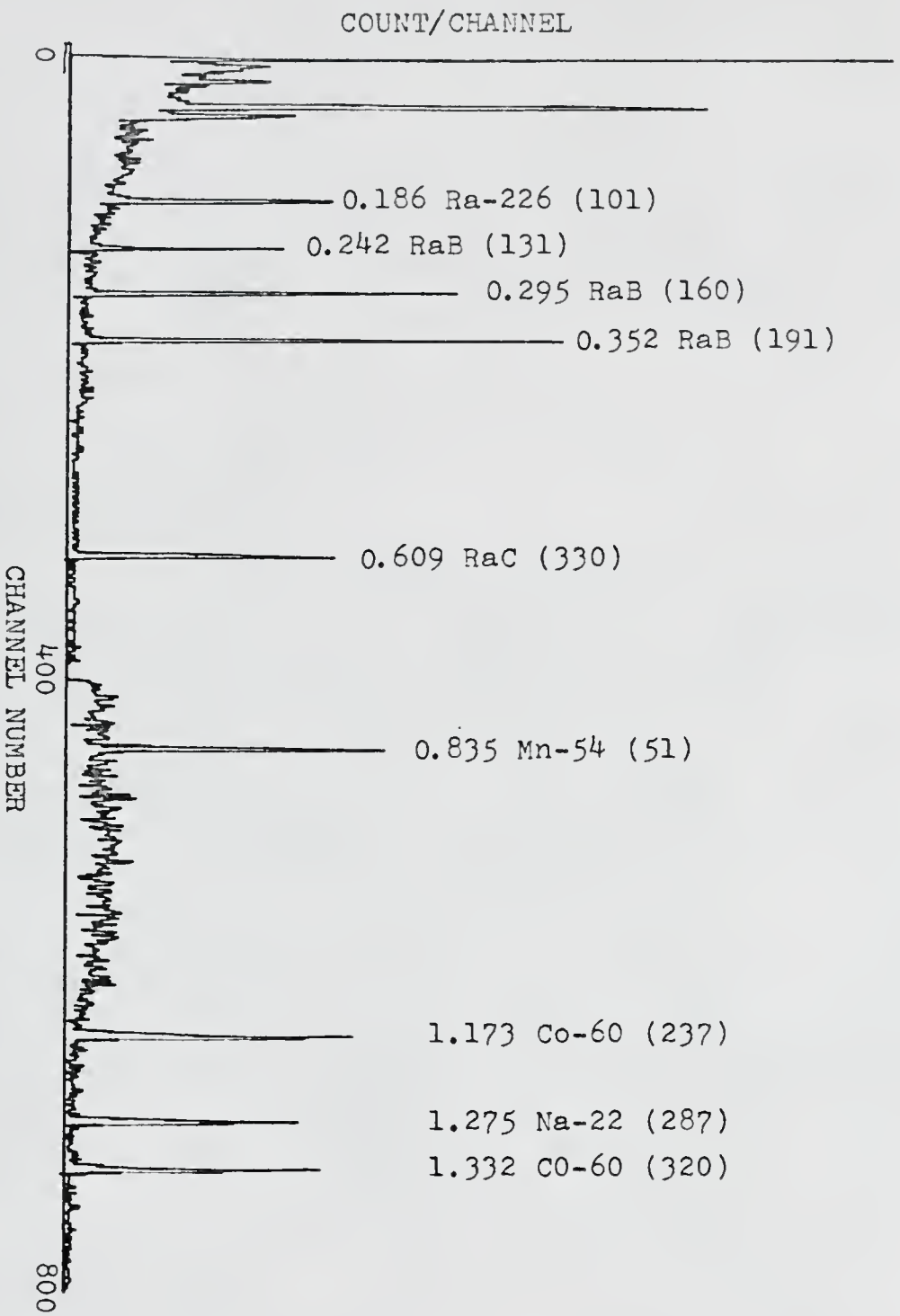

Fig.58. Ge(Li) calibration spectrum.

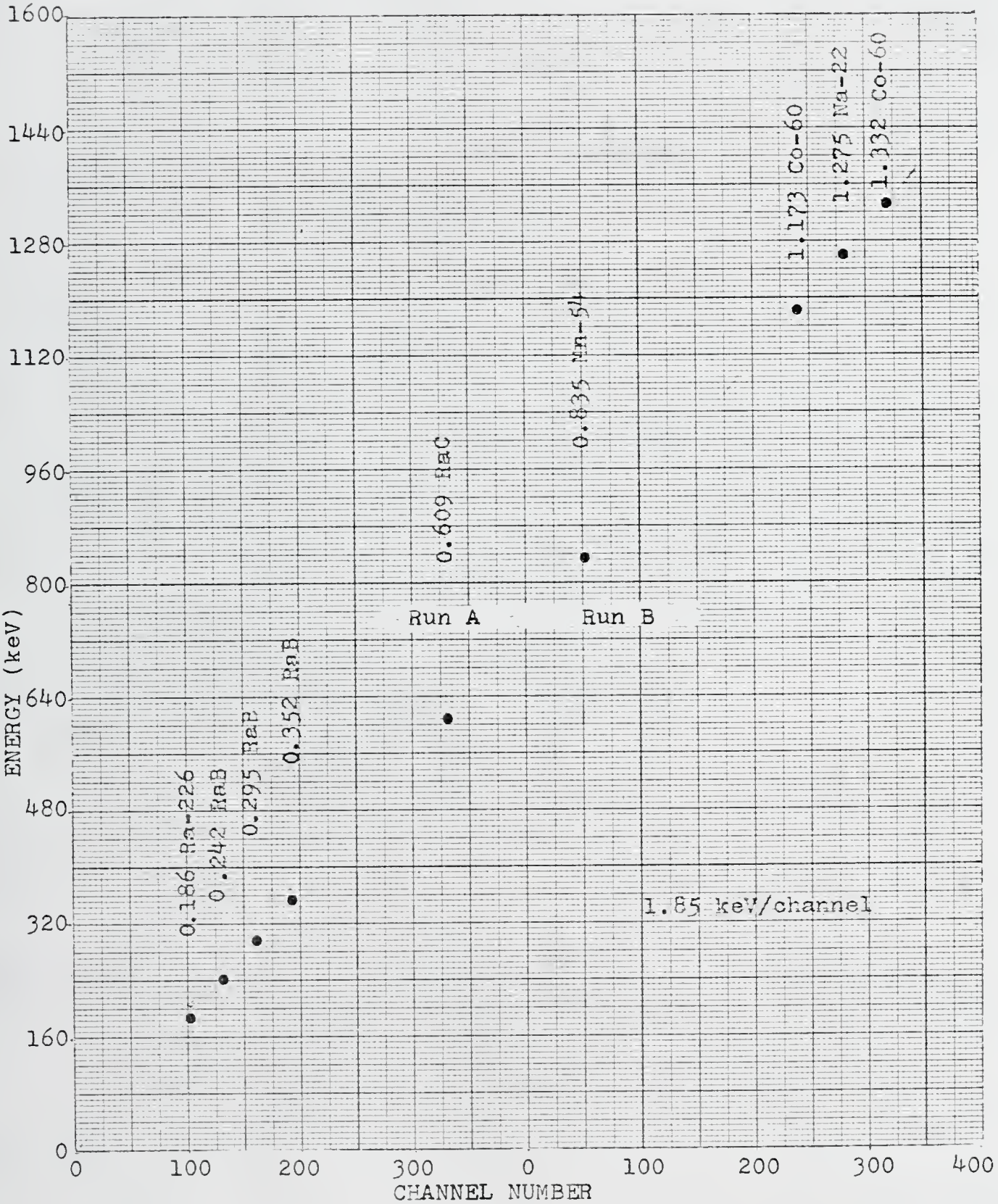

Fig. 59 Ge(Li) calibration curve.

APPENDIX D

EXAMPLE OF DIGITAL DATA

Because of noise in the plotter mechanism, some spectrum plots do not clearly show the photopeaks present. In this appendix a sample of the digital data is presented to show that this problem is indeed in the plotter.

Table 8 gives the digital data for the guarded air sample spectrum (Figure 45) between 400 keV and 800 keV. Three peaks can be easily distinguised - the 0.477 Be-7, the 0.497 Ru-103, and the 0.765 Nb-95.

Table 8

Digital Data for Guarded Air Sample Spectrum

Counts per Channel
(400-800 keV)

00	00	01	01	00	00	00	01	00	02
01	01	00	00	04 (A)	01	01	00	01	00
00	00	00	00	01	00	00	00	00	00
02	01	01	01	02	01	00	00	01	00
00	01	00	00	00	02	00	01	00	00
00	02	03	05 (B)	04	01	01	00	01	01
00	00	00	01	03	00	00	01	00	00
00	00	03	00	00	02	00	00	01	00
00	00	01	00	00	00	00	01	00	01
00	00	00	01	00	01	00	00	02	00
02	00	01	00	00	00	02	00	00	01
00	01	00	00	02	00	00	00	01	00
00	01	00	00	01	02	00	00	02	01
00	00	00	00	00	00	00	01	00	00
00	02	02	00	00	00	00	01	00	00
01	01	00	00	01	00	00	00	00	00
01	00	00	00	00	01	00	00	00	00
00	00	00	00	00	01	02	01	01	02
01	03 (C)	02	00	00	01	00	01	00	00

(A) 0.477 Be-7 100pCi
(B) 0.497 Ru-103 8pCi
(C) 0.765 Nb-95 12pCi

LIST OF REFERENCES

1. Conally, R. E. "Two-Crystal Gamma-Ray Scintillation Spectrometer," Review of Scientific Instruments 24, 458 (1953).

2. Evans, A. E., B. Brown and J. B. Marion. "Anticoincidence Shielded Gamma-Ray Spectrometer for Nuclear Reaction Studies," Review of Scientific Instruments (August, 1966).

3. Cooper, J. A., N. A. Wagman, H. E. Palmer, and R. W. Perkins. "The Application of Solid State Detectors to Environmental and Biological Problem," Battelle Memorial Institute Report, BNWL-SA-1104 (1967).

4. Hill, M. W. "An Anticoincidence-Shielded Ge(Li) Gamma-Ray Spectrometer," Nuclear Instruments and Methods, 35, 350-352 (1965).

5. Cooper, J. A. "Anticoincidence-Shielded Ge(Li) Gamma-Ray Spectrometer for High Sensitivity Counting," IEEE Transactions on Nuclear Science, NS-15, No. 3, 407-412 (June, 1968).

6. Cooper, J. A., L. A. Rancitelli, R. W. Perkins, W. A. Haller, and A. L. Jackson. "An Anticoincidence Shielded Ge(Li) Gamma-Ray Spectrometer and Its Application to Neutron Activation Analysis," Battelle Memorial Institute Report, BNWL-SA-2009 (1968).

7. Phelps, P. L., K. O. Hamby, B. Shore, and G. D. Potter. "A Ge(Li) Gamma-Ray Spectrometer of High Sensitivity and Resolution for Biological and Environmental Counting," In Radionuclides in the Environment, Advances in Chemistry, Series 93,202-230, (1970).

8. Latner, N. and C.G. Sarderso. "The HASL Ge(Li)-NaI(Tl) Low Level Counting System," IEEE Transactions on Nuclear Science, NS-19, No. 3, 141-150 (February, 1972).

9. Zimmer, W. H. "An Anticoincidence Guarded Ge(Li) Detector for Environmental Level Gamma Energy Analysis," IEEE Transactions on Nuclear Science, NS-19, No. 3, 151-154 (February, 1972).

10. Phelps, P. L. and K. O. Hamby. "Experience in the Use of an Anticoincidence Shielded Ge(Li) Gamma-Ray Spectrometer for Low Level Environmental Radionuclide Analysis," IEEE Transactions on Nuclear Science, NS-19, No. 3, 155-165 (February, 1972).

11. Ohlwiller, R. W. "The McClellan Central Laboratory's Anticoincidence Ge(Li) Spectrometers for Low Level Applications," IEEE Transactions on Nuclear Science, NS-19, No. 3, 166-171 (February, 1972).

12. Miller, G. L. "A Brief Review of Recent Advances in Compound Semiconductors for Radiation Detectors," IEEE Transactions on Nuclear Science, NS-19, No. 1, 251-259 (February, 1972).

13. Price, W. J. Nuclear Radiation Detection. New York: McGraw-Hill, 1964.

14. Webb, R. C., M. G. Hauser and R.E. Mischka. "Response of a Mineral Oil Based Liquid Scintillator to Heavily Ionizing Particles," PPAR, 26 (June, 1970).

15. Porter, C. R. "Annual Report of the Eastern Environmental Radiation Laboratory, " EPA Report EERL 71-4, 17-18 (December, 1970).

16. Douglas, G. S. Radioassay Procedures for Environmental Samples, Public Health Service Publication No. 999-RH-27 (January, 1967).

17. Bolch, W. E. "Environmental Surveillance for Radioactivity in the Vicinity of Crystal River Nuclear Power Plant: An Ecological Approach," quarterly progress report - November 1, 1970 - January 31, 1971, University of Florida.

18. Currie, L. A. "The Measurement of Environmental Levels of Rare Gas Nuclides and the Treatment of very Low-Level Counting Data," IEEE Transactions on Nuclear Science, NS-19, No. 1, 119-126 (February, 1972).

BIOGRAPHICAL SKETCH

Frank Russell Markwell was born in Miami, Florida, on November 7, 1948. In August, 1969, he received the degree of Bachelor of Science in Nuclear Engineering Sciences at the University of Florida. In September, 1969, he enrolled in the Graduate School of the University of Florida and in March, 1971, received the degree Master of Science in Engineering. Since that time he has continued his work in nuclear engineering toward the degree of Doctor of Philosophy in Engineering.

During his graduate study, he has held first, intermediate, and terminal Special Fellowships in Nuclear Science and Engineering granted by the United States Atomic Energy Commission.

During his study at the University of Florida, he has been elected to membership in the societies, Tau Beta Pi, Sigma Tau, and Phi Kappa Phi. In addition, he is a member of the American Nuclear Society and the Institute of Electrical and Electronics Engineers.

He presently holds a Second Lieutenant's commission in the United States Army - Ordinance Branch.

I certify that I have read this study and that in my opinion it conforms to acceptable standards of scholarly presentation and is fully adequate, in scope and quality, as a dissertation for the degree of Doctor of Philosophy.

William E. Bolch, Ph.D.
Chairman, Assoc. Prof. of
Environ. Engineering Science

I certify that I have read this study and that in my opinion it conforms to acceptable standards of scholarly presentation and is fully adequate, in scope and quality, as a dissertation for the degree of Doctor of Philosophy.

Mihran J. Ohanian, Ph.D.
Prof. and Chairman of Nuclear
Engineering Sciences

I certify that I have read this study and that in my opinion it conforms to acceptable standards of scholarly presentation and is fully adequate, in scope and quality, as a dissertation for the degree of Doctor of Philosophy.

Charles E. Roessler, Ph.D.
Asst. Prof. of Environmental
Engineering Science

I certify that I have read this study and that in my opinion it conforms to acceptable standards of scholarly presentation and is fully adequate, in scope and quality, as a dissertation for the degree of Doctor of Philosophy.

William H. Ellis, Ph.D.
Assoc. Prof. of Nuclear
Engineering Sciences

I certify that I have read this study and that in my opinion it conforms to acceptable standards of scholarly presentation and is fully adequate, in scope and quality, as a dissertation for the degree of Doctor of Philosophy.

Herbert A. Bevis

Herbert A. Bevis, Ph.D.
Assoc. Prof. of Environmental
Engineering Science

This dissertation was submitted to the Dean of the College of Engineering and to the Graduate Council, and was accepted as partial fulfillment of the requirements for the degree of Doctor of Philosophy.

December, 1972

Robert E. Uhrig

Dean, College of Engineering

Dean, Graduate School

MM 1 6 1.9.2.8.3